

THE UNIVERSITY OF HULL

The Role of Lipid Laden Macrophages in Airways Disease

PhD – Respiratory Medicine

by

Yvette Arabella Hayman

(Sept, 2012)

Abstract

Asthma is a chronic inflammatory disease of the airway and is often associated with Gastro-Oesophageal Reflux (GOR). Lipid laden macrophages (LLM) in the airway have previously been reported indicative of aspiration secondary to GOR. We hypothesised that lipid droplets from undigested or partially digested food may be aspirated into the airway and accumulate in scavenging macrophages thus generating an activated population that interact with other immune cells to induce an asthma-like state of disease.

Using a lipid laden alveolar macrophage index, we collected 29 broncho-alveolar lavage (BAL) samples from patients with a variety of respiratory disorders, to determine the use of this test in GOR diagnosis. We investigated the mode of uptake of unmodified lipid and other alternative sources of lipid. We attempted to generate polarised activated macrophages and to determine the activation status of LLM. We also characterised a new macrophage cell line, and compared these to PMA differentiated THP-1 macrophages.

We have shown that the LLAMI is incapable of diagnosing GOR. We showed that macrophages are capable of direct dietary lipid uptake, independently of actin or CD36. Lipid accumulation also results from the phagocytic clearance of apoptotic epithelial cells, which may account for the lack of LLAMI specificity for GOR. Our attempts to generate and distinguish polarised macrophages were unsuccessful and as a result, we were not able to determine the activation status of LLM. We demonstrated heterogeneity among primary macrophage cells isolated from BAL fluid collected from patients with varying pathologies. Particularly interesting was the finding that macrophages isolated from a patient with GOR showed distinctly greater CD36 expression. Daisy cells are novel cells which appear to be macrophage-like morphologically, functionally and phenotypically. Daisy cells have potential utility with the ability to spontaneously replicate and differentiate an advantage over THP-1 cells which require PMA stimulation.

Acknowledgements

To my supervisors Professor Alyn Morice and Dr.Simon Hart for your continued support and guidance. To Dr. Laura Sadofsky, Dr. Vincent Mann, Chris Crow and the team in the dept. of Academic Cardiovascular and Respiratory Medicine for your support and friendship. To Professor Ian Dransfield for the kind and generous gift of cells. To Dr. Kastelik and the Endoscopy Team, Mr. Cowen, Mr. Rob Bennett and the surgical team for your help and co-operation in collecting primary cells. To Ann Lowry for your help and kindness with microscopy. To James Williamson for grammatical guidance. Also to my parents for supporting and encouraging me throughout my studies.

Thank-you.

Table of Contents

ABSTRACT	II
ACKNOWLEDGEMENTS	III
TABLE OF CONTENTS	IV
LIST OF FIGURES AND TABLES	IX
ABBREVIATIONS.....	XI
1 GENERAL INTRODUCTION	1
1.1 AN INTRODUCTION TO ASTHMA.....	2
1.1.1 <i>Clinical Presentation</i>	2
1.1.2 <i>Diagnosis</i>	2
1.1.3 <i>Treatment</i>	3
1.1.4 <i>Phenotypes</i>	4
1.2 GASTRO-OESOPHAGEAL REFLUX	5
1.2.1 <i>Clinical Presentation</i>	6
1.2.2 <i>Diagnosis</i>	7
1.2.3 <i>Treatment</i>	7
1.3 THE REFLUX ASTHMA ASSOCIATION	8
1.3.1 <i>Acid</i>	10
1.3.2 <i>Enzymes</i>	11
1.3.3 <i>Bacteria</i>	12
1.3.4 <i>Food Matter</i>	12
1.4 THE ORIGIN OF THE MACROPHAGE.....	15
1.4.1 <i>Haematopoietic Stem Cells</i>	15
1.4.2 <i>Haematopoiesis in the Bone Marrow</i>	16
1.4.3 <i>Major Cytokines and Growth Factors of Myelopoiesis</i>	16
1.4.3.1 M-CSF.....	17
1.4.3.2 GM-CSF	19
1.4.3.3 G-CSF.....	19
1.4.3.4 IL-3	20
1.4.4 <i>Adhesion and Molecular Interaction in the BM</i>	20
1.4.5 <i>Functional Development of Macrophage Precursors</i>	21
1.4.6 <i>Monocyte Extravasation and Migration to the Alveoli</i>	22

1.5	MACROPHAGE ACTIVATION AND POLARISATION	24
1.5.1	<i>Classical Activation</i>	26
1.5.2	<i>Alternative Activation</i>	26
1.6	LIPIDS AND THE MACROPHAGE	28
1.7	INVESTIGATIONAL AIMS AND HYPOTHESES	29
2	GENERAL METHODS	30
2.1	CELL CULTURE AND MAINTENANCE	31
2.1.1	<i>THP-1 Cells</i>	31
2.1.2	<i>Daisy Cells</i>	31
2.1.3	<i>A549 Cells</i>	32
2.2	CELL VIABILITY AND COUNTING	33
2.3	THP-1 DIFFERENTIATION WITH PHORBOL 12-MYRISTATE 13-ACETATE (PMA)	33
2.4	TRANSMISSION ELECTRON MICROSCOPY (TEM)	33
2.5	LIPID TREATMENT	34
2.6	OIL RED O STAINING (ORO)	34
2.7	LIPID INDEX	35
2.8	FLUOROCHROME LABELLED OPSONISED ANTIGEN (BxB100)	35
2.9	OPSONISED ANTIGEN BINDING ASSESSMENT	35
2.10	CELL SURFACE FLOW CYTOMETRY	36
2.11	PREPARATION OF CYTOSPIN SLIDES	37
2.12	CELL DIFFERENTIAL STAINING	37
2.13	ASSESSMENT OF PHAGOCYTOSIS	39
2.14	HEAT AGGREGATION OF HUMAN IGG	39
2.15	PRIMARY CELL ISOLATION	39
2.16	GENE MICROARRAY	40
3	DEVELOPMENT OF AN <i>IN VITRO</i> MODEL OF GASTRO-OESOPHAGEAL REFLUX	42
3.1	INTRODUCTION	43
3.2	METHODS	44
3.2.1	<i>THP-1 Differentiation with PMA</i>	44
3.2.2	<i>Lipid Uptake Optimisation</i>	44
3.2.3	<i>Verification of Lipid Origin</i>	45
3.2.4	<i>Lipid ORO Staining Variability</i>	45
3.3	RESULTS	47

3.3.1	<i>THP-1 Differentiation with PMA</i>	47
3.3.2	<i>Lipid Uptake Optimisation</i>	47
3.3.3	<i>Verification of Lipid Origin</i>	51
3.3.4	<i>Lipid Staining Variability</i>	52
3.4	DISCUSSION.....	55
4	CHARACTERISATION OF A NEW HUMAN MACROPHAGE CELL LINE (DAISY)	57
4.1	INTRODUCTION.....	58
4.2	METHODS	59
4.2.1	<i>Light Microscopy</i>	59
4.2.2	<i>Mycoplasma Screen by Fluorescent Microscopy</i>	59
4.2.3	<i>Mycoplasma Screen by Colorimetric Assay</i>	59
4.2.4	<i>TEM</i>	60
4.2.5	<i>Assessment of Phagocytic Ability</i>	60
4.2.6	<i>Assessment of Lipid Uptake</i>	61
4.2.7	<i>Assessment of Opsonised Antigen Binding</i>	61
4.2.8	<i>Cell Surface Immunophenotype</i>	61
4.2.9	<i>Gene Microarray</i>	62
4.3	RESULTS.....	63
4.3.1	<i>Morphology of Daisy versus THP-1 cells by Light Microscopy</i>	63
4.3.2	<i>Mycoplasma Screening</i>	64
4.3.3	<i>Morphology of Daisy versus PMA/THP-1 cells by TEM</i>	65
4.3.4	<i>Assessment of phagocytosis</i>	67
4.3.5	<i>Assessment of lipid uptake</i>	69
4.3.6	<i>Opsonised Antigen Binding Capacity</i>	69
4.3.7	<i>Cell Surface Immunophenotype</i>	71
4.3.8	<i>Gene Microarray Data Analysis</i>	73
4.4	DISCUSSION	76
5	LIPID LADEN MACROPHAGES IN RESPIRATORY DISEASE	80
5.1	INTRODUCTION.....	81
5.2	METHODS	82
5.2.1	<i>Patient Recruitment</i>	82
5.2.2	<i>Lipid Staining and Indexing</i>	82
5.2.3	<i>Statistical Analysis</i>	82

5.3	RESULTS.....	85
5.3.1	<i>Primary Cell Isolation</i>	85
5.3.2	<i>Lipid Scoring of Patient BAL Samples</i>	85
5.3.3	<i>Statistical Analysis</i>	87
5.4	DISCUSSION.....	91
6	MACROPHAGE LIPID ACCUMULATION IN VITRO	93
6.1	INTRODUCTION.....	94
6.2	METHODS	96
6.2.1	<i>Induction and Detection of Apoptosis in Epithelial Cells</i>	96
6.2.2	<i>Isolation of Washed Platelets</i>	96
6.2.3	<i>Macrophage Lipid Accumulation</i>	96
6.2.4	<i>Actin-dependant Phagocytosis Inhibition</i>	97
6.2.5	<i>Blocking Lipid Accumulation</i>	97
6.2.6	<i>TEM of Intra-cellular Lipid Droplets</i>	97
6.2.7	<i>Gene Microarray</i>	98
6.3	RESULTS.....	99
6.3.1	<i>Apoptosis Induction</i>	99
6.3.2	<i>Macrophage Lipid Accumulation</i>	101
6.3.3	<i>Blocking Lipid Accumulation</i>	104
6.3.4	<i>TEM Visualisation of Lipid Droplets</i>	107
6.3.5	<i>Gene Microarray Data Analysis</i>	107
6.4	DISCUSSION	110
7	HUMAN MACROPHAGE ACTIVATION AND POLARISATION	114
7.1	INTRODUCTION.....	115
7.2	METHODS	117
7.2.1	<i>Cell line treatments</i>	117
7.2.2	<i>Enzyme-linked Immunosorbent Assay (ELISA)</i>	117
7.2.3	<i>Statistical Analysis</i>	118
7.3	RESULTS.....	119
7.3.1	<i>Immunophenotype of Polarised and Lipid Laden Macrophages</i>	119
7.3.2	<i>Comparison of Human IgG versus M-CSF treatment</i>	123
7.3.3	<i>Primary Human Alveolar Macrophages</i>	126
7.3.4	<i>ELISA Cytokine Analysis</i>	128

7.4	DISCUSSION	133
8	GENERAL CONCLUSIONS	139
9	BIBLIOGRAPHY	147
10	APPENDIX	156

List of Figures and Tables

<i>Figure 1.1 – Asthma Diagnosis Pathway</i>	4
<i>Figure 1.2 – Simplified Anatomy and Physiology of GOR</i>	6
<i>Figure 1.3 – Hematopoietic Differentiation Lineage</i>	18
<i>Figure 1.4 – Monocyte/Macrophage Migration</i>	25
<i>Figure 1.5 – Classical versus Alternative Activation of the Macrophage</i>	27
<i>Table 2.1 – Lipid Scoring of Alveolar Macrophages</i>	35
<i>Table 2.2 – Antibodies used in immunophenotyping studies</i>	38
<i>Figure 2.1 - Cytospin apparatus assembly.</i>	38
<i>Figure 3.1 – PMA treatment optimization of THP-1 cells.</i>	48
<i>Figure 3.2 – Lipid Uptake Concentration Assay</i>	49
<i>Figure 3.3 –Lipid Uptake Incubation Time Assay</i>	50
<i>Figure 3.4 – Lipid uptake verification</i>	51
<i>Figure 3.5 – Lipid staining inter-well variability</i>	53
<i>Figure 3.6 – Lipid staining inter-plate variability</i>	54
<i>Figure 4.1 – Morphology of Daisy cells by light microscopy</i>	63
<i>Figure 4.2 – Mycoplasma testing of Daisy cells by fluorescence microscopy</i>	64
<i>Figure 4.3 - Mycoplasma testing of Daisy and THP-1 cells by colorimetric micro-plate assay</i>	65
<i>Figure 4.4 – Morphology of Daisy cells by transmission electron microscopy</i>	66
<i>Figure 4.5 – Assessment of Phagocytic capability of THP-1 and Daisy cells</i>	68
<i>Figure 4.6 – Assessment of lipid uptake of THP-1 and Daisy cells</i>	70
<i>Figure 4.7 - Opsonised antigen binding capacity</i>	71
<i>Figure 4.8 – Cell surface immunophenotype</i>	72
<i>Figure 4.9 – Gene array analysis comparing PMA/THP-1 cells with THP-1 cells</i>	74
<i>Figure 4.10 – Gene array analysis comparing THP-1 cells with Daisy cells</i>	74
<i>Figure 4.11 – Gene array analysis comparing PMA/THP-1 cells with Daisy cells</i>	75
<i>Figure 5.1 – Hull Airway Reflux Questionnaire</i>	84
<i>Figure 5.2 – Cellular composition of BAL samples.</i>	86
<i>Figure 5.3 – Primary Alveolar Macrophages Stained with Oil Red O and Hematoxylin.</i>	86
<i>Table 5.1 – Patient Data</i>	88
<i>Figure 5.4 – Correlation between HARQ scores and age.</i>	89
<i>Figure 5.5 – Gender distribution of patients with GOR diagnosis.</i>	89
<i>Figure 5.6 – Correlation between LLAMI and HARQ scores.</i>	90
<i>Figure 5.7 – Comparison of means between LLAMI and GOR diagnosis.</i>	90

<i>Figure 6.1 – Induction of apoptosis in A549 cells</i>	100
<i>Figure 6.2 – Lipid staining in platelets and A549 cells</i>	102
<i>Figure 6.3 – Macrophage Lipid Accumulation</i>	103
<i>Figure 6.4 – Inhibition of Phagocytosis</i>	105
<i>Figure 6.5 – Inhibition of Lipid Uptake</i>	106
<i>Figure 6.6 – TEM Visualisation of Lipid Droplets</i>	108
<i>Figure 6.7 – Gene array analysis comparing Calogen Treated PMA/THP-1 Cells Compared with PMA only Treated THP-1 Cells</i>	109
<i>Figure 6.8 – Gene array analysis comparing Calogen Treated Daisy Cells Compared with Untreated Daisy Cells</i>	109
<i>Table 7.1 – Specific Elisa Reagents</i>	118
<i>Figure 7.1 – THP-1 cell immunophenotype</i>	121
<i>Figure 7.2 – THP-1 cell immunophenotype</i>	122
<i>Figure 7.3 – THP-1 cell immunophenotype comparision after IgG and M-CSF treatment</i>	124
<i>Figure 7.4 – THP-1 cell immunophenotype comparision after IgG and M-CSF treatment</i>	125
<i>Figure 7.5 – Primary alveolar macrophage immunophenotype</i>	127
<i>Figure 7.6 - IL-4 secretion by THP-1 cells.</i>	129
<i>Figure 7.7 - IL-4 secretion by THP-1 cells.</i>	129
<i>Figure 7.8 - IL-8 secretion by THP-1 cells.</i>	130
<i>Figure 7.9 - IL-4 secretion by THP-1 cells.</i>	130
<i>Figure 7.10 – IL-12 ELISA standard curve</i>	131
<i>Figure 7.11 – β-NGF ELISA standard curve</i>	132
<i>Figure 10.1 – Calogen Nutritional Information</i>	157
<i>Figure 10.2 – Fortijuice Nutritional Information</i>	158
<i>Table 10.1-Gene array data from Calogen treated PMA/THP-1 cells compared with PMA/THP-1 cells.</i>	159
<i>Table 10.2-Gene array data from Calogen treated Daisy cells compared with untreated Daisy cells.</i>	160

Abbreviations

ACD	acid-citrate dextrose
AM	alveolar macrophage
BAL	broncho-alveolar lavage
BM	bone marrow
BMI	body mass index
BSA	bovine serum albumin
BXB100	opsonised BSA at a working concentration of 100 ng/ml
CD(No.)	cluster of differentiation
D _{LCO}	carbon monoxide diffusing capacity of the lung
EBC	exhaled breath condensate
ECM	extra-cellular matrix
Fab	antigen binding fragment
FBS	foetal bovine serum
Fe _{NO}	fractional exhaled nitric oxide
FEV ₁	forced expiratory flow in 1 minute
FcγRI	fragment constant gamma receptor 1
FcγRII	fragment constant gamma receptor 2
FcγRIII	fragment constant gamma receptor 3
FcεRIII	fragment constant epsilon receptor 2
FITC	fluorescein isothiocyanate
G-CSF	granulocyte colony stimulating factor
GM-CSF	granulocyte/macrophage colony stimulating factor
GOR	gastro-oesophageal reflux
H ₂ O ₂	hydrogen peroxide
Hb	haemoglobin
HLA-DR	human leukocyte antigen class DR
HSC	haematopoietic stem cell
ICAM-1	immune cell adhesion molecule 1

IFN γ	interferon gamma
IL-(No.)	interleukin (No.)
LDL	low density lipoproteins
LLAMI	lipid laden alveolar macrophage index
LOS	lower oesophageal sphincter
LPS	lipopolysaccharide
M1	classically activated macrophage
M2	alternatively activated macrophage
MCP-1	macrophage chemo-attractant protein 1
M-CSF	macrophage colony stimulating factor
MHC	major histocompatibility complex
mRNA	messenger ribose nucleic acid
NGF	nerve growth factor
ORO	oil red o
oxLDL	oxidized low density lipoprotein
PBS	phosphate buffered saline
PECAM-1	platelet endothelial cell adhesion molecule
PEF	peak expiratory flow
PMA	phorbol 12-myristate 13-acetate
PS	penicillin/streptomycin
RT	room temperature
SCF	stem cell factor
T _c	cytotoxic T-cell
TCR	T-cell receptor
TEM	transmission electron microscopy
T _H	T helper cell
T _H -1	type 1 T helper cell
T _H -2	type 2 T helper cell
THP-1	human derived immortal monocytic cells

TMB	3,3' 5,5' tetramethylbenzidine
TNF α	tumour necrosis factor alpha
TNF β	tumour necrosis factor beta
VCAM-1	vascular cell adhesion molecule 1
VLA-4/5/6	very late antigen 4, 5 or 6

1 General Introduction

1.1 An Introduction to Asthma

Asthma is a disease of the airways characterised by chronic inflammation, airway hyper-responsiveness and variable, usually reversible, airflow obstruction (Chung and Adcock, 2000, Levy and Pierce, 2005, Rees, 2000). Around 300 million people have asthma, making it one of the most common chronic diseases worldwide (Levy and Pierce, 2005, Chung and Adcock, 2000, Busse, 2011) and one of the three most common causes of chronic cough (Morice and Bush, 2003a). It is estimated that 5.4 million people, or 1 in 12 adults, in the UK are currently receiving treatment for asthma (AsthmaUK, 2010) and that an asthma related death occurs every 7 hours. Caring for asthmatics costs the NHS in the region of £1 billion every year and with an average of 12.7 million lost work days per year due to asthma, the socio-economic cost is much greater.

1.1.1 Clinical Presentation

Asthma presentation is variable amongst patients and can range from mild intermittent wheezing or cough to severe episodes of airway obstruction requiring treatment and/or hospitalisation (Chung and Adcock, 2000). Triggers of an asthmatic exacerbation or 'attack' can also vary greatly among patients. Inhalation of specific allergens such as pollens (May et al., 2011), chemicals, dust and animal fur may exacerbate asthma. Ingestion of alcohol (Vally et al., 2000) and certain medications, such as aspirin, may also trigger an attack whilst respiratory infections (Micillo et al., 2000) and environmental stimuli, such as cold air inhalation (May et al., 2011), are also common triggers. Stress has also been recognised to exacerbate asthma (Chen and Miller, 2007) and where possible specific triggers should be identified and avoided in order to preserve the lung function of the asthmatic.

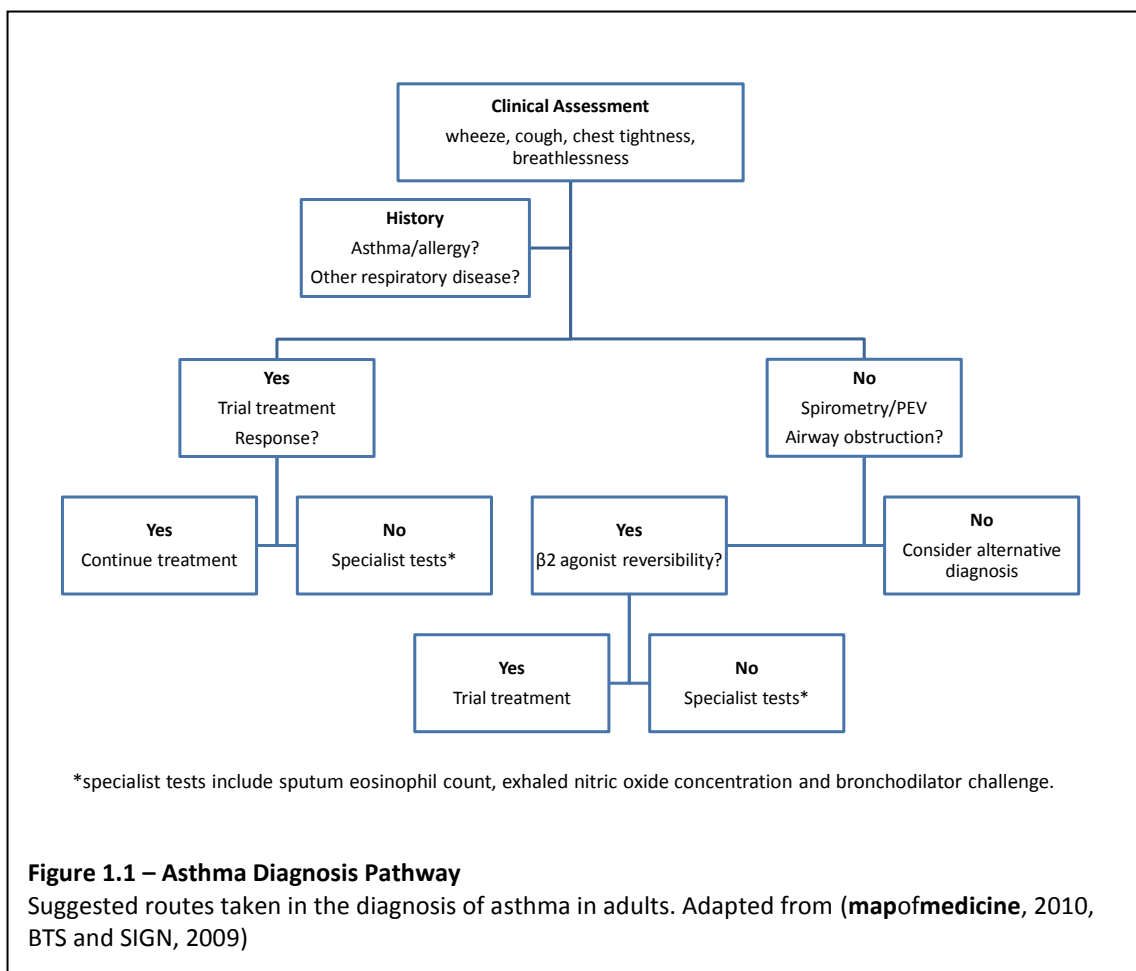
1.1.2 Diagnosis

Diagnosis can be difficult due to a varied understanding of the disease

(Morice and Bush, 2003a) between medical practitioners, the degree of reversibility of airflow obstruction in patients and other complicating respiratory conditions. It is therefore important to take a detailed history during consultation. Current guidelines issued by the British Thoracic Society and Scottish Intercollegiate Guidelines Network (BTS and SIGN, 2009) advise a highly probable asthma diagnosis if the patient describes 2 or more symptoms, i.e. wheeze, breathlessness, chest tightness or cough, and has an unexplained peripheral blood eosinophilia or an unexplained variable peak expiratory flow (PEF)/forced expiratory volume in 1 min. (FEV₁) with increasing probability if a family history of asthma and/or allergy is evident. When these diagnostic criteria are met, a trial of treatment may be initiated. However, if diagnosis is uncertain or a patient fails to respond to initial treatment, specialist referral and further testing should be carried out. Variable airflow obstruction should be confirmed with serial PEF measurements taken over a 2 week period. Preferentially, spirometry tests should be carried out where equipment is available. If obstruction is present and reversible with β_2 agonist inhalation, the diagnosis should be asthma. Where reversibility is absent, further testing should be carried out, although asthma may still be diagnosed. In practice, however, where a physician suspects asthma, trial treatments precede specialist tests and a positive response can be viewed as diagnosis confirmation. A diagram of the current diagnostic guidelines is depicted in *figure 1.1*.

1.1.3 Treatment

Treatment of asthma is as variable as the disease presentation between patients therefore treatment trials are usually necessary to determine the combination of therapy best suited to the patient. In mild asthmatics, treatment with short acting β_2 agonists when symptomatic may be sufficient. However, when asthma becomes more severe preventative measures may be taken. Inhaled corticosteroids are considered the most effective preventative treatment, but in more severe asthmatics, may be complemented with other preventative treatments. Long acting β_2 agonists and leukotriene receptor agonists can be used in this manner. Treatment regimes may be



reviewed regularly until an optimum balance is reached, where minimal pharmacological intervention achieves maximal lung function and minimal interference with the patient’s quality of life.

1.1.4 Phenotypes

Once a diagnosis of asthma has been made, patients can be categorised according to presentation and disease characteristics. This enables physicians to predict the clinical course of the individual patients’ disease progress based on previously treated asthma cases with similar characteristics. The two predominant phenotype categories are allergic and non-allergic asthma (Levy and Pierce, 2005) in which patients can be divided by the presence or absence of atopy, an elevated level of serum IgE levels associated with a pre-disposition to allergic diseases. Patients with atopy may

have a history of rhinitis, eczema, psoriasis, food allergies etc., alone or in combination and this is likely to be echoed in the family history. Asthma patients can be further sub-categorised by the age at which they first present with asthma, i.e. childhood or adulthood (Rees, 2000). Childhood asthma is difficult to diagnose before the age of 3 due to the infant respiratory tract being less rigid, allowing for frequent alveolar collapse and blockage, therefore coughs and wheezes which are not associated with asthma (Morice and Bush, 2003b). Childhood asthma is also likely to subside by early teenage years however asthma developed in later life is less transient. Further sub-categories used by physicians can reflect the exacerbation trigger such as aspirin induced, exercise induced, cold air induced asthma or less specifically, occupational asthma. Patients' symptoms will inevitably span more than one phenotype.

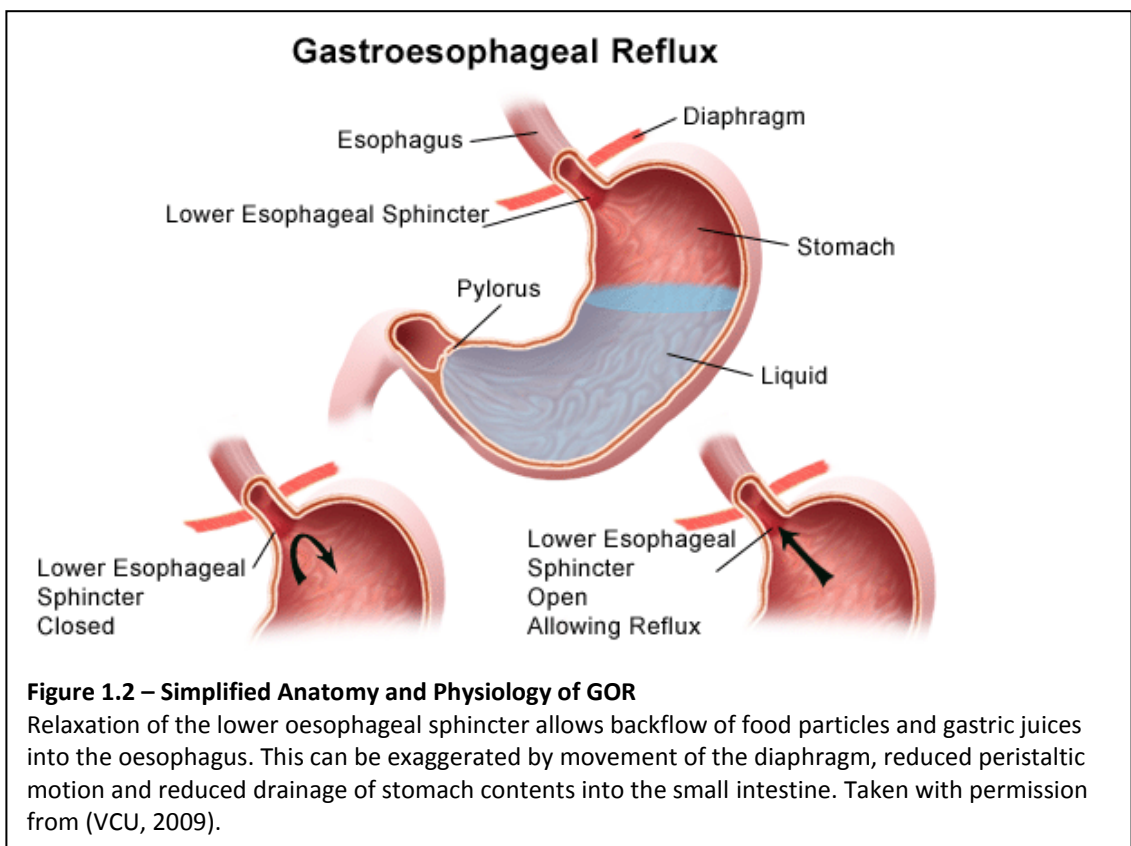
A further category termed severe or difficult asthma accounts for around 10-20% of all asthmatics (Busse, 2011, Wenzel, 2011). This represents patients who have low base-line lung function and experience almost daily symptoms and frequent exacerbations despite high dose treatment. Patients in this category often have underlying gastro-oesophageal reflux (GOR), described in 1.2, a phenomenon which is widely observed and published yet currently unexplained and are the focus of this study.

1.2 Gastro-Oesophageal Reflux

Along with Asthma, GOR is one of the most common causes of chronic cough (Everett and Morice, 2004) and aspiration of gastric contents (liquid or gaseous) into the airway is considered the primary cause (Shashkin et al., 2005). There are a number of factors which facilitate reflux such as hiatal hernia, loss of pressure at the lower oesophageal sphincter (LOS), gastric paresis and blockage of the lower gastric tract by ulcer or scar tissue (Janowitz, 1994). Impairment of normal peristalsis in both the oesophagus and intestine can also cause reflux. A diagrammatical representation of the anatomy and mechanism involved in GOR can be seen in *figure 1.2*.

1.2.1 Clinical Presentation

Reflux events are episodic occurring on average 44 times in 24 hours (Muller et al., 1999) in patients with GOR. Obvious symptoms such as heartburn may be a good indication of the disease where backflow of acidic fluid into the lower oesophagus causes pain and a burning sensation in the sternum (Janowitz, 1994). However where gaseous material is the refluxate, cough may be the only presenting feature. Therefore a detailed history taking is crucial in the diagnosis of GOR. Relaxation of the LOS is usually associated with GOR (Patti and Waxman, 2010), closing when the patient is in the supine position and so relieving symptoms of cough during sleep only to return when the patient rises. Cough in the 3 hours post-meal is also indicative and, unlike heartburn, is triggered by certain foods, even though stomach acid is neutralised by food. Relaxation of the diaphragm during speech causes loss of LOS tone below the hiatus and cough during telephone conversations or laughing is



common. Aspirated gastric contents may reach the larynx, causing a hoarse voice and sore throat, or travel further up the respiratory tract to present as a 'funny taste' (Morice and Bush, 2003a).

1.2.2 Diagnosis

Diagnosis of acid reflux can be made by investigative procedures such as 24 hour oesophageal pH monitoring with a cough diary, barium meal studies and endoscopic visualisation of the oesophagus. When patients present with frequent heartburn, caused by the retrospective flow of acidic fluid from the stomach, the patient is at risk from oesophagitis, aspiration and cancer. In such patients these methods are necessary for diagnosis, however expensive and uncomfortable for the patient they may be. Non-acid reflux is more difficult, as there are no current diagnostic tests available. It is these patients that can present with little more than a chronic cough and can advance into symptoms of an asthma-like state, if left untreated. If a diagnosis looks likely from the clinical history then the clinician may opt to begin trial pharmacological therapy and a positive response may be seen as a diagnosis. It is vitally important that a diagnostic tool for this type of reflux is developed.

1.2.3 Treatment

Non-pharmacological intervention may be beneficial, such as smoking cessation, dietary modifications and weight loss. Pharmacological treatment consists initially of a trial of proton pump inhibitors, such as Lansoprazole, or H₂ receptor antagonists, such as Ranitidine, however excess acid production may not be the cause of cough and so increasing the pH of the reflux material in this manner may not be beneficial. A second wave of therapy may then be adopted to assist passage of food matter through the gastrointestinal tract and facilitate stomach drainage. Bethanechol, a cholinergic agent can increase LOS pressure whilst Cisapride can facilitate bolus motility by stimulating acetylcholine release and therefore peristalsis along the gastric

tract (Galloway, 1993). In cases where cough persists after prolonged pharmacological trials or recurrent aspiration into the airway is present, surgical fundoplication may be the best option. Guidelines as to the appropriate procedure are detailed by Stefanidis *et al* (2010).

The effectiveness of surgery in the resolution of typical acid reflux symptoms such as heartburn and regurgitation are undisputed. Short term outcomes following surgery seem positive also when focussing on symptoms of cough, with one study reporting 82% complete or partial improvement of cough, 6 months post-fundoplication (Allen and Anvari, 1998). However, long term outcomes on cough post-surgery are less impressive. One study investigating the effectiveness of Nissen fundoplication in 90 patients referred to the same surgeon after no or only partial improvement was seen post pharmacological intervention (Chen and Thomas, 2000). At 12-46 month follow up, 93% of patients reported complete abolition of the typical reflux symptom of heartburn. However 46% of patients had concurrent atypical symptoms of which 17% reported cough, pre-surgery. Of these only 13% reported complete abolition of symptoms post-surgery and 46% reported no change whatsoever. A similar study performed retrospectively at Hulls very own specialist NHS cough clinic was performed on all patients referred for surgery following non-response to reflux therapy for chronic cough (Faruqi *et al.*, 2012). Of the 47 patients that underwent fundoplication, 85% complained of typical gastric symptoms of heartburn, dyspepsia and/or indigestion concurrent to the presenting chronic cough. A complete response shortly after surgery was reported in 45% of patients and partial response in 19%. However at a mean follow up of 3.8 years, 41% of patients remained symptomatic. A further study reported 49.5% non-resolution of cough at a mean follow up of 27.4 months (Brown *et al.*, 2011).

1.3 The Reflux Asthma Association

GOR has long been associated with asthma, in particular which is difficult to treat. Recent prevalence studies have shown that around 50% of adults and children

with difficult to treat asthma also have GOR and this figure may be higher in adults alone (Mathew et al., 2004). It is of no surprise that such problems arise involving both the digestive and respiratory tract given our unique anatomical position. As evolution has served to progress man's ability to move on two legs, thus freeing the hands for other possibly more useful acts, the angle at which the oesophagus joins the stomach has altered to our disadvantage. Food descends directly down the oesophagus into the stomach, travelling through the thorax under low pressure and into the abdomen, where pressure is increased (Pacheco-Galvan et al., 2011). This unfortunate anatomy allows for less resistance to backflow of ingested material and a tendency for reflux. Perhaps unsurprisingly, an association between asthma and obesity has been increasing recently. One study, using a large cohort of non-smoking, difficult-to-treat asthmatic adults, demonstrated that GOR was present in a significantly greater number of patients with a body mass index (BMI) >30 (van Veen et al., 2008). In addition, it was found that BMI inversely correlated with sputum eosinophils and fractional exhaled nitric oxide (FeNO) indicating that eosinophilia was not a contributing factor in mechanisms linking obesity, GOR and asthma. A further study showed sputum neutrophils to be significantly increased in obese asthmatics versus both non-obese asthmatic and non-obese non-asthmatic subjects, whereas eosinophils were significantly increased only in obese asthmatics versus non-obese control subjects (Scott et al., 2011). Further to this finding, serum free fatty acid levels negatively correlated with sputum neutrophils in males alone whilst BMI positively correlated with neutrophils most significantly in females alone. The latter statement being in agreement with the former study, given that the study cohort consisted largely of females (~70%). Could the differing effects of obesity between sex be a result of adipose tissue distribution, being predominantly abdominal in females and potentiating reflux by increasing the thoracic/abdominal pressure gradient? Studies of this nature are scarce at present, and the association between GOR, asthma and obesity warrants thorough investigation.

The acquired ability to speak has also proven detrimental to human

health in that the descent of the larynx during early infancy interferes with the protective mechanism of the laryngeal sphincter and promotes aspiration (Pacheco-Galvan et al., 2011). Whilst many of us are familiar with the symptoms of acid reflux, during which backflow of liquid stomach contents produce a burning sensation, the phenomenon of non-acid or silent reflux is less known. Around half of patients with GOR experience solely liquid reflux which in 70% of cases can reach the proximal oesophagus. The other half of GOR patients will experience a mixture of liquid and gas reflux which increases the frequency of proximal oesophageal irritation to 92% (Pacheco-Galvan et al., 2011). In such cases where gaseous refluxate is present, ascent of such stomach contents into the upper airways, the throat and beyond, is feasible and aspiration into the lungs themselves is likely.

1.3.1 Acid

The damaging effects of such aspiration reach far beyond the obvious acid insult although this is not insignificant. A unique study measuring lung pH directly with indicator paper during routine bronchoscopy showed that patients with GOR had a significantly lower lung pH than controls at pH 5.13 and pH 6.08 respectively (Mise et al., 2010). Whilst the stomach and to a certain extent, the oesophagus have protective mechanisms in place to withstand acidic material, the airways do not and so, whilst many people experience reflux to a tolerable degree, some patients with more severe reflux and aspiration exhibit debilitating, sometimes fatal respiratory symptoms. Ironically, this is something I recently experienced myself. The severity of reflux/aspiration is evidenced in a study reporting that 79% of patients with recurrent acute lung injury have GOR concurrently in comparison with 26% of patients with single episode acute lung injury and 49% of controls (Bice et al., 2011). Interestingly, patients with cystic fibrosis have been shown to have a significantly reduced exhaled breath condensate (EBC) pH which is further reduced during exacerbation (Khlusov et al., 2005). Indeed, exercise also appears to be a contributing factor to acid induced respiratory symptoms with a study showing that of 20 asthmatic and 11 non-asthmatic

subjects, 79% were found to have abnormal oesophageal pH readings during half hour periods of exercise (Peterson et al., 2009). Studies of both mice and man have shown that inhalation of acidic vapour caused increased airway sensitivity to methacholine, neutrophilia, increased protein levels, increased tissue permeability and increased lactate dehydrogenase in EBC suggesting acid aspiration causes cell, probably epithelial, damage (Shimizu et al., 2007, Allen et al., 2009, Barbas et al., 2008). Whilst these studies have shown treatment of excess stomach acid with proton pump inhibitors to significantly reduce respiratory symptoms (Luthy et al., 2008) in addition to reducing pH and oxidative stress marker 8-isoprostane in EBC (Shimizu et al., 2007), others have shown this not to be the case owing to the cohort inclusion of patients with non-acid reflux (Asano and Suzuki, 2009).

1.3.2 Enzymes

Indeed, reflux material may well be acidic; however post meal material is less so and acid is not the only damaging ingredient. The protease enzyme pepsin present in the stomach and required for the breakdown of ingested protein, has been shown to be cytotoxic to human bronchial epithelial cells when active at pH 2 (Bathoorn et al., 2011). Pepsin was shown to be present in increased levels in children with cystic fibrosis and of the children with higher pepsin levels, so too was IL-8 concentration (McNally et al., 2011). This did not, however, correlate with lung function, suggesting the possibility that pepsin alone *in vivo* may not be the pathological entity. Perhaps an altered airway pH is required to activate pepsin to become detrimental? This certainly seems to be the current view (Bardhan et al., 2012). In addition to pepsin, matrix metalloprotease-9, a type IV collagen degrading enzyme produced by macrophages, has been found to be up-regulated in a mouse macrophage cell line when treated with gastric fluid for 24 hours (Cheng et al., 2010). Activation of the macrophages by gastric fluid was observed at relatively low concentrations (1/1000 dilution) to be toll-like receptor-4 dependant, a mechanism shared by bacterial activation, which was detected by tumour necrosis factor alpha

(TNF α) production. This finding suggests an interesting role of macrophages in aspiration induced airway remodelling.

1.3.3 Bacteria

Whilst many reviews have suggested bacterial load as a source of reflux mediated airways disease, few studies have investigated the prevalence of gastric flora colonising the lungs. One such study however has shown the bacteria *Helicobacter pylori* CagA+ to be significantly increased in the airways of patients with GOR (Batool et al., 2011). A second study also showed that human tracheal epithelial cells exposed to acid showed significantly increased binding of the bacteria *Streptococcus pneumoniae* in a pH and time dependent manner (Ishizuka et al., 2001). Maximal binding was seen following exposure to pH 2.5 for 5 hours although similar results were observed with exposure to pH 1.5 for just 1 hour. This was significantly inhibited, though not abolished, by the platelet activating factor inhibitor Y-24180 under all conditions. One larger study of 150 children with GOR showed that whilst airway cultures were positive for one or more of *Streptococcus pneumoniae*, *Haemophilus influenza*, *Moraxella catarrhalis* and *Staphylococcus aureus*, this was not reflective of gastric cultures (Chang et al., 2005). However, one of the study exclusion criteria was a clinical history of primary aspiration which may skew the data. Nevertheless further studies into the clinical prevalence and relevance of gastric microbial colonisation of the airways are required to establish its importance.

1.3.4 Food Matter

Aspiration of large particulate food matter will often result in particles becoming lodged in the large airways producing an unexplained cough. These cases can usually be resolved with radiological or bronchoscopic investigation and removal of the offending obstruction. When particulate matter is partially digested, however, identification can be more difficult. In humans, aspiration of partially digested plant material has been found to cause pathological lesions termed 'lentil pneumonia' only

uncovered at autopsy (Morehead, 2009). A neutrophilic infiltration has been observed in rodent models 4-6 hours post aspiration of either acid or small non-acidified gastric particles. When the two insults were combined, this neutrophilia was sustained for 48 hours post aspiration, and coupled with reduced arterial oxygenation levels in concordance with diagnostic values of acute respiratory distress syndrome (Raghavendran et al., 2011, Jaoude et al., 2010). The true pathogenesis of all components of homogenised meals have yet to be investigated; however one area in particular has become of interest.

Homogenised lipids may also be present in refluxate and can be detected in the airways indefinitely following ingestion by alveolar macrophages using established lipid staining techniques (Midulla et al., 1998). Studies regarding the use of such techniques as a reliable diagnostic tool of reflux and aspiration have been extensive. Using the lipid laden alveolar macrophage index (LLAMI) scoring system first described by Colombo and Hallberg (1987) to quantify the levels of macrophage ingested lipids in the airways, findings have so far been somewhat inconclusive. In this method, alveolar macrophages are obtained by sequential instillation of physiological saline solution during bronchoscopy and the aspirated fluid collected (broncho-alveolar lavage, BAL). Cells can then be isolated by centrifugation, mounted onto glass slides and stained before being scrutinised under light microscopy. This method is somewhat subjective, relying on the technical experience of the observer which may, in part, account for the inter-study variance.

One study reported that LLAMI was found to be significantly raised in BAL from children diagnosed with GOR, compared with children presenting recurrent pneumonia and healthy children (Ahrens et al., 1999). Another study reported that LLAMI was significantly raised in children with respiratory symptoms and this significance increased when analysing the group of cystic fibrosis patients (Kazachkov et al., 2001). In 448 6-month-old to 16-year-old patients with persistent wheeze, bronchitis or pneumonia, LLAMI was found not to correlate with oesophageal pH; however, the authors did not report the difference, if any, of LLAMI between GOR and

non- GOR patients (Kitz et al., 2012).

In adults diagnosed with aspiration (based on clinically witnessed aspiration, positive barium swallow or reflux oesophagitis) showing abnormal radiology, LLAMI greater than 100 was statistically found to be 94% sensitive and 89% specific at identifying aspiration with a 71% positive and 98% negative predictive value (Adams et al., 1997). A further study showed that LLAMI taken from induced sputum as opposed to BAL fluid was significantly raised in patients with abnormal oesophageal pH, which significantly correlated with the number of reflux events (Parameswaran et al., 2000). In addition, a LLAMI of above 7, considerably lower than other studies, had a 90% sensitivity and a 89% specificity for reflux with an 80% positive and a 95% negative predictive value.

In patients with laryngeal cleft, LLAMI was found to be significantly raised in type 2, where aspiration is likely, compared with type 1 clefts (Wenzel, 2011), although this was not significantly different between patients showing aspiration or non-aspiration by modified barium swallow techniques (Kieran et al., 2010) . In lung transplant recipients, LLAMI was found to be more effective at identifying silent micro-aspiration during acute graft dysfunction than oesophageal pH monitoring, with a sensitivity of 82.3% and a specificity of 76.4% (Busse, 2011). A similar study found the same sensitivity and specificity in a smaller cohort and that foreign material found in BAL fluid did not correlate with either LLAMI or oesophageal pH abnormality (Hopkins et al., 2010). In a separate study including a range of patients with differing pathologies including HIV and haematological disorders, LLAMI was found to be raised across the entire range of diseases compared to healthy control subjects; this was significantly higher in HIV patients in relation to opportunistic infection (Basset-Leobon et al., 2010).

Combined, these findings show an unquestionable presence of lipid laden macrophages in respiratory disease; however the diagnostic use of the LLAMI is still debatable. Undoubtedly, the varying reports have had differing patient inclusion/exclusion criteria, in addition to differing methods of GOR diagnosis. How, then, can studies using pH monitoring for example be compared with studies using

clinical history suggestive of GOR be compared? Until a reliable and reproducible method for the diagnosis of GOR can be established, studies of this nature cannot be concluded upon, yet the purpose of such studies is to establish exactly that. One thing which can be certain is that the macrophage is present in vast numbers in the airways and so the clinical relevance of lipid laden cells must be investigated.

1.4 The Origin of the Macrophage

Haematopoiesis, the production and maintenance of all blood and lymphatic cell compartments, is a complex and highly regulated process. Circulating blood cells have a limited lifespan and need to be continually replaced in order to maintain healthy populations. In addition to this, populations need to adapt in response to stresses such as infection, hypoxia or bleeding, in order to maintain the health of the individual. This requires a complicated, inducible and reversible expansion of particular populations of cells, up to 10 fold that of the normal population size. It is therefore not surprising that haematopoiesis, as a whole, is not yet fully understood. The macrophage itself, although ultimately residing in tissue, is also born of this process and shall be discussed here.

1.4.1 Haematopoietic Stem Cells

What is understood is that all blood cell populations, macrophages included, arise from a single multi-potent stem cell (Bender et al., 1987) first demonstrated by Till and McCulloch in 1961, when spleens of irradiated mice were repopulated with cells of all lineages arising from implanted haematopoietic cells. These cells, now known as haematopoietic stem cells (HSC), can be distinguished by their ability not just to differentiate and mature into cells of all lineages but also by their ability to self renew. HSC are themselves the progeny of embryonic toti-potent stem cells (Haig, 1992), and in adults reside in the red bone marrow (BM) found in the sternum, ribs, pelvis, vertebrae and skull (Harmening, 1997) therefore these are the areas in which haematopoiesis takes place. Phenotypically, in mice, these cells express

stem cell antigens (Sca-1 and c-kit) whilst remaining lineage unspecific (Lin^-). The same is thought to be true in the human haematopoietic system (Zhu and Emerson, 2002), which suggest HSC differentiation is influenced by the cells' environment.

1.4.2 Haematopoiesis in the Bone Marrow

Active adult BM contains approximately 1.3×10^{12} cells, weighing 2.6 kg and releasing 200 billion erythrocytes and 70 billion neutrophils into circulation each day (Gunsilius et al., 2001). BM is compartmentalised into vascular sinuses. In these areas blood vessels insert into the marrow and are surrounded by a layer of epithelial cells and the haematopoietic blood cell producing spaces or 'chords'. Here, the HSC can be found, making up 0.05-0.5 % of the cells within the BM (Gunsilius et al., 2001). Within the chord spaces, distinct areas of cell production can be found where colonies of cells of specific cell lineage are produced. Under normal circumstances colonies are surrounded in all dimensions by specialised bone marrow stromal cells comprising reticulum cells, histiocytes, fat cells, endothelial cells, osteoblasts and fibroblast-like cells (Orlovskaya et al., 2008) which not only provide structural support, but also trans-membrane ligands, extracellular matrix (ECM) components and soluble proteins (Krause, 2002, Harris et al., 1997). Together, these stromal cells form a specialised microenvironment which provides vital cell-cell interactions, cell-ECM interactions and soluble ligands known collectively as growth factors.

1.4.3 Major Cytokines and Growth Factors of Myelopoiesis

According to the current theory, HSC express low levels of surface receptors to a diverse range of growth factors and cytokines (Krause, 2002, Haig, 1992). This low level and non-lineage specific expression means that cellular differentiation can progress down any one of the cell lineages. For a schematic diagram of the various cell lineages refer to *figure 1.3*. The type, combination and concentration of cytokines/growth factors in the surrounding environment are crucial in determining the

fate of the HSC.

Cytokines are polypeptide molecules produced by cells that induce differentiation and/or provide activation signals, in either an autocrine or paracrine fashion via receptors (Haig, 1992). They are produced in low concentrations by activated cells and usually have a relatively short half life in circulation. Whilst many are secreted in a soluble form, membrane bound forms are also produced, highlighting a need for stem cells to be enclosed in their specific microenvironment in order for normal differentiation to take place. Cytokines and their functions are still being discovered; however some of the major cytokines known to be involved in myelopoiesis, the production of cells of myeloid origin as opposed to lymphoid origin, are discussed briefly here.

1.4.3.1 M-CSF

Macrophage colony stimulating factor (M-CSF) is readily produced by stromal cells in the BM in both soluble and membrane bound forms (Barreda et al., 2004). Other cells which express M-CSF include activated monocytes and lymphocytes, which indicate a role in induced haematopoiesis during crisis. The presence of M-CSF serves to stimulate proliferation, differentiation and survival of primitive cells of the monocyte/macrophage lineage and to activate monocytes and macrophages to stimulate production of other cytokines such as granulocyte colony stimulating factor (G-CSF), granulocyte/macrophage colony stimulating factor (GM-CSF), Interleukins 1, 6 and 8 (IL-1, IL-6, IL-8), TNF α and interferons. Expression is up

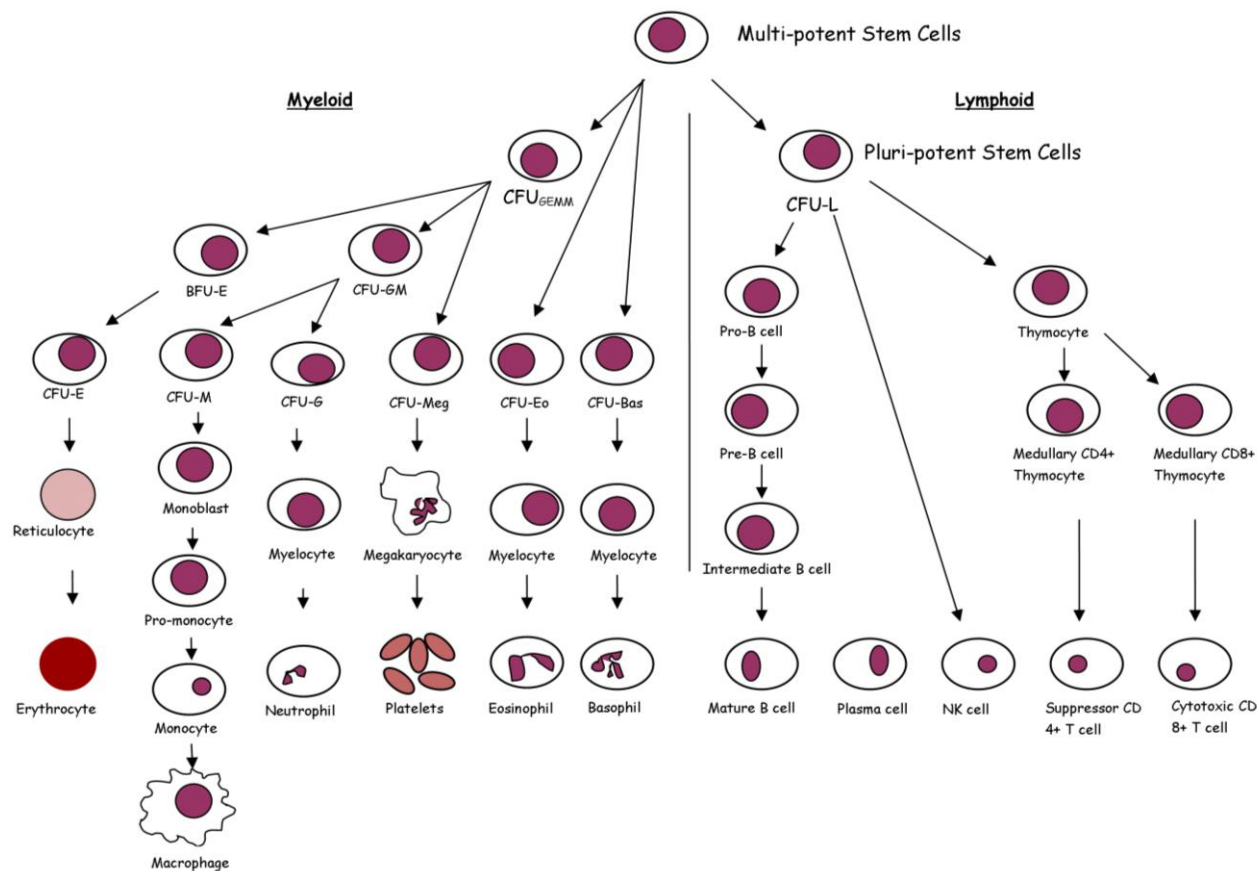


Figure 1.3 – Hematopoietic Differentiation Lineage

Cells of the immune system originate from a single self-renewing population of stem cells which reside in the bone marrow. Subsequent differentiation gives rise to colony-forming units (CFU) which have lymphocyte (L), erythrocyte (E), granulocyte (G), monocyte (M), megakaryocyte (Meg), eosinophil (Eo) and basophil (Bas) generating capacity but no longer have self-renewing ability. Adapted from (Howard and Hamilton, 2002, WebSpidersLimited, 2012b).

regulated by other cytokines such as GM-CSF, TNF α , interferon gamma (IFN γ) and IL-1.

Only cells which mature along the myeloid lineage express the corresponding receptor to M-CSF (CD115), which becomes expressed at increasing levels as the cells mature. M-CSF signalling is negatively regulated by binding of a c-Cbl molecule to the phosphokinase domain of the receptor which initiates internalisation, ubiquitination and degradation of the receptor. Also, signalling can be inhibited by molecules such as P56 (Barreda et al., 2004).

1.4.3.2 *GM-CSF*

Granulocyte macrophage colony stimulating factor (GM-CSF) is also produced by stromal cells in the bone marrow and by activated macrophages and lymphocytes. GM-CSF promotes proliferation and maturation of macrophages from their stem cell precursors in a dose dependant manner. At low concentrations, macrophage colony formation is stimulated and cells are protected from apoptosis, whilst at high concentrations, proliferation is stimulated (Barreda et al., 2004). GM-CSF also increases the biological activity of macrophages including antigen presentation, chemotaxis, enzyme synthesis, release of reactive oxygen species and phagocytosis. GM-CSF down regulates expression of the M-CSF receptor on macrophages and thus inhibits M-CSF induced growth.

The GM-CSF receptor (CD116) is expressed at low levels by CD34+ precursor cells and other cells, however as the precursor cells mature into granulocytes and monocytes, receptor expression increases whilst in other cell types receptor expression diminishes. In response to GM-CSF and inflammatory mediators, the alpha chain of the receptor is released in a soluble form to regulate the response by binding, thus “mopping up” circulating GM-CSF (Barreda et al., 2004).

1.4.3.3 *G-CSF*

Monocytes and macrophages are the main producers of granulocyte colony stimulating factor (G-CSF), which stimulates production of neutrophils but has

no effect on growth of monocytes. However, G-CSF in combination with IL-3 does stimulate growth of precursor cells and plays an important role in mobilising cells from the bone marrow to the peripheral blood. In addition, G-CSF down regulates inflammatory cytokine production by activated monocytes. The G-CSF receptor (CD114), although largely found on neutrophils, can also be found on monocytes and myeloid leukaemic cells (Barreda et al., 2004).

1.4.3.4 *IL-3*

IL-3 has one of the broadest target specificities of all the growth factors, promoting development of the earliest progenitor cells. It is largely produced by activated T-cells but can also be produced by stromal cells of the bone marrow. IL-3 alone is capable of supporting colony formation of multi-lineage, granulocyte/macrophage lineage amongst others.

The corresponding receptor (CD123) is found on early and more mature progenitor cells (although not on the most primitive stem cells) in addition to monocytes/macrophages, B-cells, and granulocytes (Barreda et al., 2004). IL3 is known to play a role in directing differentiation towards the myeloid lineage in synergy with stem cell factor (SCF), IL1, IL6, IL11, and G-CSF (Barreda et al., 2004) Once differentiated, the HSC becomes a pluri-potent stem cell committed to the myeloid lineage. This early differentiation from stem cell to progeny is undoubtedly irreversible, however the later stages of differentiation into mature cells is debated to be reversible (Haig, 1992).

1.4.4 Adhesion and Molecular Interaction in the BM

In order for effective haematopoiesis to take place, cell-cell interactions are required between the HSC, more committed haematopoietic cells, and stromal cells (Krause, 2002). This requires expression of binding molecules on both the stem and stromal cells, to allow transduction of signals and messages between cells. The signals are transmitted either via gap junctions or by ligand/receptor binding via jagged/notch,

which are both trans-membrane receptors (Krause, 2002). Upon binding of a ligand to a notch receptor, the internal portion of the receptor is cleaved and translocates to the nucleus where it interacts with cofactors to modify transcription of the DNA and thus protein production. In the absence of notch signalling, cells differentiate, therefore notch directs cells towards primitive precursor formation and inhibition of differentiation by mechanisms which are currently unknown (Krause, 2002).

In addition to cell-cell interactions, binding of stem cells to the ECM occurs within the bone marrow. The ECM is comprised of fibronectin, collagen and laminin, to which HSC bind and receives signals via integrins, Ig-like molecules, cadherins, selectins and mucins (Krause, 2002). The most well known of these are the integrins very late activation antigen 4 (VLA-4) and vascular cell adhesion molecule 1 (VCAM-1) on stromal cells. Loss of VLA-4 binding to fibronectin leads to cells exiting the bone marrow into the peripheral blood (Krause, 2002). The binding of cells to the ECM maintains cells in a quiescent (G_0) stage of the cell cycle (Krause, 2002), i.e. prevents both proliferation and apoptosis, thus maintaining a population of cells in 'stand-by' mode, capable of re-entering the cell cycle when required.

Cellular and molecular interaction within the BM microenvironment is crucial in determining cell fate and adhesion is critical. Recently however, a hypothesis has emerged that cells are not strictly bound in their individual niche and may travel to other sites within the BM via the bloodstream, based on findings of persistent populations of HSC in peripheral blood of healthy individuals (Wagers et al., 2002). This may well be proven to be the case, however, adhesion is still a necessity in either scenario and lack of adhesion molecule expression may contribute to impaired haematopoiesis.

1.4.5 Functional Development of Macrophage Precursors

As the monocytic lineage progresses, cells begin to show characteristics of the mature cell. Cells express IgG receptors from as early as the monoblast stage and are capable of phagocytosing IgG-coated red blood cells. The cells termed monoblasts

also express lysozyme and esterase enzymes, though only in small quantities. Production of peroxidase begins with differentiation of the monoblast into promonocytes which are now capable of phagocytosis of opsonised bacteria. Receptors to the complement proteins (CR1 and CR2) appear (Bender et al., 1987) by the monocyte stage and allows for phagocytosis of C3b coated antigens. As cell surface receptor expression is modified, cells are guided through maturation by an array of cytokines or growth factors, many of which are secreted by the surrounding stromal cells in soluble form or as membrane bound molecules. Cells exit the bone marrow and enter peripheral circulation as monocytes where they may remain for several days.

1.4.6 Monocyte Extravasation and Migration to the Alveoli

Within 70 hours, monocytes are released into circulation from the bone marrow and begin migrating into surrounding tissues. Initially extravasation through the blood vessel wall begins with tethering, or weak binding of the monocyte to endothelial cells. Weak binding of monocytes, as with all leukocytes, is achieved by interactions between L selectin (CD62L) on the monocyte cell surface and P and E selectins (CD62P and CD62E) on the endothelial cell surface with corresponding lectin carbohydrate ligands (Muller and Randolph, 1999, Maus et al., 2002). This weak interaction serves to slow the motion of the circulating monocyte and results in rolling along the endothelium as the selectin molecules and ligands bind and break repeatedly. Eventually, the monocyte slows to a point at which it becomes immobilized and firm adhesion is achieved by binding of β 2 integrin molecules (CD11a/CD18, CD11b/CD18 and CD11c/CD18) on the monocyte cell surface to members of the Ig super family ICAM-1 (CD54) and VCAM-1 (CD106) on the surface of the endothelial cells in a magnesium dependent manner (Muller and Randolph, 1999). Circulating monocytes primarily express high levels of CD11b/18 and low levels of CD11c/18, however, during extravasation this expression is reversed (Beekhuizen and van Furth, 1993).

Monocytes become activated by binding of C-C and C-X3-C chemokine receptor ligands MIP-1 α , MCP-1, MIP-3 α , MIP-3 β and fructalkine bound to heparin

sulphate on the endothelial surface (Muller and Randolph, 1999) which induce a conformational change to other adhesion proteins allowing higher affinity binding (Beekhuizen and van Furth, 1993). Following adhesion and activation, migration then takes place with homophilic interactions between platelet endothelial cell adhesion molecule (PECAM-1, CD31) molecules found on monocytes and at the tight junctions of endothelial cells, along with binding of β 1 integrins VLA-4 and VLA-5 (CD49d/CD29 and CD49e/CD29, respectively) to their corresponding ligands VCAM-1 (CD106) and fibronectin (Shang et al., 1998, Maus et al., 2002). The monocyte is thus directed to migrate between endothelial cells and into the ECM. Monocytes then make their way into tissue and organs where they differentiate into macrophages and remain for several months.

Mature macrophages are widely distributed throughout the human body, and serve to patrol the surrounding tissue for invading pathogens. The distribution of monocytes/macrophages into different areas of the body is apparently random, although can be influenced by cytokines during immune responses. Whilst sharing many characteristics, macrophages residing in different anatomical locations display discrete, yet distinct, phenotypes and functions. In the alveoli, macrophages need to be able to respond quickly to unusual antigen load and so, although originating from circulating monocytes, may well be capable of self expansion. This theory arose from experiments using isolated lung explants which in the absence of a blood supply showed expansion of the alveolar macrophage (AM) population. This was later shown to arise from division and migration of interstitial cells and not the AM itself (Bowden, 1976), although subsequent studies in which blood monocytes were labelled with [3 H-TdR] thymidine failed to prove this (Riches and Henson, 1986). Whether the AM population is capable of self renewal or not, it is clear that the cells do at least originate from circulating monocytes and ultimately the BM, even if not directly (Landsman and Jung, 2007). Repopulation of the alveoli following whole body irradiation and BM transplant can take up to a year (Landsman and Jung, 2007).

The process of macrophage tissue migration to the alveoli is not yet fully

understood; however, elegant studies by Rosseau *et al* (2000) and Eghtesad *et al* (2001) have shed some light. The alveolar epithelium is made up of squamous type 1 and cuboidal type 2 pneumocytes or epithelial cells. Together, these studies showed that type 1 pneumocytes constitutively express ICAM-1 and integrin-associated protein (CD47) along with low levels of human leukocyte antigen DR (HLA-DR) and VCAM-1. Levels of ICAM-1 and VCAM-1 could be increased with TNF α stimulation. Type 2 pneumocytes expressed low levels of ICAM-1 and CD47 in addition to high levels of HLA-DR, which were not affected by TNF α . No PECAM-1, P-selectin or E-selectin expression was seen in either cell types. Blocking of CD47, which is also expressed by circulating monocytes, almost completely ablated trans-epithelial migration in addition to significant inhibition by blocking of CD11b/18. Blocking of either CD11a/18 or CD11c showed no inhibitory effect. Blocking of ICAM-1 showed no effect on transmigration despite being the ligand for CD11b/18, suggesting the presence of an alternative ligand. A combination of blocking VLA-4, VLA-5 and VLA-6 inhibited transmigration by 75%, whereas individually blocking these molecules had a lesser effect. TNF α was shown to up-regulate the CCL5 chemokine RANTES (Regulated upon Activation, Normal T-cell Expressed, and Secreted) production by type 1 pneumocytes and macrophage chemo attractant protein 1 (MCP-1) production by type 2 pneumocytes and transmigration has been shown to be dependent on MCP-1 concentration. A schematic diagram demonstrating monocyte/macrophage migration from circulation through the alveoli can be seen in *figure 1.4*.

1.5 Macrophage Activation and Polarisation

Once in the tissue, the mature functional macrophage is capable of eliciting a specialised immune response upon activation (Gordon, 2007). Macrophages however, do not express adapted antigen receptors like the T- and B- cell lymphocyte populations and so are capable only of distinguishing groups of non-self antigens as opposed to individual antigens. In order for macrophages to become active in the tissue, they must first encounter a stimulus. Current understanding suggests there are

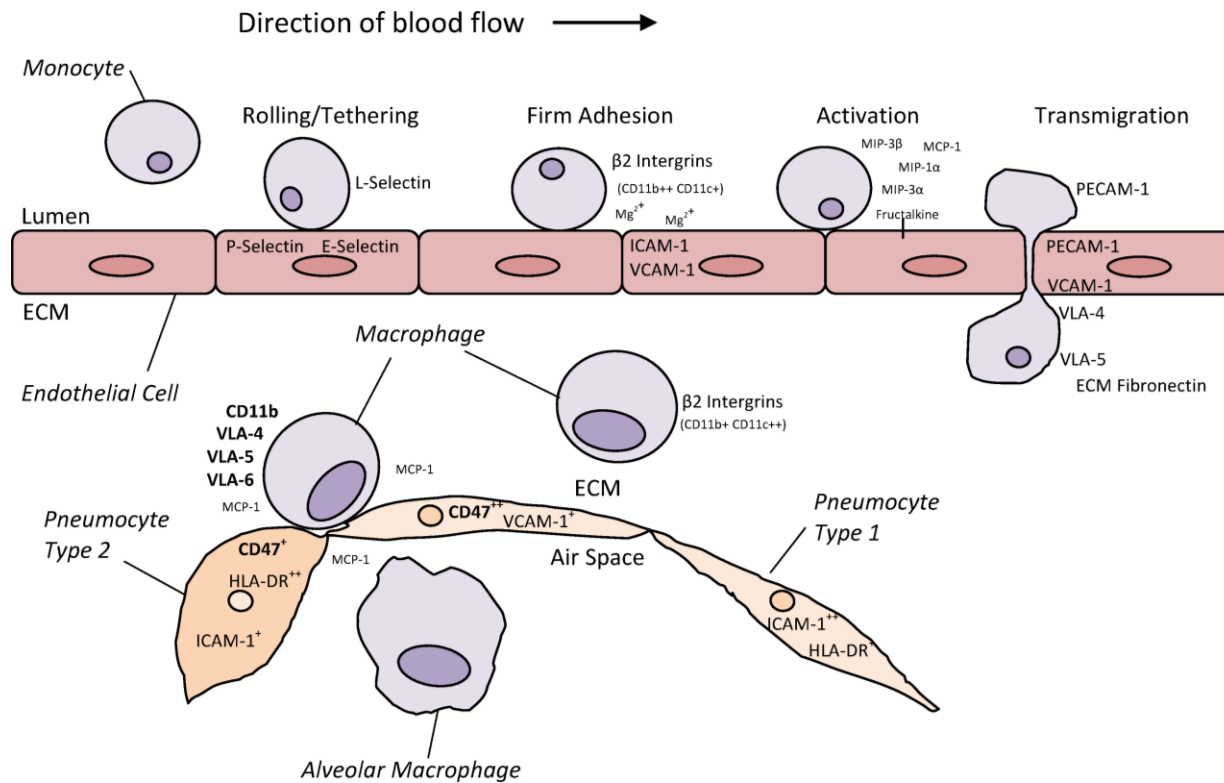


Figure 1.4 – Monocyte/Macrophage Migration

Circulating monocytes loosely attach to endothelium by binding of selectin molecules to their corresponding ligands. Firm adhesion then takes place by binding of β2 intergrins on the monocyte to ICAM-1 and VCAM-1 molecules on the endothelial cell. Next monocytes become activated by a number of C-C and C-X3-C chemokines or fructalkine bound to heparin sulphate on the endothelial cell. Transmigration takes place by homophilic binding of PECAM-1 molecules and binding of VLA-4/VLA-5 on the monocyte to VCAM-1 on the endothelial cell and fibronectin respectively. Tissue macrophages alter β2 intergrin molecule expression from CD11b⁺⁺/CD11c⁺ to CD11b⁺/CD11c⁺. Trans-epithelial migration into the alveoli is dependent on MCP-1 concentration and involves CD11b, VLA-4,5 and 6 on the macrophage and CD47 on the pneumocyte although the mechanism has yet to be fully elucidated.

2 possible mechanisms of activation.

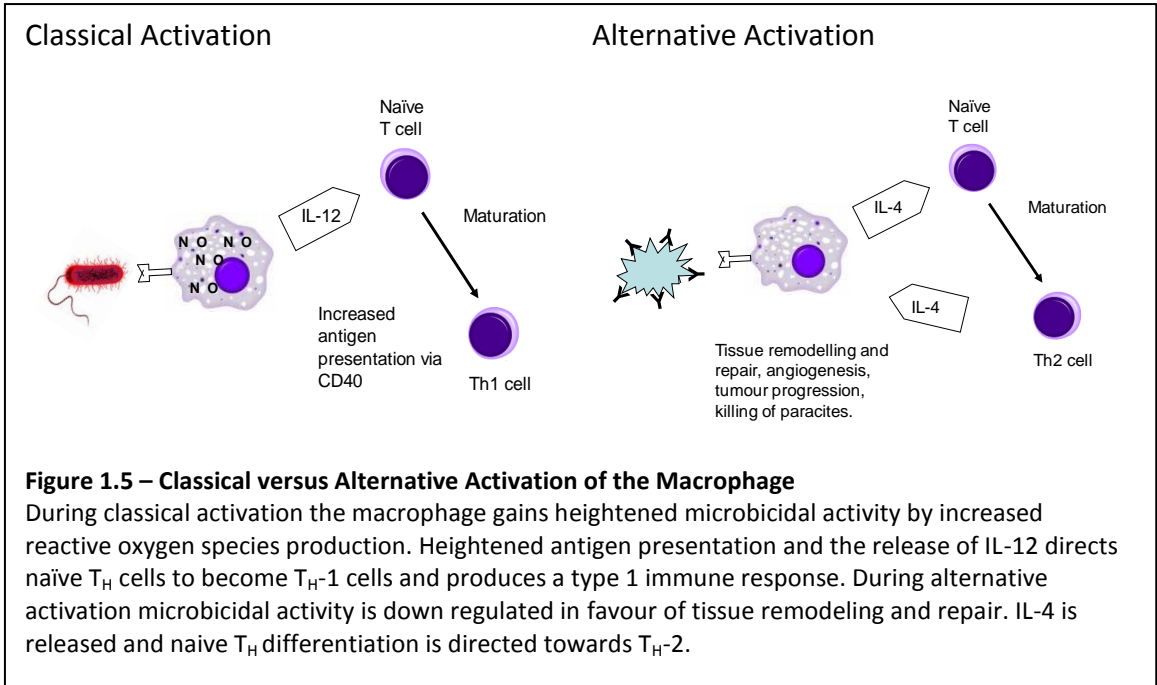
1.5.1 Classical Activation

Classical macrophage activation can be induced by the cytokines IFN γ , TNF α , and GM-CSF, or the constituent of a bacterial cells wall, lipopolysaccharide (LPS) (Mantovani et al., 2007, Anderson and Mosser, 2002, Mosser and Edwards, 2008). This results in a macrophage with heightened microbicidal activity, by production of reactive oxygen and nitrogen species. Also antigen presentation takes place, which produce a number of pro-inflammatory cytokines (IL-1 β , IL-6, IL-12, IL-18, IL-23 and TNF α) and are capable of inducing T_H-1 cell polarisation (Mantovani et al., 2007, Bouhleb et al., 2007, Mosser and Edwards, 2008, Verreck et al., 2006). However this is not the only state of activation possible.

1.5.2 Alternative Activation

Macrophages may also be activated by an alternative stimulus, such as immune complex, glucocorticoid, secosteroids (e.g. vitamin D) or the cytokines IL-4, IL-10 and IL-13 (Mantovani et al., 2007, Anderson and Mosser, 2002, Mosser and Edwards, 2008). Such cells have anti-inflammatory effects producing cytokines IL-8, IL-10 and TGF β , and are involved in the T_H-2 response, scavenging of apoptotic cells, angiogenesis, tissue repair and remodelling (Bouhleb et al., 2007, Verreck et al., 2006). A diagram comparing classical and alternative macrophage activation can be seen in *figure 1.5*. To reflect the activated macrophage involvement with T_H cell responses, the same nomenclature has been adopted in that classically activated macrophages are termed M1 and alternatively activated, M2. Whilst M1 macrophages are a well established population of cells, M2 cells have not yet been fully investigated and incorporate a number of emerging sub-types based on function and phenotype.

Activation of macrophages has also been found to be both inducible and reversible in mouse and man (Stout and Suttles, 2004, Porcheray et al., 2005, Bouhleb et al., 2007, Anderson and Mosser, 2002), demonstrating not only heterogeneity



among active macrophage populations, but also plasticity. Studies to find definitive markers to identify and distinguish M1 and M2 cells have proven difficult, owing to the responsive nature of activated macrophages, adapting to addition but also to removal of activating stimuli. A small number of cell surface molecules have been suggested as distinguishing markers. The family of three low affinity IgG antibody receptors (CD16, CD32 and CD64) are reported to be up-regulated in M1 but not M2 macrophages (Martinez et al., 2006, Xu et al., 2007, Komohara et al., 2006). CD14, the LPS receptor is reported to be down regulated during differentiation from monocyte to macrophage, though expression is reported to be higher in M2 than M1 cells (Verreck et al., 2006). In M2 macrophages, a number of scavenger receptors are also reported to be up-regulated, namely the haemoglobin scavenger receptor (CD163) (Xu et al., 2007, Komohara et al., 2006, Porcheray et al., 2005), macrophage scavenger receptor class A (CD204) and the mannose scavenger receptor (CD206) (Porcheray et al., 2005). Although promising markers of activation, further work is necessary to identify activated cell sub-types before any of the markers can be used definitively. The B7 co-

stimulatory molecules CD80 and CD86 are expressed by macrophages (Burastero et al., 1999, Schweitzer and Sharpe, 1998, Balbo et al., 2001) however in lung tissue, the environment dictates that alveolar macrophages express little or no B7 molecules. This finding may be due to that fact that the airways are constantly exposed to foreign material and therefore are required to have a certain degree of tolerance to antigen. It has, however, been found in asthmatic airways specifically, that macrophages chronically express higher levels of CD80 than in non-asthmatics and that allergen challenge results in an increase in CD86 (Burastero et al., 1999). Moreover, in the asthmatic airway, simultaneous co-stimulation with both CD80 and CD86 resulted in enhanced IL-4 and IL-5 production by antigen specific T_H cells generated by the investigators (Balbo et al.), a profile often associated with asthma.

1.6 Lipids and the Macrophage

The macrophage is also capable of scavenging lipid and plays an important role in the development of atherosclerosis. Macrophages express the class A scavenger receptor and CD36 (Moore and Freeman, 2006), both capable of binding modified low density lipoproteins (LDL) in circulation. In hyper-lipidaemic individuals, macrophages become heavily loaded with lipid droplets and are termed 'foam cells'. It is thought that lipid accumulation activates the macrophage to express the classical inflammatory phenotype; however the mechanisms of activation have yet to be elucidated. Studies have shown both M1 and M2 cells are present in atherosclerotic plaques, yet switch phenotype to M1 only during disease development (Bouhlef et al., 2007, Mosser and Edwards, 2008). The foam cell is not exclusive to atherosclerotic plaques and has in fact been reported in the airway in a number of studies (Ahrens et al., 1999, Parameswaran et al., 2000, Adams et al., 1997, Kazachkov et al., 2001). Studies show that foam cells present in the airway are indicative of, although not wholly exclusive to, patients with aspiration secondary to gastro-oesophageal reflux disease, which is discussed in 1.3. Although studies have been carried out as to the mode of uptake of circulating modified LDL in the development of foam cells, alveolar

macrophage lipid uptake has so far been overlooked.

1.7 Investigational Aims and Hypotheses

In summary, asthma is a chronic inflammatory disease of the airway and is often associated with GOR. The alveolar macrophage makes up to 70% of the immune cells populating the airway and is capable of antigen presentation and modulation of the immune response. The alveolar macrophage is also capable of lipid uptake which may activate and induce an inflammatory phenotype by mechanisms currently unknown. Lipid laden macrophages in the airway have previously been reported to be indicative of aspiration secondary to GOR and have been discussed. We hypothesise that lipid droplets from undigested or partially digested food may be aspirated into the airway and accumulate in scavenging macrophages. Foam cell formation in the airway thus generates activated macrophages that interact with other immune cells and tissue to induce an asthma-like state of disease.

Using oil red o staining and the lipid index, we propose to collect samples of alveolar macrophages from a large cohort of patients with a variety of respiratory disorders and controls, to determine a correlation between GOR and extent of foam cell formation in the airway. In addition, we propose to investigate the activation status of foam cells generated by uptake of unmodified lipid and compare this to classically and alternatively activated macrophages. In addition, we propose to investigate the mode of uptake of unmodified lipid by the macrophage and elucidate the cytokine profile of the generated foam cells. We also propose to characterise a new cell line, a derivative of the human monocytic THP-1 cell line and to compare these as a model for the human alveolar macrophage.

2 General Methods

All materials stated in this chapter were purchased from Sigma-Aldrich, Dorset, UK unless otherwise stated.

2.1 Cell Culture and Maintenance

All immortal cell lines were originally purchased from ATCC-LGC Middlesex, UK and were cultured at 37°C with 5% CO₂ in a humidified atmosphere. All cells were maintained and cultured in RPMI 1640 media supplemented with 10% v/v Foetal Bovine Serum (FBS) and *Penicillin/ Streptomycin* (PS), at concentrations of 100 U/ml and 0.1 mg/ml respectively (Gibco, Paisley, UK). All tissue culture techniques were performed in a Unimat² class 2 safety cabinet (Medical Air Technology, Oldham UK).

2.1.1 THP-1 Cells

The human derived myeloid cell line THP-1 was used throughout this project as a model for primary human macrophages and was a kind gift from Professor Ian Dransfield of the University of Edinburgh. THP-1 cells were maintained and cultured in suspension to between 60-80% confluence. During passage cells were transferred to 20 ml universal tubes, centrifuged (205 x g, 3 min.) and re-suspended in media before being diluted approximately 1/3 every 2-3 days.

2.1.2 Daisy Cells

The new progenitor cell line, now termed Daisy, was also used throughout this project and a kind gift from Professor Ian Dransfield. These cells were originally sent to us under the assumption that they were regular THP-1 pre-monocytic cells, as labelled, previously cultured by Professor Dransfield's team. They were shipped as live cells suspended in culture media and contained in an airtight polyethylene tube. Unfortunately the cells were misplaced during transit and did not reach our labs for culture until 2 weeks after they were initially shipped. When the cells arrived in our laboratory it was noted that the media had retained its original red colour and deemed

feasable to try and salvage any remaining live cells by cell culture. On doing to it became apparent that a good proportion of the cells were infact still alive and proliferating well, although rather than being suspended, the cells had transformed to become semi-adherent. The reason for this transformation is unclear. As the cells were shipped in an air tight container it is possible that hypoxia had played a role, selecting out a robust sub-population of cells able to survive with very little or no oxygen. Alternatively hypoxia or nutrient starvation had activated the cells to differentiate and transform in this way. Needless to say these altered cells which resembled macrophages at first look were deemed interesting and worthy of further investigation and so were maintained throughout this study.

The cells were maintained and cultured to between 60-80% confluence. During passage adherent cells were lifted using a cell scraper, transferred with the suspended fraction to 20 ml universal tubes and centrifuged (205 x g, 3 min.). Cells were then re-suspended in media before being diluted approximately 1/3 every 2-3 days and re-seeded.

2.1.3 A549 Cells

A549 bronchial epithelial cells, used briefly in this project, were previously stored in liquid nitrogen. Cells were defrosted, washed with phosphate buffered saline (PBS) and centrifuged (205 x g, 3 min.) before being re-suspended in supplemented media. Cells were seeded onto tissue culture flasks and allowed to adhere overnight. During passage non adherent cells were removed by washing with PBS. Adherent cells were detached with the addition of TrypLE™ Express (Gibco) trypsin enzyme and incubated to 37°C for 5 min. before gentle agitation. Detached cells were washed with PBS and centrifuged (205 x g, 3 min.) before being re-suspended in supplemented RPMI1640 media. Cells were then diluted approximately 1/5 every 2-3 days and re-seeded.

2.2 Cell Viability and Counting

Adherent cells were harvested by replacing cell culture media with ice cold PBS. Cells were kept at 4°C and agitated frequently. Cell suspensions were transferred to 20 ml universal tubes, centrifuged (205 x g for 5 min.) and the supernatant discarded before cells were re-suspended in 1 ml PBS. An aliquot of the cell suspension (10 µl) was added to an equal volume of trypan blue Solution (0.4 % w/v) and using a Neubauer haemocytometer, examined under light microscopy. Cells with compromised membranes were unable to extrude the stain, therefore staining blue and were considered non-viable (Strober, 2001). To determine the concentration of the cell suspension in cells/ml, the number of cells counted was multiplied by 1×10^4 , as the haemocytometer held a total volume of 0.1 µl, and then multiplied by 2 to account for the dilution with trypan blue. Cell suspensions were diluted as appropriate to allow accurate enumeration of live cells during experimentation.

2.3 THP-1 Differentiation with Phorbol 12-Myristate 13-Acetate (PMA)

In order to generate cells with mature macrophage characteristics, THP-1 cells were stimulated to differentiate with PMA. Cells were cultured at a density of 0.5×10^6 cells/ml. Conditions of culture are described in 2.1. PMA was added to the culture media at a concentration of 50 nM and the cells incubated for 24 hours. Cells were then washed 3 times with PBS and fresh PMA free media added. Cells were incubated for a further 24 hour recovery period before any further treatments were applied.

2.4 Transmission Electron Microscopy (TEM)

For the study of cell morphology at high resolution, cells were subjected to TEM. Cells were centrifuged (200 x g, 3 min.) and fixed in iso-osmotic 2.5% glutaraldehyde diluted in sodium cacodylate buffer (pH 7.3) and post-fixed in 1%

osmium tetroxide. Cells were then stained with 1% uranyl acetate and dehydrated through an ethanol series and eventually propylene oxide. Finally, cells were embedded in epon resin. Ultrathin sections were cut on a Leitz UC6 ultra microtome with a diamond knife. Images were obtained in a Jeol 2010 transmission electron microscope running at 120kV using a Gatan US4000 digital camera. TEM was graciously performed by Ann Lowry of the University of Hull microscopy suite.

2.5 Lipid Treatment

In order to study lipid accumulation as a model for reflux aspiration, cells were treated with a high fat liquid meal. PMA/THP-1 cells and Daisy cells were plated at a cell density of 0.5×10^6 cells/ml in wells of a 24 well tissue culture plate containing 1 ml cell suspension and a sterile glass cover slip. Conditions of culture are described in 2.1. After 24 h the media was replaced with media containing 10% v/v Calogen and the cells incubated for a further 24 h at 37°C. Cover-slips were then removed, washed 5 times in PBS and stained with oil red o, counterstaining with hematoxylin. The oil red o staining protocol is described in 2.6.

2.6 Oil Red O staining (ORO)

Staining of intracellular lipid droplets was performed using the ORO stain. This stain is more soluble in lipid than in solvent, staining non-polar lipids a bright red colour. A stock solution was prepared in advance (dissolving 0.5 % w/v of stain into isopropanol and stirring for 20 min.) and kept in the dark. Working solutions were freshly prepared combining 60 % stock solution with 40 % distilled water. This was stirred for 5 min. then allowed to stand for a further 5 min. before being filtered through a 0.2 µm syringe filter and transferred to a glass staining chamber. Slides were immersed in the stain for 20 min. before being rinsed thoroughly in distilled water. Slides were counterstained for 3 min. with Mayer's Haematoxylin followed by 2-3 drops of 0.1% w/v sodium bicarbonate for 30 sec. Slides were then allowed to dry and glass cover slips mounted using Kaiser's glyceringelatine mounting media.

2.7 Lipid Index

The lipid index was adopted throughout this study as a method of quantification of lipid accumulation. Cells adhered to glass slides or cover slips were washed 5 times with PBS and stained with ORO as described in 2.6. Stained macrophages were identified and scored according to the system described by Colombo and Hallberg (1987) during a study into recurrent aspiration in children. Each macrophage counted was simply assigned a score from 0-4 dependent on the degree of lipid staining and is described in *table 2.1*. When 100 macrophages had been scored the scores were added to give a total score, or lipid index, for the sample of between 0-400.

2.8 Fluorochrome Labelled Opsonised Antigen (BxB100)

Antibody coated antigen conjugated to FITC were prepared and used as a model for opsonised antigen in order to compare the cells opsonised antigen binding abilities. Stock solutions were prepared 'in house'. Biotin labelled bovine serum albumin (BSA) was diluted in PBS to a concentration of 500 ng/ml. Mouse monoclonal fluorescein isothiocyanate (FITC) conjugated anti-biotin antibody was added at a concentration of 170 ng/ml and the solution placed on ice, in the dark for 30 min. Stock solutions were stored at -20°C in the dark and diluted to give a working concentration of 100 ng/ml BSA when necessary.

2.9 Opsonised Antigen Binding Assessment

To quantify the cells opsonised antigen binding ability, FACS was used. Cells were harvested and counted as previously described in 2.2., filtered through a 70 µm cell strainer (BD Biosciences, Oxford, UK) and sufficient cell suspension containing 1×10^5 cells was then transferred to wells of a 96 well tissue culture plate with a removable plastic insert (BD Biosciences). The plate was centrifuged (350 x g, 3 min.,

Table 2.1 – Lipid Scoring of Alveolar Macrophages

Score Assigned	Degree of Staining
0	No staining
1	0-25%
2	25-50%
3	50-75%
4	75-100%

Macrophages were mounted onto slides and stained with ORO stain for lipid. Macrophages were scored according to the degree of staining observed and the total sample score calculated by addition of 100 individual macrophages scores (Colombo and Hallberg, 1987).

4°C) and the cells washed twice with PBS (100 µl). Fluorescent opsonised antigen (50µl) was then added at a concentration of 100 ng/ml, details of which are described in 2.8. The plate was gently agitated and incubated at 4°C for 30 min. Cells were washed (PBS; 100 µl) and centrifuged (300 x g; 5 min., 4°C) twice before being re-suspended in 500 µl FACSFlow Buffer (BD Biosciences) and analysed on a FACSAria II™ flow cytometer (BD Biosciences), running BD FACSDiva version 6.1.3 software, counting ten thousand cells per sample.

During analysis a gate (P1) was applied to the live cell population based on forward side scatter characteristics. This gate was applied to a histogram of fluorescence to all subsequent samples within the same experiment and statistical data generated to include mean fluorescence intensities.

2.10 Cell Surface Flow Cytometry

FACS was used to determine cell surface expression of a number of markers of mature macrophage functionality. Cells were harvested and counted as previously described in 2.2, filtered through a 70 µm cell strainer (BD Biosciences) and sufficient cell suspension to contain a total of 1×10^5 cells was then transferred to wells of a 96 well tissue culture plate with removable plastic insert (BD Biosciences). The plate was centrifuged (350 x g, 3 min., 4°C) and the cells washed twice with PBS (100

µl). Purified primary antibodies (50µl) were then added at a concentration of 20 µg/ml, details of which are described in *table 2.2*. All antibodies were purchased from AbD Serotec (Oxford, UK) as mouse monoclonal antibodies in a purified un-conjugated format, except CD32 which was generated 'in house' and a generous gift from Dr. Simon Hart. One well was left unlabelled. The plate was gently agitated and incubated at 4°C for 30 min. Cells were washed (PBS; 100 µl) and centrifuged (350 x g; 5 min., 4°C) twice and the supernatant discarded. The secondary rabbit anti-mouse FITC conjugated detection antibody was then added (50µl; 50 µg/ml). The plate was gently agitated and incubated for 30 min. at 4°C in the dark to avoid quenching of the fluorochrome. The cells were washed as previously described and re-suspended in 500 µl FACSFlow Buffer (BD Biosciences) before being analysed on a FACSAria II™ flow cytometer (BD Biosciences), running BD FACSDiva version 6.1.3 software and counting ten thousand cells per sample. During analysis a gate (P1) was applied to the live cell population based on forward side scatter characteristics. This gate was applied to a histogram of fluorescence to all subsequent samples within the same experiment and statistical data generated to include mean fluorescence intensities.

2.11 Preparation of Cytospin Slides

To prepare cells for staining, visualisation and analysis, live cells were mounted onto glass slides using a Shandon Cytospin 3 (Thermo-Shandon Ltd., Runcorn, UK) centrifuge and apparatus. Cytospin apparatus was assembled to include a polypropylene funnel, glass slide, as depicted in *figure 2.1*. Cell suspensions were adjusted to a concentration of 1×10^6 cells/ml, 10 µl of which was transferred into a polypropylene funnel. Apparatus was placed into the Cytospin 3 and centrifuged (300 rpm, 5 min.) before being dismantled and the slides allowed to air-dry.

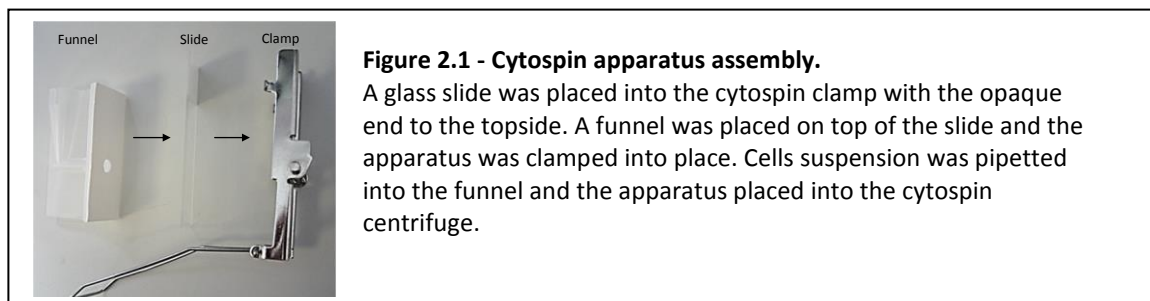
2.12 Cell Differential Staining

Cell differential staining was performed to distinguish macrophage cells using a Reastain Quick-Diff Kit (Reagen Ltd, Toivala, Finland) containing solutions of

Specificity	Description
CD11b	α M2 integrin commonly used as a monocyte to macrophage differentiation marker
CD14	Pattern recognition receptor which binds LPS and is expressed by human monocytes and macrophages
CD16	Low affinity Fc γ RIII receptor up-regulated in classically activated macrophages
CD23	Low-affinity Fc ϵ RII receptor up-regulated on alternatively activated macrophages
CD24	Adhesion molecule expressed by granulocytes but not macrophages
CD32	Low affinity Fc γ RII receptor up-regulated on classically activated macrophages
CD36	Class B scavenger receptor which binds long chain fatty acids and oxLDL
CD64	High affinity Fc γ RI receptor up-regulated in classically activated macrophages
CD80	T-cell co-stimulatory molecule required for TH1 differentiation
CD86	T-cell co-stimulatory molecule required for TH2 differentiation
CD163	Hb scavenger receptor up-regulated on alternatively activated macrophages
CD206	Mannose receptor up-regulated on alternatively macrophages

Table 2.2 – Antibodies used in immunophenotyping studies

Table of antibodies used during investigation of cell surface molecule phenotyping by flow cytometry of THP-1 and Daisy cells. A description of each molecule is also given.



methanol (A), Eosin Y (B) and Azur II (C). Solutions A, B and C were transferred to glass staining chambers. Cytospin slides previously prepared as described in 2.11 were sequentially dipped fifteen times in each staining solution before being rinsed thoroughly with tap water. Slides were allowed to air dry before a glass cover slip was mounted using DPX mountant for histology. Slides were then examined under the microscope and macrophages identified and quantified as a percentage of total cells.

2.13 Assessment of Phagocytosis

To determine the cells phagocytic capability as a function of maturity, cells were incubated with zymosan particles. PMA/THP-1 cells and untreated Daisy cells were cultured to 80% confluence in wells of a 24 well tissue culture plate containing sterile glass cover-slips. Conditions of culture are described in 2.1. Media was aspirated and replaced with fresh media containing 1 mg/ml zymosan, a protein-carbohydrate complex constituent of yeast cell walls and cells were returned to the incubator for a further 60 min. Cover-slips containing adherent cells were then removed from the wells and washed 5 times in PBS before being differentially stained as described in 2.12. Phagocytosed zymosan appeared as white rings in the cellular cytoplasm.

2.14 Heat Aggregation of Human IgG

Human IgG antibodies were aggregated using heat for use as an economical cell stimulator (resembling opsonised antigen) to generate M2 alternatively activated macrophages. Human IgG was diluted in PBS at a concentration of 20 mg/ml and heated to 63°C for 30 min. Stock solutions were stored at -20°C and thawed as necessary.

2.15 Primary Cell Isolation

In order to confirm *in vitro* findings in primary human tissue, primary cells were isolated from BAL fluid. All tissue culture techniques were performed in a

Unimat2 class 2 safety cabinet (Medical Air Technology, Oldham, UK). Human primary cells were obtained from excess BAL fluid obtained from patients undergoing diagnostic bronchoscopy procedures. BAL was obtained by sequential instillation of three, 10-20 ml aliquots of physiological saline (0.9%) solution into the airway followed by immediate aspiration. Samples were kept on ice during transportation to the laboratory. Cells were filtered through a 100 µm cell strainer (BD Biosciences), to remove excess mucus, and centrifuged (300 x g for 10 min.) before being re-suspended in 1 ml PBS.

2.16 Gene Microarray

Gene microarray analysis was performed to provide a clearer picture as to the origin of the daisy cells and to provide a bank of data for future reference when studying lipid accumulation and metabolism of macrophages. mRNA was extracted from cultured cells using a NucleoSpin® RNA II Kit (Macherey-Nagel GmbH & Co KG, Duren, Germany). Adherent cells cultured in a T25 tissue culture flasks were washed (5 times with 5ml PBS) and lysed directly in the flask using the lysis buffer provided (600 µl supplemented with 10% v/v β-mercaptoethanol). Lysate was transferred to a micro-centrifuge tube containing a NucleoSpin® filter and centrifuged at 11000 x g for 1 min. to reduce viscosity. Ethanol (70% v/v; 600 µl) was then added to the filtrate to adjust RNA binding conditions. RNA was transferred to a micro-centrifuge tube containing a NucleoSpin® RNA II column and centrifuged (11000 x g for 30 sec) discarding the collection tube. The column was placed in a clean collection tube and membrane desalting buffer (350 µl) was then passed through by centrifugation (11000 x g; 1 min.), discarding the flow-through. Contaminating DNA was digested by incubation with 10% v/v rDNase in reaction buffer (15 min.; RT). rDNA wash washed through the column by addition of buffer RA2 (200 µl) and centrifugation (11000 x g; 30 sec.). A second wash was performed by passing buffer RA3 (600 µl) through the column by centrifugation (11000 x g; 30 sec.) followed by a third wash (250 µl; 11000 x g; 2 min.) discarding flow-through after each wash. Finally the mRNA was eluted into a clean collection tube by

passing RNase free water (60 μ l) through the column by centrifugation (11000 x g; 1 min.)

mRNA was then quantified on a Qubit™ 1.0 fluorometer (Invitrogen, Paisley, UK). Firstly a dye working solution was prepared diluting Quant-iT™ RNA reagent in Quant-iT™ RNA buffer (0.5% v/v) allowing 200 μ l for each standard or sample. Secondly, standards and samples were prepared diluting 1 μ l of each standard or sample in 199 μ l of dye working solution. Standards comprised of a negative (0 ng/ μ l) and a positive (10 ng/ μ l) control solution. Finally standards and samples were quantified taking fluorescence readings at 630/680 nM.

Samples were transferred on ice and analysed for gene expression profiles by the Bioscience Technology Facility, Biological Sciences, University of York, using an Agilent gene array system. Samples were prepared and analysed in duplicates of 4 and the data filtered and analysed by the Facility. Further data analysis was performed by us using Microsoft Excel 2010 software.

3 Development of an *in vitro* model of Gastro-Oesophageal Reflux

3.1 Introduction

Many of the methods described in this project were used repeatedly throughout. Therefore, this chapter will describe in detail the development of such methods.

The THP-1 cell line used throughout this project was stimulated with PMA to induce monocyte to macrophage differentiation. PMA is a potent agonist of protein kinase C which induces the raf/MAPK/ERK signalling pathway to promote cell differentiation. In addition, PMA induces up-regulation of p21 which promotes G₁/S phase cell cycle arrest via negative regulation of cyclin dependant kinase-2 and subsequent binding of hypo-phosphorylated retinoblastoma protein to E2F (Traore et al., 2005). Although knowledge of the mechanism by which PMA induces THP-1 cell differentiation has improved, a complete understanding is yet to be achieved. However, this method of differentiation is relatively standard in research, although optimisation was necessary and will be described here.

Lipid accumulation by PMA stimulated THP-1 cells and the new Daisy macrophage cell line, characterised in *chapter 4*, was central to this project as a model for reflux aspiration. Lipid was presented in the form of Calogen, a medically available complete liquid meal which contains 50% w/v lipid comprising of a combination of sunflower and canola oil. This form of lipid in the context of a complete meal was deemed representative of post meal stomach contents with the exclusion of reduced pH and enzymes. Quantification of cellular lipid accumulation by ORO staining and lipid indexing was verified to confirm that lipid accumulation was reproducible and that this method of quantification was reliable. These results will also be presented in this chapter.

3.2 Methods

3.2.1 THP-1 Differentiation with PMA

During optimisation of PMA stimulated THP-1 cell differentiation, cells were cultured at a density of 0.5×10^6 cells/ml. Conditions of culture are described in 2.1.1. PMA was added to the culture media at concentrations of 10, 20, 30, 40, 50, 100 and 150 nM and the cells incubated for 24, 48 and 72 hours. Cells were visualized under light microscopy using an Olympus CK2 inverted microscope (Olympus, Southend-on-Sea, UK) under phase contrast at 20x magnification. Images were captured on an Olympus C-5060 wide zoom digital camera (Olympus). Differentiation was determined by visual identification of key characteristics such as cell adherence, increased nucleus:cytoplasm ratio and mitotic growth inhibition.

3.2.2 Lipid Uptake Optimisation

During optimisation PMA/THP-1 and Daisy cells were incubated with concentrations of Calogen ranging from 5 % v/v to 50 % v/v and for lengths of time ranging from 1-24 hours. Calogen osmolarity was adjusted from 150 mOsm/L to 287 mOsm/L with the addition of 40.07 g NaCl/L to match that of the cell culture media. This was calculated by dividing the difference in osmolarity (137) by the number of molecules to which NaCl disassociates in water, i.e. 2, and multiplying the answer (68.5) by the molecular weight (58.5) to give g/L. Calogen was then diluted v/v in culture media maintaining the osmolarity at an isotonic level.

PMA/THP-1 cells and Daisy cells were plated at a cell density of 0.5×10^6 cells/ml in each well of a 24 well tissue culture plate containing 1 ml cell suspension and a sterile glass cover slip. Conditions of culture are described in 2.1. After 24 h the media was replaced with media containing 5, 10, 15, 20, 25, 30, 35, 40, 45 and 50 % v/v Calogen and the cells incubated for a further 24 h at 37°C. Cover-slips were then removed, washed 5 times in PBS and stained with ORO, counterstaining with hematoxylin and mounted onto glass slides with kaisers glyceringelatine mounting

media.. ORO staining protocol is described in 2.6. A similar method was used to determine optimum incubation time using only 10 % v/v Calogen diluted in cell culture media and incubated for 1, 2, 3, 4, 5, 6 and 24 h. Again cover-slips were removed after treatment, washed 5 times in PBS and stained with ORO and haematoxylin.

3.2.3 Verification of Lipid Origin

In order to verify that lipid accumulating in the cultured macrophages was a result of direct uptake from Calogen, this high fat liquid meal was compared with a fat free liquid meal, namely Fortijuce. The ingredients of both these products can be found in *figures 10.1 and 10.2* of the appendix. The osmolarity of the Fortijuce was adjusted similarly from 750 mOsm/L to 287 mOsm/L by a 1 in 2.61 dilution in distilled water. Fortijuce was then also diluted to a 10 % v/v concentration in supplemented RPMI 1640 media. Daisy cells were seeded and treated as before (0.5×10^6 cells/ml; 24 h) before being washed and stained with ORO and haematoxylin and mounted onto glass slides with kaisers glyceringelatine mounting media. Untreated cells were compared with 10 % v/v Calogen treated and 10 % v/v Fortijuce treated cells.

3.2.4 Lipid ORO Staining Variability

PMA/THP-1 cells and Daisy cells were plated at a cell density of 0.5×10^6 cells/ml in each well of a 24 well tissue culture plate containing 1 ml cell suspension and a sterile glass cover slip. Conditions of culture are described in 2.1. After 24 h, the media was replaced with media containing 10 % v/v Calogen and the cells incubated for a further 4 h at 37°C. Cover-slips were then removed, washed 5 times in PBS and stained with ORO, counterstained with hematoxylin and mounted onto glass slides with Kaiser's glyceringelatine mounting media. ORO staining protocol is described in 2.6. Lipid scoring was then performed on slides prepared from all 24 wells from both the PMA/THP-1 plate and the Daisy plates and the method repeated twice more to give n = 3 in both cases. Inter-well variability of each plate was calculated by taking the mean of lipid scores from all 24 wells and calculating the standard deviation using Microsoft

Excel 2010 software. The coefficient of variation was then calculated by dividing the standard deviation by the mean and multiplying this value by 100, to give the value as a percentage. Similar calculations were performed to determine inter-plate variability by pooling the raw data from all 3 plates prepared for each of the 2 cell types.

3.3 Results

3.3.1 THP-1 Differentiation with PMA

THP-1 cells can be stimulated to differentiate into macrophages by PMA. Optimisation of this method was performed stimulating THP-1 cells with varying concentrations of PMA for varying lengths of time. The results can be seen in *figure 3.1*. At a concentration of 30 nM PMA (A) or less (not shown) cells remained in suspension and appeared not to have undergone differentiation. At a concentration of 40 nM PMA (B) cells began to take on an appearance of differentiated macrophages indicated by adherence, increased nucleus:cytoplasm ratio and mitotic growth inhibition, after 48 hours of treatment. Treatment with a concentration of 50 nM PMA (C) or more (not shown) for 24 hours consistently gave rise to cells with this morphology.

3.3.2 Lipid Uptake Optimisation

Macrophage lipid accumulation was central to this project, therefore optimal conditions for lipid accumulation were sought. PMA/THP-1 and Daisy cells were first incubated with varying concentrations of Calogen, a high fat liquid meal for 24 h at 37°C. Results of these experiments can be seen in *figure 3.2*. Subsequent staining with ORO showed lipid accumulation at all concentrations however at concentrations above 15% v/v Calogen, cytotoxicity was also observed. Maximal lipid accumulation and minimal cytotoxicity was seen at a concentration of 10% v/v Calogen.

Optimal incubation time was also investigated using 10% v/v Calogen. Results of these experiments can be seen in *figure 3.3*. Subsequent ORO staining showed lipid accumulation after as little as 1 hour. Accumulation increased over time and maximal accumulation was seen after 24 h incubation with 10% v/v Calogen.

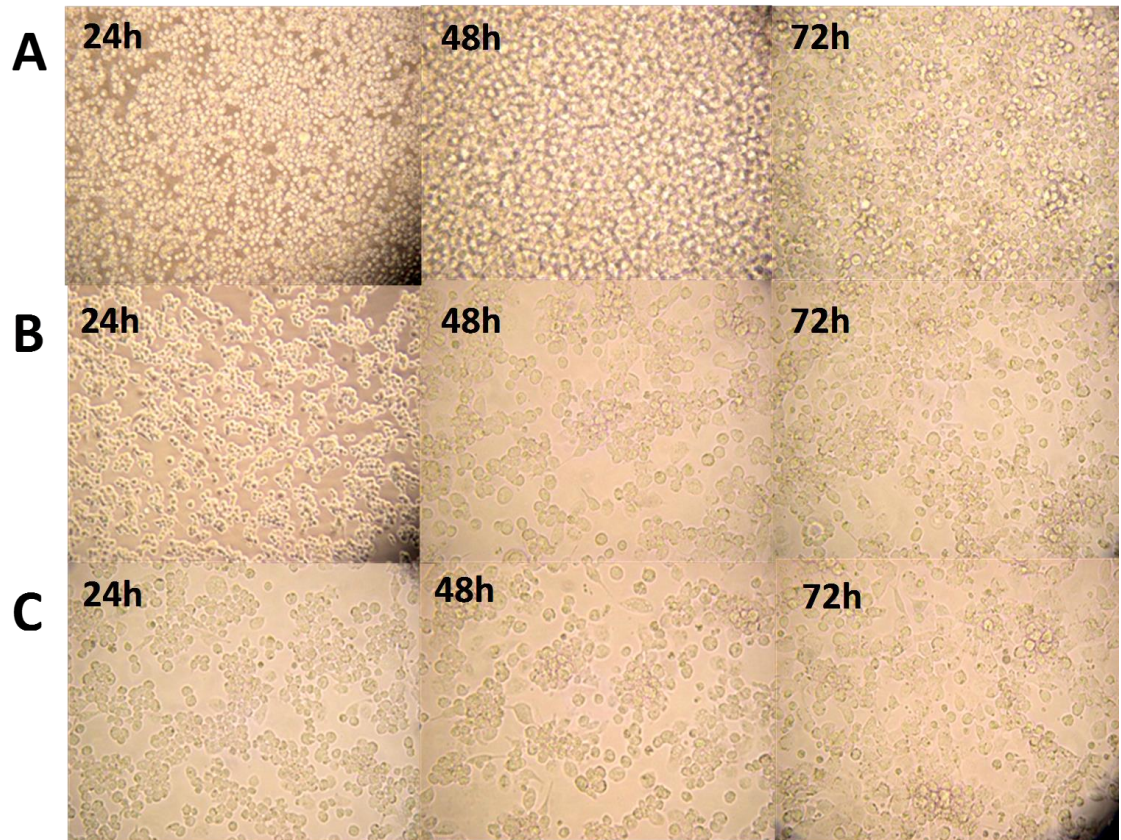
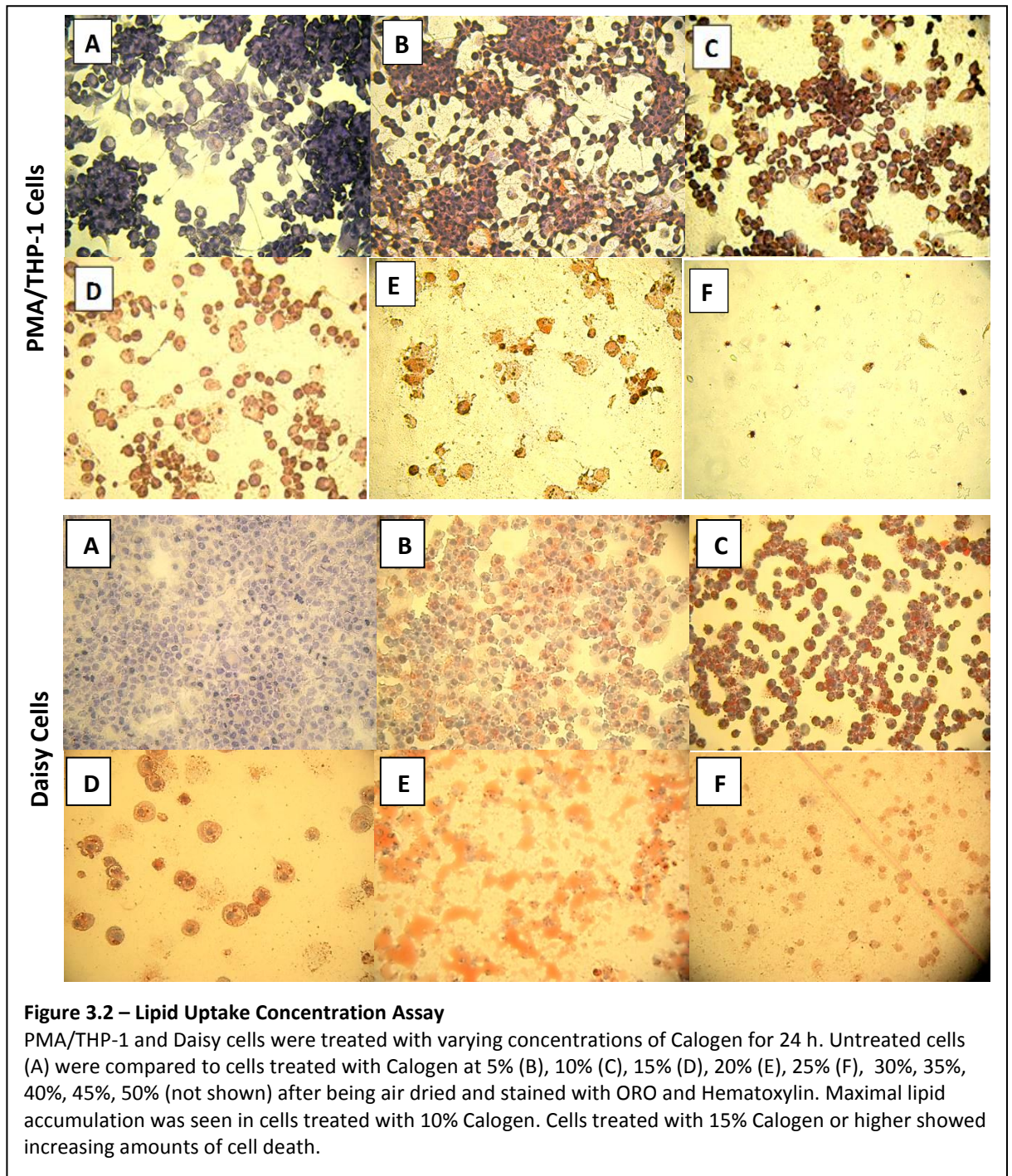
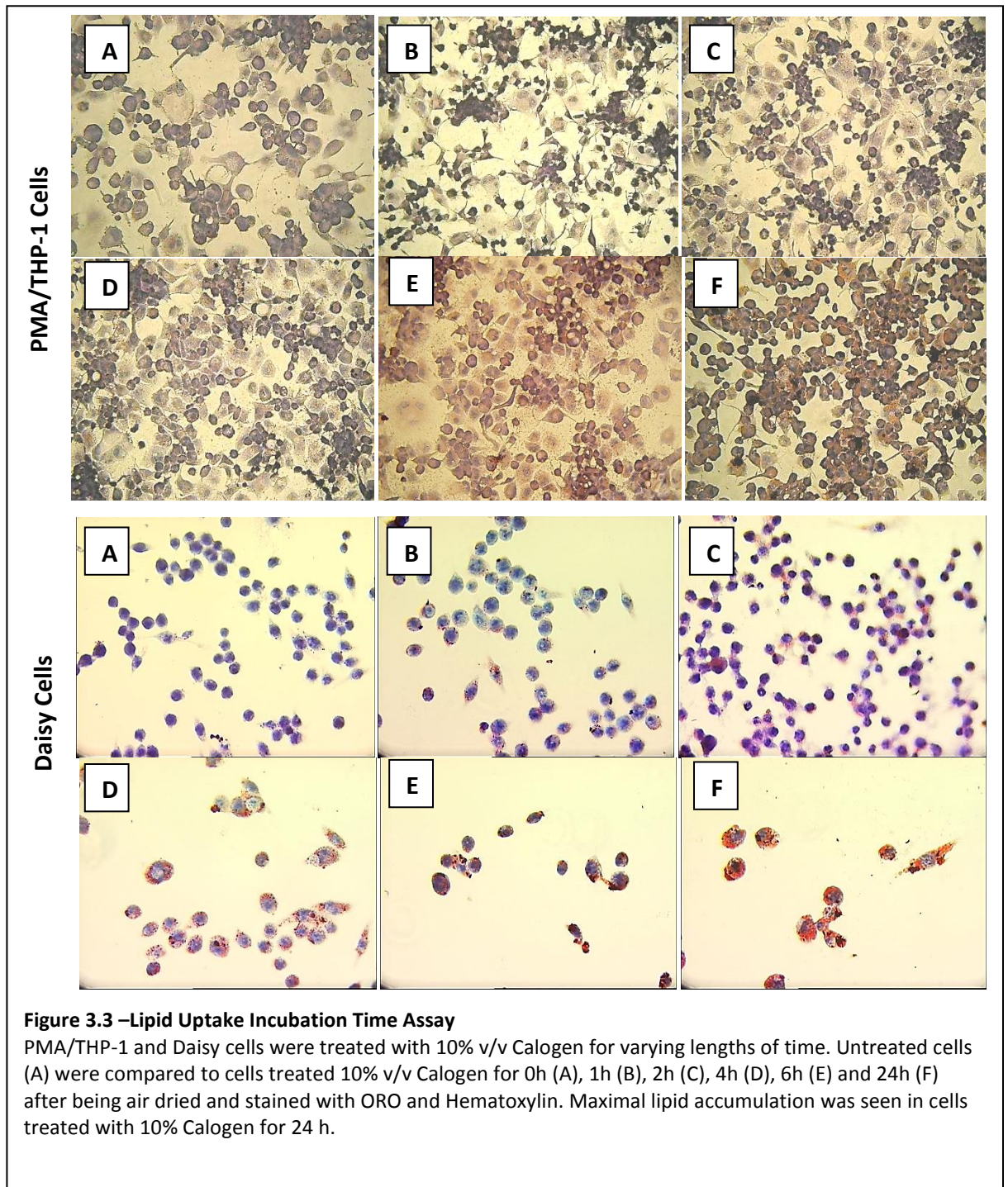


Figure 3.1 – PMA treatment optimization of THP-1 cells.

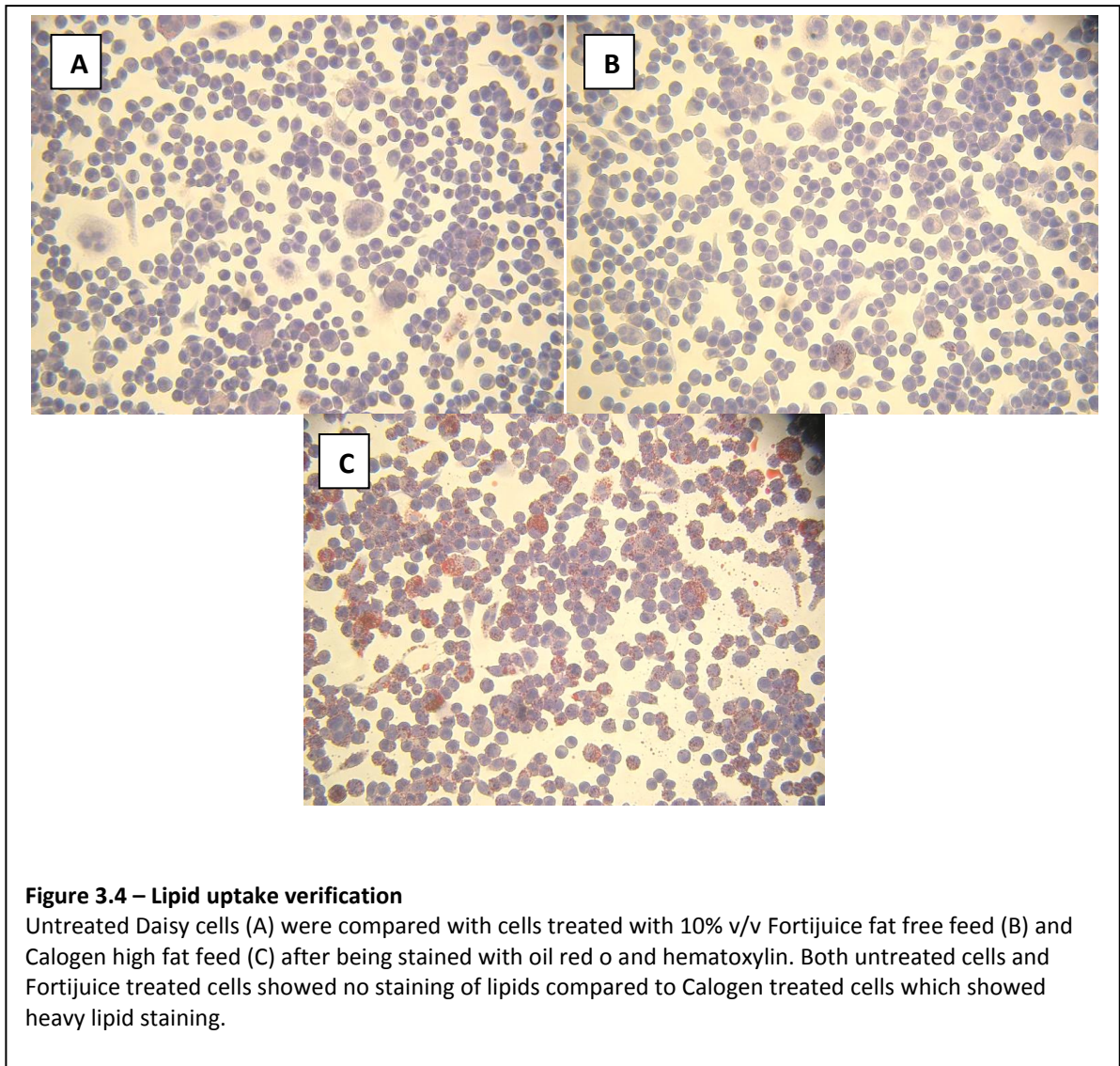
THP-1 cells were seeded into a 24 well plate at 0.5×10^6 cells/ml. PMA was added to the culture media at varying concentrations and incubated for 72 h. At 24 h intervals the cells were examined under the microscope. At a concentration of 30 nM PMA (A) or less (not shown) cells remained in suspension and appeared not to have undergone differentiation. At a concentration of 40 nM PMA (B) cells took on an appearance of differentiated macrophages indicated by adherence, increased nucleus:cytoplasm ratio and mitotic growth inhibition, after 48 hours of treatment. Treatment with a concentration of 50 nM PMA (C) or higher (not shown) for 24 hours consistently gave rise to cells with this morphology.





3.3.3 Verification of Lipid Origin

To verify intracellular lipid accumulation seen in previous experiments was a result of direct extracellular lipid uptake, Daisy cells were incubated with both a high fat liquid meal (Calogen) and a fat free liquid meal (Fortijuce) under identical conditions. Results can be seen in *figure 3.4*. After 24 hours incubation cells were washed and stained with ORO and hematoxylin and compared with untreated cells. Both untreated and fat free Fortijuce treated cells showed no lipid staining whilst high fat Calogen treated cells showed heavy lipid staining.



3.3.4 Lipid Staining Variability

PMA/THP-1 and Daisy cells were seeded into wells of 2 separate 24 well tissue culture plates and treated with high fat Calogen as described in 2.5 reducing the incubation time to a sub-maximal uptake period of 4 hours. This was in order for total lipid accumulation to be detectable therefore the variability of the lipid accumulation, staining and scoring protocols be measurable. Cells were then stained with ORO and scored using the lipid index scoring system as described in 2.6 and 2.7 respectively. All 24 wells from each plate were stained and scored and the experiment repeated twice more. Inter-well variability of each plate was calculated by taking the mean of lipid scores from all 24 wells and calculating the standard deviation using Microsoft Excel 2010 software. The coefficient of variation was then calculated by dividing the standard deviation by the mean and multiplying this value by 100 to give the value as a percentage, results of which can be seen in *figure 3.5*. Similar calculations were performed to determine inter-plate variability by pooling the raw data from all 3 plates prepared for each of the 2 cell types, results can be seen in *figure 3.6*.

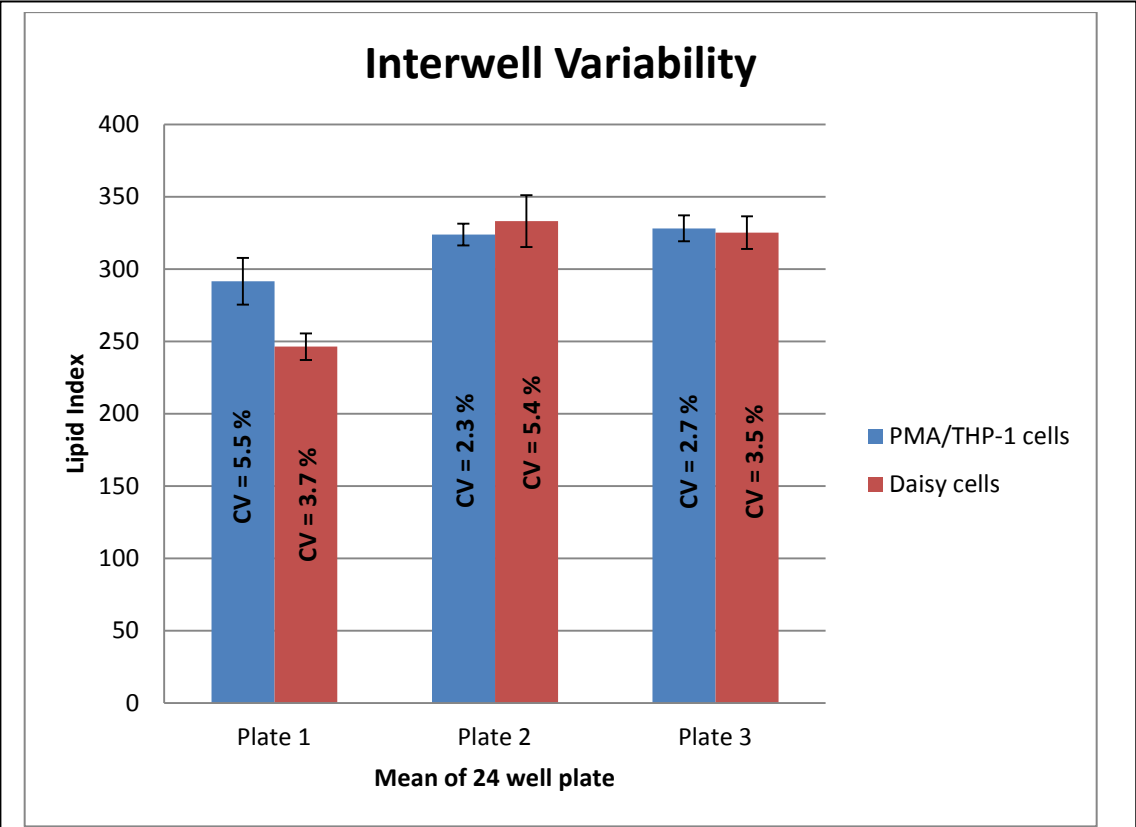


Figure 3.5 – Lipid staining inter-well variability

PMA/THP-1 and Daisy cells were seeded into wells of 24 well tissue culture plates and treated with Calogen for a period of 4 hours. Cells were then stained with ORO and scored using the lipid index scoring system. All 24 wells from each plate were stained and scored and the experiment repeated twice more. The mean of lipid scores from all 24 wells was calculated along with standard deviation (error bars) and coefficient of variance using excel software. The coefficient of variation for lipid stained PMA/THP-1 cells ranged from 2.3-5.5 %. The coefficient of variation for lipid stained Daisy cells ranged from 3.5-5.4 %.

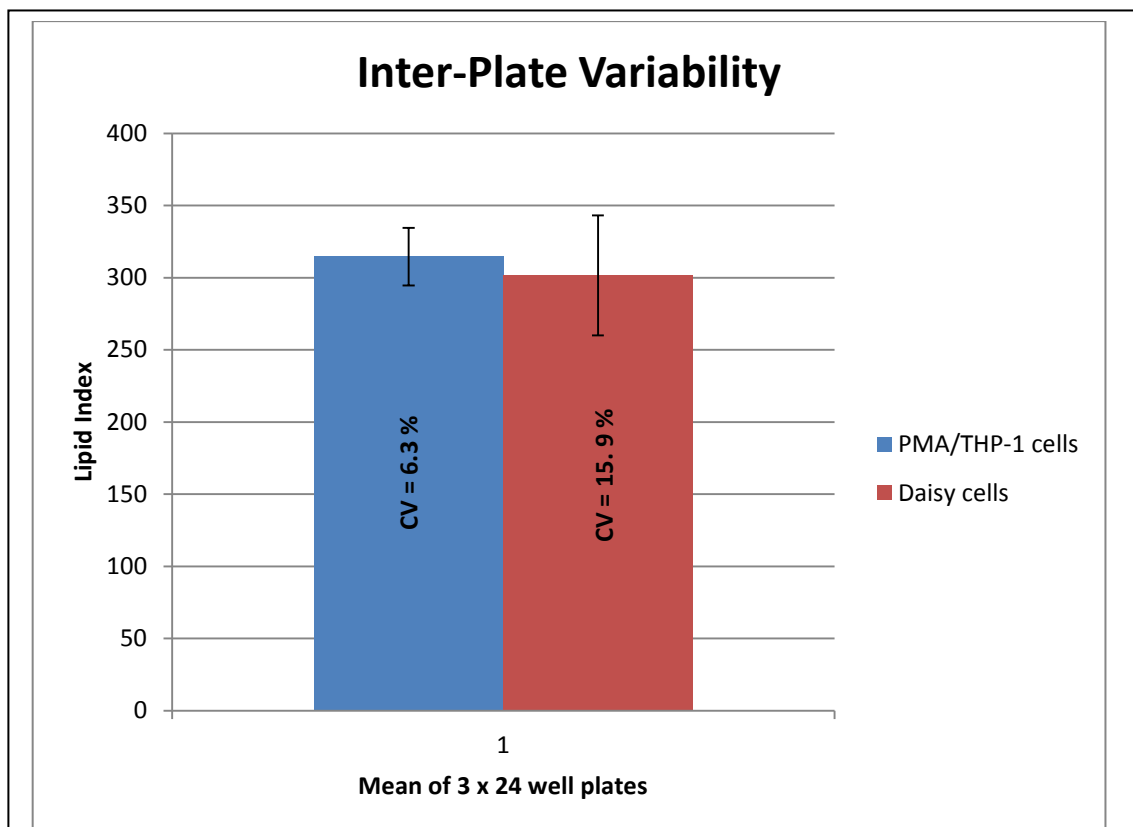


Figure 3.6 – Lipid staining inter-plate variability

PMA/THP-1 and Daisy cells were seeded into wells of 24 well tissue culture plates and treated with Calogen for a period of 4 hours. Cells were then stained with ORO and scored using the lipid index scoring system. All 24 wells from each plate were stained and scored and the experiment repeated twice more. The mean of lipid scores from all 24 wells across 3 separate plates was calculated along with standard deviation (error bars) and coefficient of variance using excel software. The coefficient of variation for lipid stained PMA/THP-1 cells was 3.6 %. The coefficient of variation for lipid stained Daisy cells was 15.9 %.

3.4 Discussion

PMA stimulation of pre-monocytic THP-1 cells to differentiation into macrophages is a well established methodology. Exact experimental conditions vary, however, between published groups. We therefore intended to establish optimal conditions for use in this study. Whilst a concentration of 30 nM PMA or less appeared to have no effect on the cells, a concentration of 40 nM PMA showed cells to take on an appearance of differentiated macrophages indicated by adherence, increased nucleus:cytoplasm ratio and mitotic growth inhibition, after 48 h of treatment. Treatment with a concentration of 50 nM PMA, or higher, for 24 h consistently gave rise to cells with this morphology. It was thus concluded that the latter treatment be used consistently throughout this study.

Lipid uptake by PMA/THP-1 and Daisy cells was fundamental to this project and was also required optimisation. PMA/THP-1 and Daisy cells were treated with varying concentrations of Calogen, a lipid rich medically available complete meal. This was thought suitable to represent stomach contents in the context of unmodified lipids, proteins, carbohydrate, vitamins and minerals with the exclusion of reduced pH and enzymes. Lipid accumulation was seen with 24 h treatments of Calogen diluted in cell culture media at all concentrations. Cells treat with 15% Calogen or higher showed increasing amounts of cell death. As osmolarity of Calogen was adjusted to match that of the cell culture media the reason for cell death is less clear. The pH of undiluted Calogen was measured at 1.8. When diluted at 10% v/v however the buffering effect of the cell culture media compensated this. Calogen did, over the 24 h incubation period, separate in the media, forming a layer of lipid on top of the media. This may have prevented gas exchange at higher concentrations, but we were unable to quantify this.

PMA/THP-1 and Daisy cells were also treated with 10% v/v Calogen for varying lengths of time. Whilst slight lipid accumulation was seen after just 1 h, maximal lipid accumulation was seen in cells treated with 10% Calogen for 24 h. Therefore these conditions were considered optimal for consistent use throughout this project.

In terms of verifying intracellular lipid droplet origin, both untreated cells and cells treated with fat free Forti juice showed no lipid accumulation at all. This rules out the theory that lipids could accumulate by intra-cellular lipogenesis from metabolism of protein or carbohydrate. Compared with Calogen treated cells, which showed high levels of lipid accumulation when treated under identical conditions, this would suggest the origin of lipid is direct absorption from Calogen.

Whilst investigating the sensitivity of the lipid accumulation and staining protocols optimised in this study it was found that the inter-well variability of cells of the same passage treated identically showed a low degree of variability. PMA/THP-1 cell inter-well variance across 3 separate 24 well plates treated on 3 separate occasions ranged from 2.3-5.5 %. Daisy cells were almost equally invariable ranging from 3.5-5.4 %. When comparing results from 3 separate plates the PMA/THP-1 cell inter-plate variance was still low, at 6.3 %. However, the inter-plate variance of Daisy cells increased to 15.9 %. The difference seen here may be due to the fact that scores on one of the Daisy cell plates were slightly lower than the other 2 plates making inter-plate variability higher, whereas inter-well variability remained low. The reason for this could be related to cell passage number as Daisy cells have so far been found to be temperamental with regards to optimal culture conditions. As this is a new cell line, optimal cell density is still being established during cell maintenance which appears to affect cell adherence and presumably cell activation. In comparison cell activation of THP-1 cells has been regulated with optimisation of PMA treatment.

4 Characterisation of a New Human Macrophage Cell Line (Daisy)

4.1 Introduction

Macrophages are the predominant mononuclear phagocytes of the innate immune system and have a fundamental role in inflammatory processes throughout the body. The macrophage upon activation is capable of eliciting a specialised immune response, the primary function of which is dictated by the stimulus and the environment in which the macrophage resides (Stout and Suttles, 2004).

In vitro experiments requiring human macrophages currently require mitogenic (e.g. PMA) stimulation of a macrophage precursor cell line (e.g. THP-1 or U937) or *ex vivo* maturation of circulating primary monocytes. PMA stimulation activates protein kinase C resulting in phosphorylation of a number of downstream signalling molecules (Traore et al., 2005). This activation of intracellular signalling is long lasting and has been shown to regulate gene expression in a manner that is not comparable to human monocyte-derived macrophages (Kohro et al., 2004).

We have derived a unique sub-clone of the THP-1 cell line capable of spontaneous and perpetual differentiation into macrophage-like cells. This cell line, termed 'Daisy', was derived, albeit by accident, from a THP-1 clone sent to use as a gift. Upon initial culture of the cells it was clear they were not regular THP-1 cells, given that a large proportion quickly became adherent to the plastic tissue culture flask in which they were incubated. This phenomenon is not seen with THP-1 cells, which normally grow in suspension. For this reason it was decided to characterise the new sub-clone to investigate key features of a mature macrophage and compare results with native THP-1 cells and THP-1 cells stimulated with PMA.

4.2 Methods

4.2.1 Light Microscopy

Cells cultured in T25 plastic tissue culture flasks were visualised on an Olympus CK2 inverted microscope (Olympus, Southend-on-Sea, UK) using phase contrast at 20x magnification. Images were captured on an Olympus C-5060 wide zoom digital camera (Olympus).

4.2.2 Mycoplasma Screen by Fluorescent Microscopy

THP-1 and Daisy cells were tested for mycoplasma infection using a MycoFluor™ mycoplasma detection kit (Molecular Probes, Paisley, UK). Cells were cultured at 80% confluence for 24 h in wells of a 24 well tissue culture plate containing sterile cover slips. Conditions of culture are described in 2.1. Cell culture media was aspirated and 1.9 ml fresh culture media was added to each well. Concentrated MycoFluor™ reagent (supplied) was brought to room temperature before being diluted 1 in 20 in each well and incubated for 10 min. Adherent cells attached to cover slips were then removed, mounted on glass slides and sealed with supplied sealant, previously melted. Positive control slides were prepared pipetting 5 µl of mycoplasma MORFS (supplied) onto a glass slide before covering and sealing with a cover slip. Slides were visualised on a Nikon Eclipse 80i fluorescence microscope (Nikon, Surrey UK) with a 365 nm excitation filter and a band-pass filter at 100x oil immersion magnification. Images were captured on a Photometrics Coolsnap ES digital camera (Photometrics, Tucson, USA).

4.2.3 Mycoplasma Screen by Colorimetric Assay

Colorimetric mycoplasma testing was performed by Sam Drennan of the Cancer Research group (Daisy Building, Castle Hill Hospital, Cottingham, UK) using a MycoProbe™ detection kit (R&D, Abingdon, UK). Briefly, after washing a 24 well tissue culture plate twice with wash buffer, 50 µl of diluted detection probes were added to

each well. Sample (cell culture supernatant collected and diluted 10x with cell lysis diluent) and controls were then added to corresponding wells (150 μ l) and incubated at 65°C for 60 min. Samples were then transferred (150 μ l) to a streptavidin coated plate and incubated at room temperature for 60 min with gentle agitation. The plate was then washed before further incubations at room temperature with gentle agitation of anti-digoxigenin conjugate added (200 μ l; 60 min.), substrate solution (50 μ l; 60 min.) and amplifier solution (50 μ l; 30 min.). Finally, stop solution was added (50 μ l) and optical density measured on a micro-plate reader with 490 nm filter subtracting readings at 650 nm to allow for corrections. Average readings from duplicate samples or controls were then calculated before subtracting the negative control reading. Samples reading <0.05 were deemed negative, 0.05-0.1 inconclusive and >0.1 positive for mycoplasma infection.

4.2.4 TEM

PMA/THP-1 cells and untreated Daisy cells were cultured to 80% confluence in T75 tissue culture flasks containing 20 ml culture media at a cell density of 0.5×10^6 cells/ml. Conditions of culture are described in 2.1. Cells were detached by replacement of culture media with ice cold calcium and magnesium-free PBS. Flasks were refrigerated and periodically agitated until cell detachment was complete. Detached cells were then centrifuged (400 x g; 5 min.) and transported on ice. Transmission electron microscopy was then performed as stated in 2.4 of the general methods chapter.

4.2.5 Assessment of Phagocytic Ability

PMA/THP-1 and Daisy cells were cultured, incubated with zymosan beads and differentially stained as described in 2.12 and 2.13. Quantification of phagocytosis was performed by calculating the phagocytic index. The number of beads seen in each of 100 cells was counted and divided by 100 to give the average number of beads per cell. This was performed on 3 separate slides created on 3 separate

occasions. The mean of the scores was then calculated and an unpaired, 2 tailed t-test performed for samples with unequal variance using Microsoft Excel 2010 software.

4.2.6 Assessment of Lipid Uptake

The ability of PMA/THP-1 and Daisy cells to take up unmodified lipid was assessed. PMA/THP-1 cells and untreated Daisy cells were cultured in wells of a 24 well tissue culture plate containing sterile glass cover slips. Conditions of culture are described in 2.1.1. Cells were incubated with 10% v/v Calogen lipid rich liquid meal for a sub-optimal treatment time of 4 hours before being washed and stained as described in 2.6. Cells were then scored as described in 2.7. Slides from each of 24 wells of a 24 well tissue culture plate were scored and 3 plates were tested on 3 separate occasions. The mean of the scores was then calculated and an unpaired, 2 tailed t-test performed for samples with unequal variance using Microsoft Excel 2010 software.

4.2.7 Assessment of Opsonised Antigen Binding

PMA/THP1 and untreated Daisy cells were assessed for their ability to bind opsonised antigen. Fluorescent labelled opsonised antigen was generated in house as described in 2.8 and its binding to cells was analysed by flow cytometry as described in 2.10. The mean fluorescence was subjected to an unpaired, 2 tailed t-test performed on separate cell combinations for samples with unequal variance using Microsoft Excel 2010 software.

4.2.8 Cell Surface Immunophenotype

Cell surface Immunophenotype of untreated THP-1 cells, PMA/THP-1 cells and untreated Daisy cells was assessed by flow cytometry as described in 2.10. Data was entered into SPSS Statistics version 19 software and statistically significant differences in cell surface molecule expression were calculated. Initially, an independent samples Kruskal-Wallis test was performed to highlight significant

differences in expression across all 3 cells types. Subsequent post hoc testing using Mann-Whitney was then used to identify specific differences in expression.

4.2.9 Gene Microarray

Untreated THP-1 cells, PMA stimulated THP-1 cells and Daisy cells were analysed for gene expression profiles as described in 2.16. Data was filtered using Microsoft Excel 2010 software to compare differences in gene expression by the fold change.

4.3 Results

4.3.1 Morphology of Daisy versus THP-1 cells by Light Microscopy

Morphology of the new 'Daisy' THP-1 sub-clone was assessed by light microscopy comparing Daisy cells with both native THP-1 cells and THP-1 cells stimulated with PMA. Images of these observations can be seen in *figure 4.1*. Native THP-1 cells (A) appeared classical in morphology growing predominantly in suspension and round, un-clumped cells with a small proportion of cells (<5%) very loosely adhering to the bottom of the tissue culture flask. Such cells became detached upon gentle agitation.

THP-1 cells stimulated with PMA (B) appeared slightly larger than native THP-1 cells and were firmly adhered to the tissue culture flask. These cells also appeared to clump together and were flattened with some pseudopodia.

Daisy cells (C) appeared distinct in that whilst a large proportion of cells grew in suspension and resembled native THP-1 cells, a monolayer of cells firmly adhered to the tissue culture flask. The adherent fraction of cells appeared larger and more flattened than the suspended cells however did not clump together and showed relatively long pseudopodia, in some cases appearing as long stretched out cells.

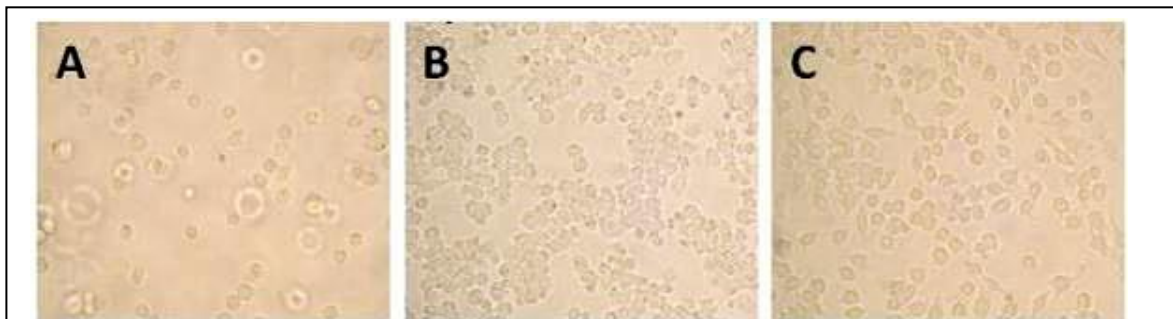


Figure 4.1 – Morphology of Daisy cells by light microscopy

THP-1 cells (A) appear predominantly suspended with some loosely adherent, flattened cells making up no more than 5% of the total cells. When treated with 50 nM PMA for 24 hours (B) and allowed 24 hours recovery, THP-1 cells become adherent forming 'clumps' with increased cytoplasm and inhibited mitotic growth. Daisy cells (C) originally thought to be THP-1 cells show predominantly strongly adherent cells with a flattened morphology and pseudopodia without 'clumping'.

4.3.2 Mycoplasma Screening

Given the unusual cell culture behaviour of the Daisy cells, mycoplasma infection was suspected when no bacterial infection was observed. Mycoplasma was screened for using 2 separate methods for clarity. Results of the first screen using a MycoFluor™ Mycoplasma Detection Kit (Molecular Probes) can be seen in *Figure 4.2*. Mycoplasma morphs (A), supplied by the manufacturer as a positive control, appeared as tiny fluorescent specs ranging from 0.1-0.3µm at 60x magnification. Under the same settings mycoplasma infected HEK cells (B) showed specs similar in size to the control morphs along with large fluorescent cell nuclei of approximately 2µm in diameter. Daisy cells (C) showed only large fluorescent cell nuclei.

Using a colorimetric method of detection, as seen in *figure 4.3*, positive controls were red in colour and had an optical density of 1.8 which was above the 1.5 cut-off value described in the supplier's manual. The negative control whilst still showing some colouration had a value of 0.4 which was below the 0.5 cut-off value described in the manufacturers manual. Both THP-1 and Daisy cells showed no colouration and had an optical density of 0.3, below that of the negative control.

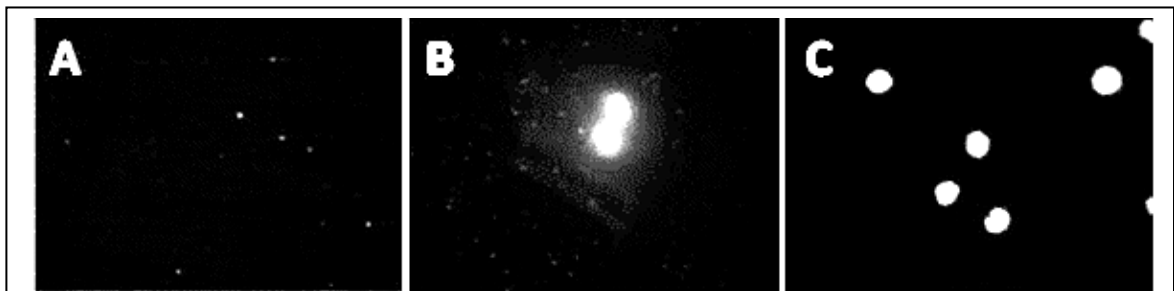


Figure 4.2 – Mycoplasma testing of Daisy cells by fluorescence microscopy

Mycoplasma morphs (A), supplied by the manufacturer as a positive control, appear as tiny fluorescent specs ranging from 0.1-0.3µm at x60 magnification. Under the same settings mycoplasma infected HEK cells show specs similar in size to the control morphs along with large fluorescent cell nuclei of approximately 2µm in diameter. Daisy cells (C) show only large fluorescent cell nuclei concluding that these cells are mycoplasma negative.

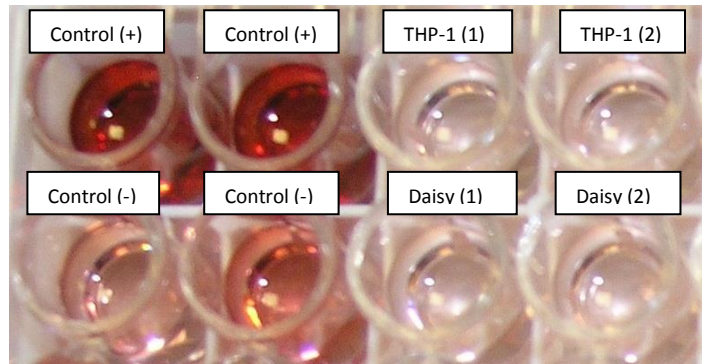


Figure 4.3 - Mycoplasma testing of Daisy and THP-1 cells by colorimetric micro-plate assay

Cell culture supernatants were tested for mycoplasma infection using a MycoProbe™ kit (R&D). Readings were calculated by subtracting the negative control average value from the sample average value. Final readings were positive control – 1.8, negative control 0.4, THP-1 cells -0.3 and Daisy cells - 0.3 confirming assay success and no mycoplasma infection.

4.3.3 Morphology of Daisy versus PMA/THP-1 cells by TEM

TEM was then performed on THP-1 cells stimulated with PMA and untreated Daisy cells. Results can be seen in *figure 4.4*. Cells appeared similar in size and shape both with crescent shaped nuclei. The nuclei of the PMA/THP-1 cells showed large areas of loosely coiled euchromatin, appearing as light grey areas, whilst Daisy cells showed a high degree of tightly coiled heterochromatin, appearing as dark grey areas. The membrane of PMA/THP-1 cells showed some ruffling whilst the Daisy cells showed a high degree of ruffling and pseudopodia. Both cells showed round vesicular inclusions within the cytoplasm of various sizes however they appeared to a higher degree in Daisy cells. Cholesterol clefts appearing as long thin clear sections in the cytoplasm also appeared in both cell types, yet again, to a higher degree in Daisy cells.

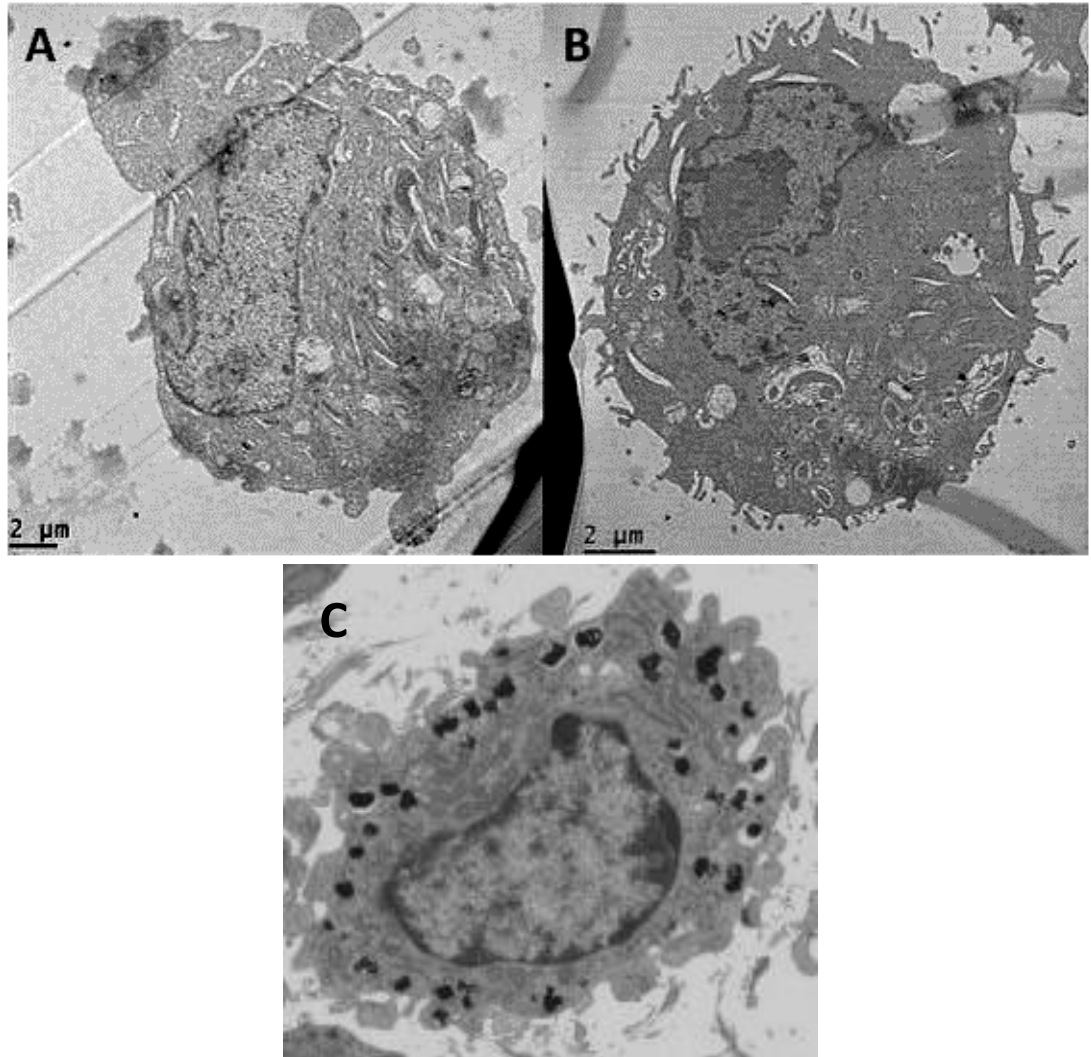
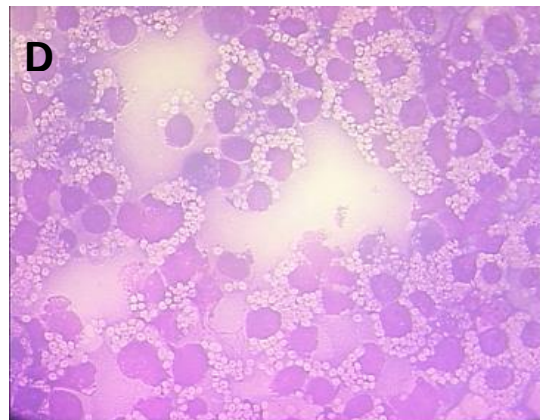
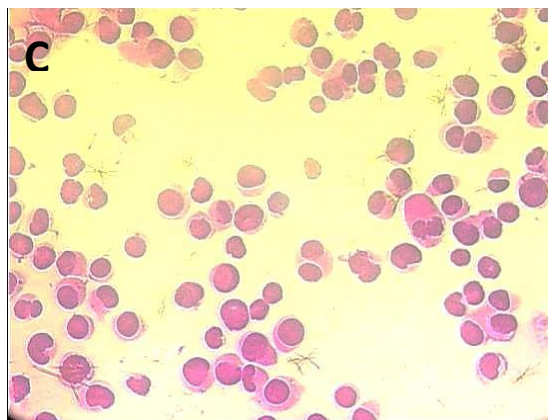
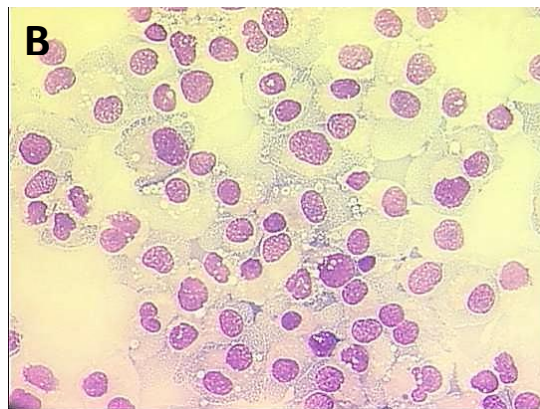
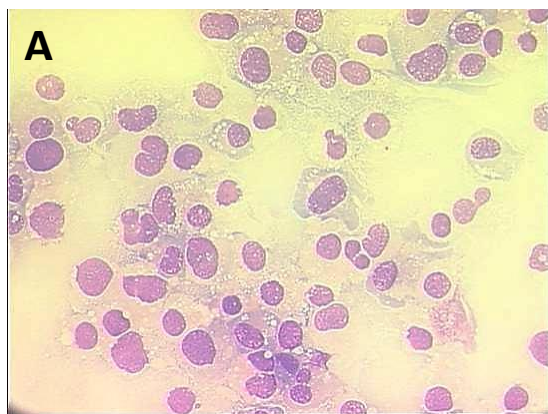


Figure 4.4 – Morphology of Daisy cells by transmission electron microscopy

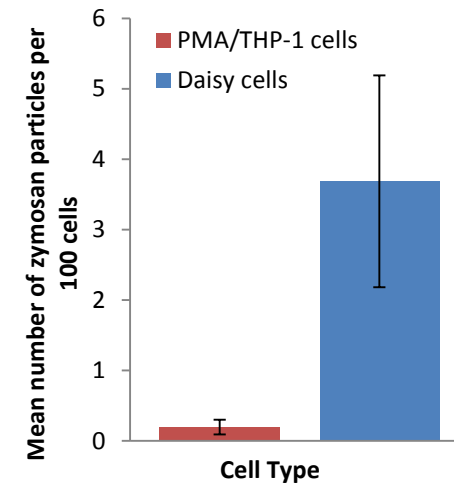
THP-1 cells (A) treated with PMA (50nM;24h) appear approximately 14μm in diameter with a large crescent shaped nucleus containing predominantly euchromatin. The cell membrane is slightly ruffled and there appears a number of vesicular inclusions and cholesterol clefts. Daisy cells (B) appear similar in size, shape and granularity however show a higher proportion of heterochromatin, pseudopodia and vesicular inclusions. Both (A) and (B) show similarities with a human macrophage (C) taken from (Gschmeissner)

4.3.4 Assessment of phagocytosis

The ability of the cells to phagocytose micro-particles was investigated using zymosan, a commercially available yeast cell preparation. Results can be seen in *figure 4.5*. PMA/THP-1 and Daisy cells were incubated with zymosan particles as described in 2.13 and differentially stained as described in 2.12. A phagocytic index was calculated by counting the number of zymosan particles within the cytoplasm of 100 cells and dividing this by 100 to give an average. Whilst PMA/THP-1 cells showed some phagocytosis, few particles per cell were observed and a large number of cells showed no phagocytosis. Daisy cells showed a large number of cells containing many zymosan particles although variation across 3 separate experiments was high. Statistically there was no difference between the phagocytic index of the 2 cell types.



Phagocytic Index



	PMA/THP-1	Daisy
mean	0.20	3.69
median	0.13	4.2
range	0.06-0.4	0.86-6
std dev	0.18	2.6

Figure 4.5 – Assessment of Phagocytic capability of THP-1 and Daisy cells

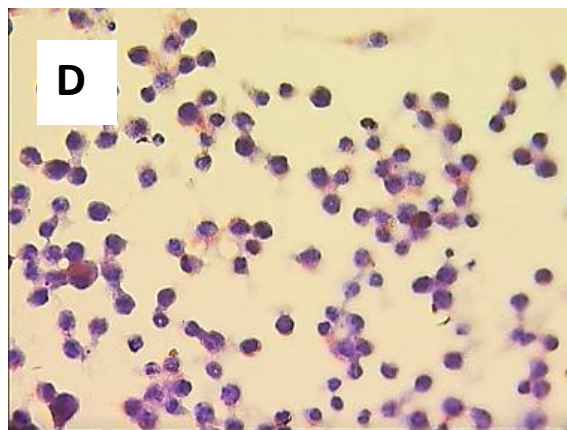
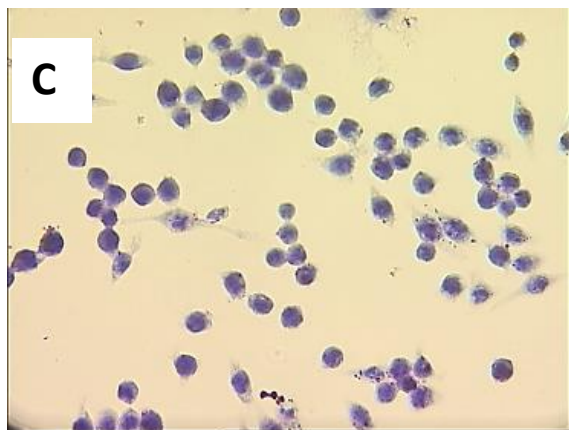
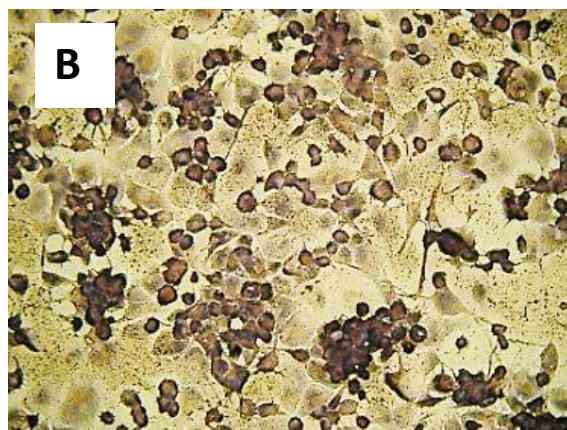
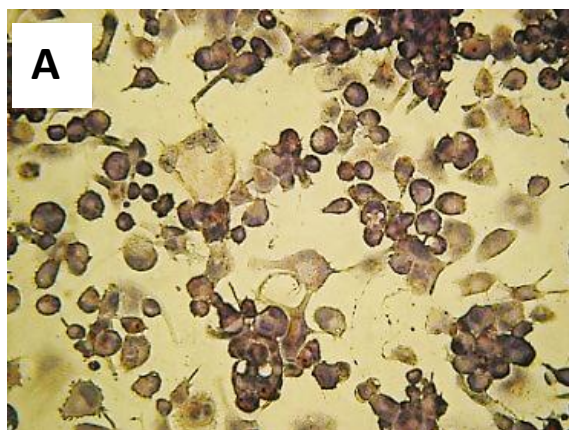
PMA (50nM;24h) treated THP-1 cells (A) were differentially stained and compared to (B) THP-1 cells treated with PMA and zymosan (1 ng/ml;1h). (C) Untreated Daisy cells were also stained and compared with (D) Daisy cells treated with zymosan. Zymosan treated cells show phagocytosis of zymosan particles appearing as small purple dots surrounded by a white ring, approximately 3µm in diameter at 40X magnification, contained within the cell cytoplasm. A phagocytic index was calculated (graph, right) by counting the number of zymosan particles within the cytoplasm of 100 cells and dividing this by 100 to give an average. Whilst THP-1 cells showed some phagocytosis, Daisy cells showed a marked though not significant increase in phagocytosis by comparison.

4.3.5 Assessment of lipid uptake

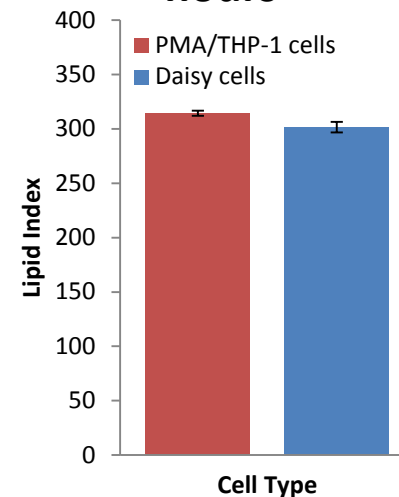
Lipid uptake was assessed comparing PMA/THP-1 cells with Daisy cells. Cells were incubated for 4 hours with Calogen high fat liquid meal before being washed and stained with ORO and haematoxylin. This was repeated on 3 separate occasions. Slides were then scored and a mean calculated across 3 x 24 slides for each cell type. The results can be seen in *figure 4.6*. Both cells accumulated lipid after 4 hours with the majority of cells showing between 50-75% lipid staining. Statistical analysis showed no significant difference in the amount of lipid accumulation between the 2 cell types.

4.3.6 Opsonised Antigen Binding Capacity

The ability of PMA/THP-1 and untreated Daisy cells to bind opsonised antigen was compared and the results can be seen in *figure 4.7*. Opsonised antigen was created *in vitro* incubating biotin labelled BSA with FITC labelled mouse anti-biotin monoclonal antibody. Cells were then incubated with the BSA/antibody complex and binding was assessed using mean fluorescence values obtained by flow cytometry. This was repeated on 5 separate occasions. THP-1 cells both untreated and PMA stimulated bound very little opsonised antigen, with mean fluorescence between 36-110 arbitrary units. Statistically no difference was seen between these 2 cell types. However, Daisy cells showed very high opsonised antigen bind in the region of 1030-4010 arbitrary fluorescence units, an increase statistically significant to $p=0.02$.



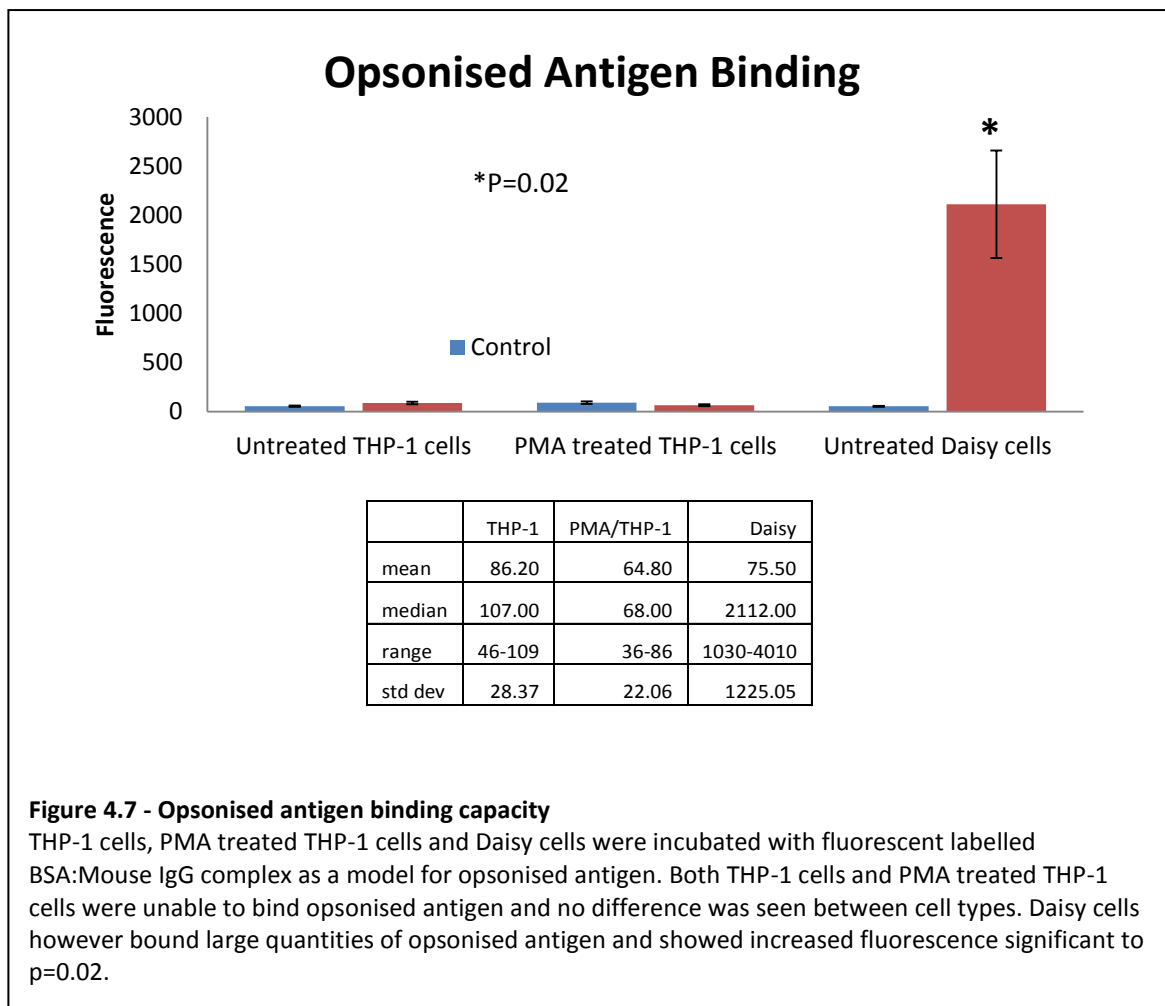
Lipid Index at 4 hours



	PMA/THP-1	Daisy
mean	314.50	301.57
median	321.00	318.50
range	267-338	228-349
std dev	19.93	48.00

Figure 4.6 – Assessment of lipid uptake of THP-1 and Daisy cells

PMA (50nM;24h) treated THP-1 cells (A) were stained with oil red o and hematoxylin and compared with cells treated with 10 % v/v Calogen (B), a high fat liquid meal containing sunflower and canola oil for 4 hours. Untreated Daisy cells (C) were also stained and compared with Calogen treated cells (D). Slides were then scored and a mean calculated across 3 x 24 slides for each cell type. Statistical analysis showed no significant difference in the amount of lipid accumulation between the 2 cell types.



4.3.7 Cell Surface Immunophenotype

Cell surface immunophenotype of untreated THP-1, PMA/THP-1 and untreated Daisy cells was compared using flow cytometry to assess expression levels of key cell markers. Results can be seen in *figure 4.8*. All 3 cell types showed differing expression profiles. PMA/THP-1 cells show significant increases in CD14, CD11b, CD36 and CD86 with decreased CD32 expression compared with untreated THP-1 cells. Daisy cells showed decreased CD14 and CD11b with increased CD80, CD163 and CD206 expression when compared with PMA/THP-1 cells.

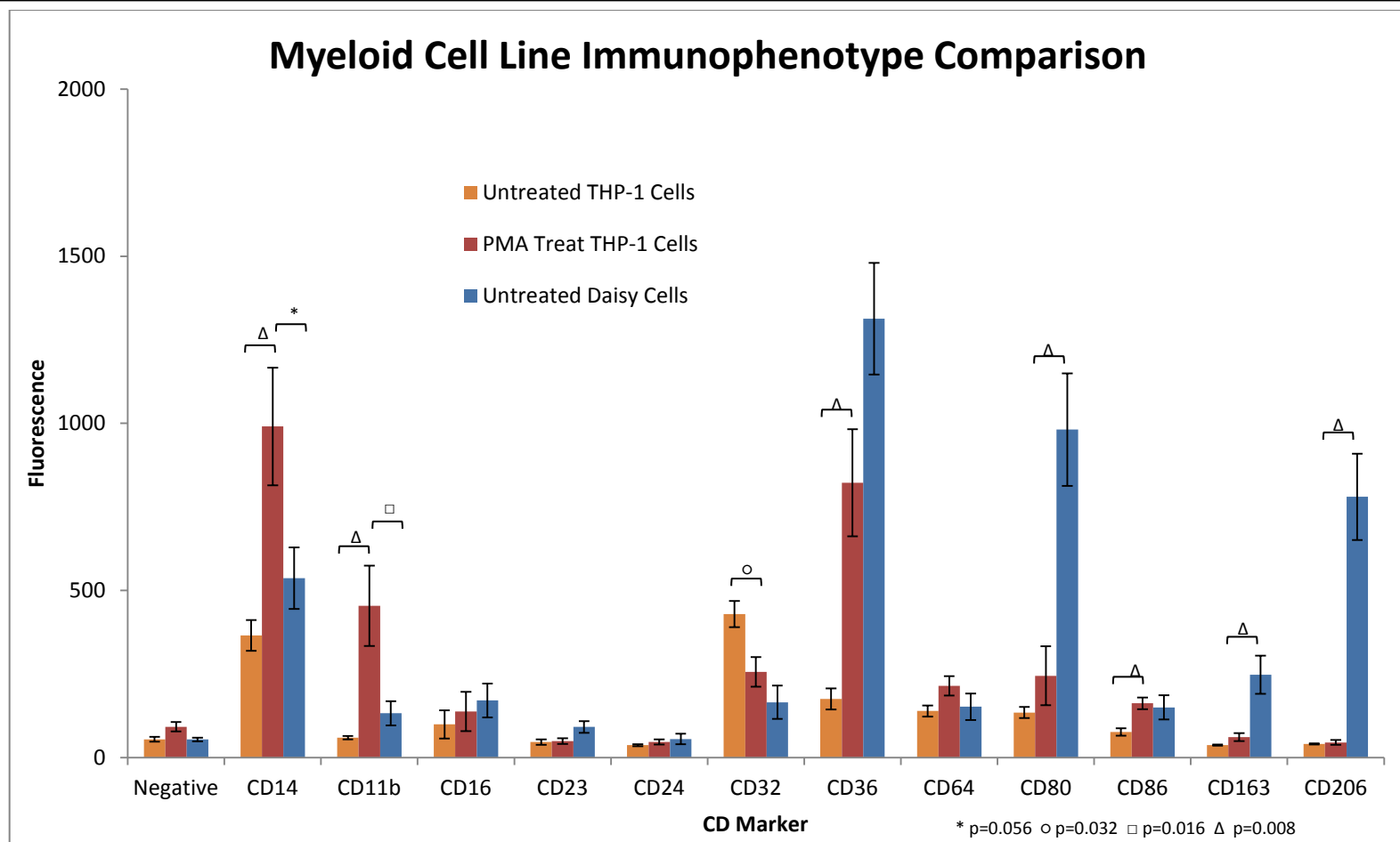


Figure 4.8 – Cell surface immunophenotype

PMA stimulated (50µg/ml; 24h followed by 24h recovery) THP-1 cells show significant increases in CD14, CD11b, CD36 and CD86 with decreased CD32, compared with native THP-1 cells. Compared with untreated, differentiated cells, Daisy cells show decreased CD14 and CD11b with increased CD80, CD163 and CD206.

4.3.8 Gene Microarray Data Analysis

To determine the extent of the genetic differences between the new Daisy cells and their progenitor THP-1 cells with or without PMA stimulation, mRNA was extracted and sent for microarray analysis using a Agilent microarray system. Data was analysed using Microsoft Excel 2010 to count genes which were either up or down regulated by categorical fold changes. The result can be seen in *figures 4.9-4.11*. Upon PMA stimulation of THP-1 cells 7863 genes showed fold change differences of 2 or greater. The majority of these genes were 2-3 fold different and decreasing in number as fold change increased. When comparing untreated THP-1 cells to Daisy cells the difference in gene expression was considerably higher. A total of 39797 genes showed a difference of greater than 2 fold, however the greatest number of genes showed a 10-20 fold change difference in expression. In addition 1793 genes showed over a 100 fold change compared to 47 in the previous comparison. When comparing PMA/THP-1 cells with Daisy cells a total of 39761 genes were expressed with at least a 2 fold change difference, with the majority having 10-20 fold change difference and almost equal number of genes having 5-10 fold change difference.

Difference in Gene Regulation of PMA/THP-1 Cells Compared with THP-1 Cells

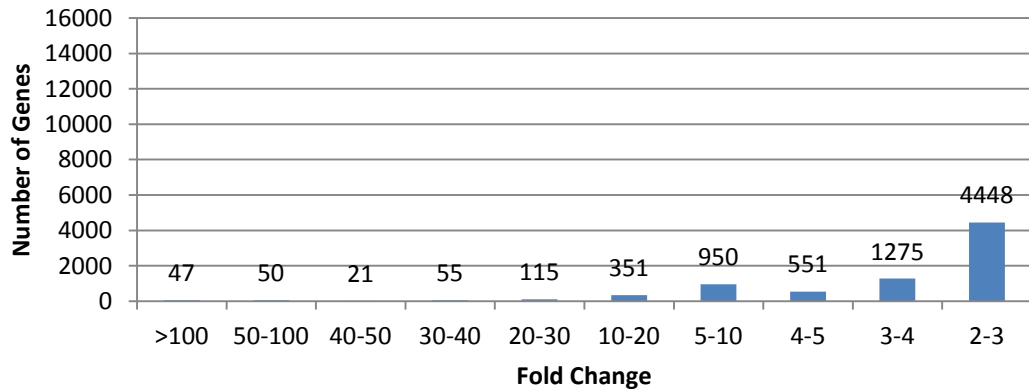


Figure 4.9 – Gene array analysis comparing PMA/THP-1 cells with THP-1 cells

Gene microarray analysis of PMA-THP-1 and THP-1 cell mRNA showed 7863 genes with fold change differences of 2 or greater. The 4448 of these genes were 2-3 fold different, with numbers of genes decreasing in number as fold change increased. 47 genes showed over a 100 fold change.

Difference in Gene Regulation of THP-1 Cells Compared with Daisy Cells

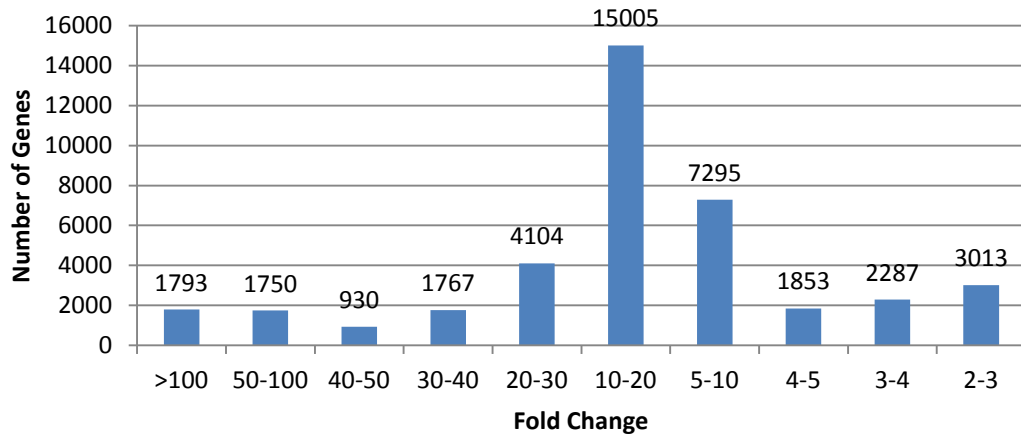


Figure 4.10 – Gene array analysis comparing THP-1 cells with Daisy cells

Gene microarray analysis of THP-1 and Daisy cell mRNA showed a total of 39797 genes with fold change differences of greater than 2 fold. The greatest number of genes showed a 10-20 fold change difference in expression. 1793 genes showed over a 100 fold change.

Difference in Gene Regulation of PMA/THP-1 Cells Compared with Daisy Cells

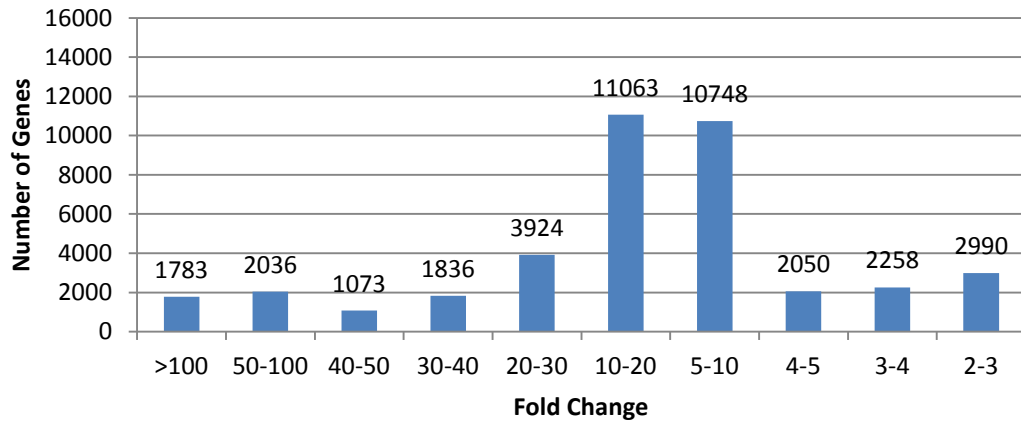


Figure 4.11 – Gene array analysis comparing PMA/THP-1 cells with Daisy cells

Gene microarray analysis of PMA/THP-1 and Daisy cell mRNA showed a total of 39761 genes with fold change differences of greater than 2 fold. The greatest number of genes showed a 10-20 fold change difference in expression however almost equal number of genes showed a 5-10 fold change difference. 1783 genes showed over a 100 fold change.

4.4 Discussion

In vitro experiments using human macrophages currently require mitogenic stimulation of a macrophage precursor cell line or *ex vivo* maturation of circulating primary monocytes. We have derived a unique sub-clone of the THP-1 cell line capable of spontaneous perpetual differentiation into macrophage-like cells termed 'Daisy'. Having confirmed that the cells were not activated by mycoplasma, characterisation of this cell line was performed in order to validate its use in this and future projects as an alternative to PMA stimulated THP-1 cells.

Morphologically these cells adhere to cell culture plastic in the absence of PMA stimulation, unlike unstimulated THP-1 cells, which would indicate monocyte to macrophage maturation. Upon closer inspection by TEM these cells show similar structural morphology to PMA stimulated THP-1 cells and both compared well with published images of human macrophages. However a higher proportion of euchromatin was seen in PMA stimulated THP-1 cells which would signify increased DNA transcription processing. The significance of this finding is that PMA stimulation is potent and long lasting, which may mask any subsequent activity during *in vitro* experiments. Daisy cells showed much less loosely coiled chromatin which could indicate these cells are in a more 'resting' state which may be advantageous in the experimental setting.

A fundamental role of a mature macrophage is to phagocytose foreign and damaged self-material and so it was necessary to determine whether the Daisy cells were capable of phagocytosis. Cells were incubated with yeast derived zymosan particles and a phagocytic index was determined as a method of quantification. Daisy cells were capable of phagocytosis with many cells ingesting many particles. In comparison PMA/THP-1 cells also showed phagocytic capability although cells ingested fewer particles. This difference was not statistically significant however, probably due to a higher variation in the phagocytic index of the daisy cells. This variation could be due to that fact that whilst both cell types were initially seeded at the same cell density, Daisy cells continued to proliferate whereas PMA stimulated THP-1 cells did

not. Therefore Daisy cells had the potential to outgrow the nutrient supply of the culture media which may have inhibited phagocytic activity to deferring degrees during repeat experiments.

The ability to ingest lipid was also compared as an indication of cell maturity as macrophages are well known to accumulate lipid in diseases such as atherosclerosis. In this instance both cell types were equally capable of lipid accumulation as demonstrated with ORO staining and lipid index quantification methods.

The ability of macrophages to bind opsonised antigen was determined not by specific IgG receptor expression measurements but by incubation of the cells with fluorescent antibody coated BSA particles. The reason for this was that there are a number of specific opsonised antigen receptors on the cell surface however we were interested initially in the cells' general binding capacity only, rather than specific receptor binding. Surprisingly PMA/THP-1 cells were barely able to bind these particles despite subsequently showing expression of all three IgG receptors (CD16, CD32 and CD64). However, Daisy cells were able to bind large amounts of opsonised antigen indicating a significant difference between the two cell types and one which needs further investigation.

Cell surface phenotype studies were undertaken by FACS analysis. A panel of antibodies were chosen to indicate myeloid cell origin (CD11b, CD14 and absence of CD24), cell maturity (CD16, CD23 and CD64) and macrophage activation (CD163 and CD206) in addition to investigating the expression of co-stimulatory molecules (CD80 and CD86) and a known lipid receptor (CD36). These experiments showed significant differences between un-stimulated THP-1 cells, PMA/THP-1 cells and Daisy cells. Firstly upon PMA stimulation THP-1 cells showed a significant increase in CD14, the lipopolysaccharide receptor, and CD11b, one of the major cell adhesion molecules expressed by macrophages. The latter was expected as monocytes become adherent with macrophage differentiation however an increase in CD14 was not expected as mature macrophages would ordinarily down-regulate expression of this

molecule. Daisy cells showed similar expression levels of both these molecules to that of un-stimulated THP-1 cells despite being adherent in contrast. Perhaps CD11b then is not the major cell adherence molecule isotype expressed by these cells but one of either CD11a or CD11c. As discussed in *chapter 1.4.6.* mature tissue macrophages down-regulate CD11b and up-regulate CD11c which could indicate a more mature macrophage phenotype of Daisy cells over PMA stimulated THP-1 cells. Expression of the 3 IgG receptors was similar across all cell types except that un-stimulated THP-1 cells showed a higher expression of CD32. Also very little IgE receptor was expressed by any of the cells but was expected due to relatively low levels of circulating IgE antibody *in vivo*. No CD24, the granulocyte adhesion molecule, was seen in any of the cells either, and coupled with CD14 expression, this confirms the myeloid origins of our Daisy cells as this molecule is only expressed by cells of the monocyte/macrophage lineage. A significant increase in expression of CD36, the macrophage lipid scavenger receptor, was seen in THP-1 cells with PMA stimulation and a similarly high expression was seen in Daisy cells. With regards to activation untreated THP-1 cells showed no expression of markers of activation, as expected. Upon PMA stimulation, THP-1 cells showed an increase in expression of CD86, a co-stimulatory molecule required for anti-inflammatory T-cell differentiation. Un-stimulated Daisy cells however, showed high expression of CD80, a co-stimulatory molecule required for pro-inflammatory T-cell differentiation. In contrast, Daisy cells also showed expression of alternative (anti-inflammatory) activation markers CD163 and CD206. These were not expressed by THP-1 cells stimulated or not.

Lastly, during gene array analysis, THP-1 cells showed at least a 2 fold up/down regulation of 7863 genes when stimulated with PMA. Daisy cells expressed almost 40000 genes with at least a 2 fold difference in levels of transcription regardless of whether we compared them to THP-1 cells or PMA stimulated THP-1 cells. This demonstrates that the Daisy cell line has become distinct, on a genetic level, from its progenitor the THP-1 cell. The phenotypical result of these genetic differences is currently unclear and further pathway analysis is required.

In conclusion, Daisy cells are genetically distinct cells which appear to be macrophage-like cells morphologically, functionally and phenotypically. Phagocytosis, lipid accumulation and opsonised antigen binding assessments all show these cells to be functionally mature. Whilst DNA transcription activity appears low by TEM, phenotype analysis shows these cells to be active in, most likely, an alternative fashion. It is our opinion that the Daisy cells have potential utility for this and future studies with the ability to spontaneously replicate and differentiate, these cells could eliminate the need for constant blood donation in human macrophage research and eliminate cell signalling interference by PMA stimulation.

In the context of studying aspiration, Daisy cells appear to be superior in that they accumulate lipids equally as well as the PMA stimulated counterparts, though have a greater ability to bind and phagocytose other particulate matter. As previously discussed, during reflux events a number of substances may be aspirated into the airways and cleared away by airway resident macrophages. These particles have the potential to induce an inflammatory response or modify an existing response via macrophages. Primary macrophages are the ideal tool for studying such effects though in our studies have proven to be difficult to obtain in useful quantities. Daisy cells would therefore serve as a readily available tool to uncover the effect of such aspirated materials *in vitro*.

5 Lipid Laden Macrophages in Respiratory Disease

5.1 Introduction

Using the lipid laden macrophage scoring system (LLAMI) first described by Colombo and Hallberg (1987), studies to quantify the levels of macrophage ingested lipids in the airways have so far been somewhat inconclusive. The combined findings show an unquestionable presence of lipid laden macrophages in respiratory disease, however, the diagnostic use of the LLAMI in GOR is still debatable. Undoubtedly, the varying reports have had differing patient inclusion/exclusion criteria, in addition to differing methods of GOR diagnosis, which may contribute to the lack of specificity.

We wanted to undertake a study to include patients diagnosed with GOR based on clinical history and Hull Airway Reflux Questionnaire (HARQ) scores (Morice et al., 2011), without reference to oesophageal pH studies which exclude patients with silent or non-acid reflux. Using excess BAL fluid taken from patients undergoing diagnostic bronchoscopy to extract cells from the airway, we proposed to determine whether a greater LLAMI could be attributed to reflux of both the acid and non-acid phenotype collectively.

5.2 Methods

5.2.1 Patient Recruitment

All patients attending the specialist cough clinic to undergo diagnostic bronchoscopy procedures in the Endoscopy department, Castle Hill hospital between June 2009 and June 2011 were approached for recruitment to the study. Written consent was obtained by the attending physician for the use of any excess broncho-alveolar lavage (BAL) fluid for research purposes. Patients were also asked to complete the HARQ prior to sedation which can be seen in *figure 5.1*. Patient data was collected post-diagnosis and anonymised for the purposes of this study. Whilst many patients consented to donate excess lavage fluid, this was not always possible due to difficulties with the procedure. Insufficient samples were discarded though this was purely random. During sample collection and analysis patient history and diagnosis was unknown therefor this was essentially a blind study.

5.2.2 Lipid Staining and Indexing

Primary cells were collect by broncho-alveolar lavage and isolated as described in 2.15. Cells were mounted onto glass slides as described in 2.11 before being stained with ORO and quantified using the lipid index scoring system as described in 2.6 and 2.7 respectively.

5.2.3 Statistical Analysis

Acquired data was entered into a statistical data base and analysed using IBM SPSS version 19 software. Firstly, Spearman rank order correlations were performed in order to determine significant correlations between any of the variables. Secondly, a Mann-Whitney test was performed to compare means within groups i.e. GOR and non-GOR.

REFLUX COUGH QUESTIONNAIRE

Name: _____

D.O.B: _____ UN: _____

DATE OF TEST: _____

Please circle the most appropriate response for each question

Within the last MONTH, how did the following problems affect you?						
0 = no problem and 5 = severe/frequent problem						
Hoarseness or a problem with your voice	0	1	2	3	4	5
Clearing your throat	0	1	2	3	4	5
The feeling of something dripping down the back of your nose or throat	0	1	2	3	4	5
Retching or vomiting when you cough	0	1	2	3	4	5
Cough on first lying down or bending over	0	1	2	3	4	5
Chest tightness or wheeze when coughing	0	1	2	3	4	5
Heartburn, indigestion, stomach acid coming up (or do you take medications for this, if yes score 5)	0	1	2	3	4	5
A tickle in your throat, or a lump in your throat	0	1	2	3	4	5
Cough with eating (during or soon after meals)	0	1	2	3	4	5
Cough with certain foods	0	1	2	3	4	5
Cough when you get out of bed in the morning	0	1	2	3	4	5
Cough brought on by singing or speaking (for example, on the telephone)	0	1	2	3	4	5
Coughing more when awake rather than asleep	0	1	2	3	4	5
A strange taste in your mouth	0	1	2	3	4	5

TOTAL SCORE _____ /70

Figure 5.1 – Hull Airway Reflux Questionnaire

Patients recruited to the study were asked to fill in the HARQ prior to sedation and bronchoscopy.

5.3 Results

5.3.1 Primary Cell Isolation

Primary alveolar macrophages were obtained from patients by BAL as described in 2.15. To assess the cellular composition of the samples, slides produced were differentially stained and counted, examples of which can be seen in *figure 5.2*.

Macrophage populations were around 70% in the majority of samples, except where neutrophilic and/or red cell contamination was present. In these cases, the macrophage population was reduced to around 30% of the total cells. Average macrophage counts from BAL fluid were obtained by multiplying the total cell count by the percentage of macrophages counted on the differential stained slide. This was found to be around 1×10^5 macrophages per ml of lavage fluid collected. The amount of lavage collected was usually between 5-10 ml.

5.3.2 Lipid Scoring of Patient BAL Samples

Patient BAL samples collected were processed as described above and 2 cytopsin slides were produced for each sample. One slide was stained with a differential staining kit and the other slide stained with ORO lipid stain. The latter was examined under light microscopy and scored according to the lipid index scoring system described in 2.7. Examples of lipid staining of primary human macrophages in this manner can be seen in *figure 5.3*.

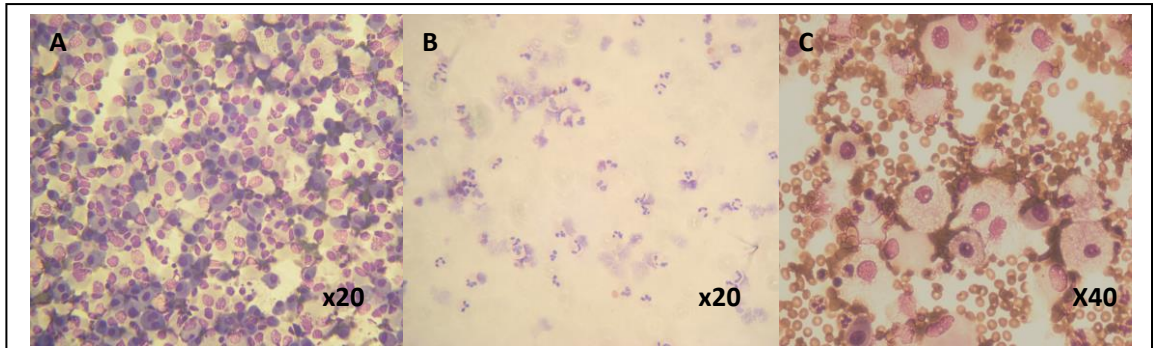


Figure 5.2 – Cellular composition of BAL samples.

BAL samples were collected from patients undergoing bronchoscopy. Samples were processed, counted and stained with a cell differential staining kit as described in the methods. Cellular composition of a relatively healthy patient (A) showed around 70-90% macrophages. From patients with infectious airway disease (B) the predominant cell population was neutrophilic with around 30% macrophages. Where patients were suspected to have a malignant tumour of the airway, blood contamination was common (C).

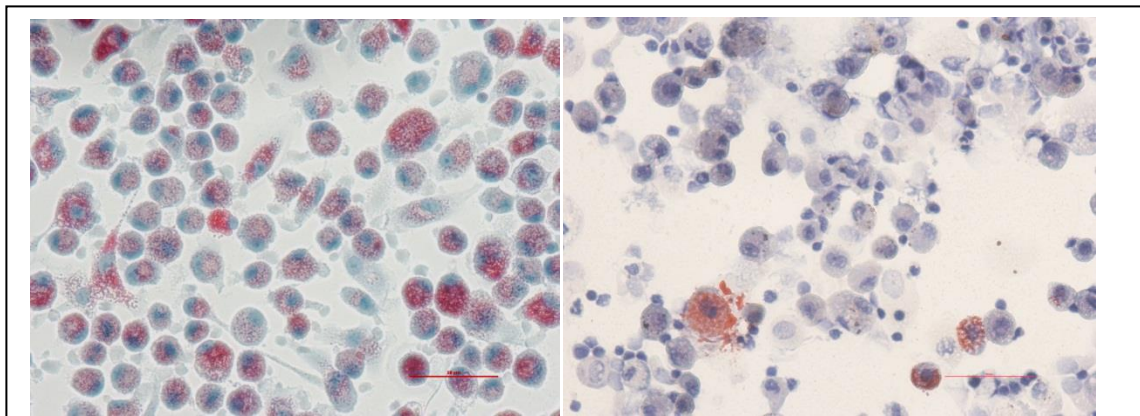


Figure 5.3 – Primary Alveolar Macrophages Stained with Oil Red O and Hematoxylin.

Random patient BAL samples were processed mounted onto glass slides using Cytospin methodology. Cells were stained for lipids using Oil Red O and counterstained with Mayers Hematoxylin. Lipid droplets stained vivid red and were easily distinguishable against the purple counterstain. Patients showed a high degree of variability of lipid accumulation. Patient (A) shows many cells with lipid accumulation whilst patient (B) shows only a few cells with lipid accumulation.

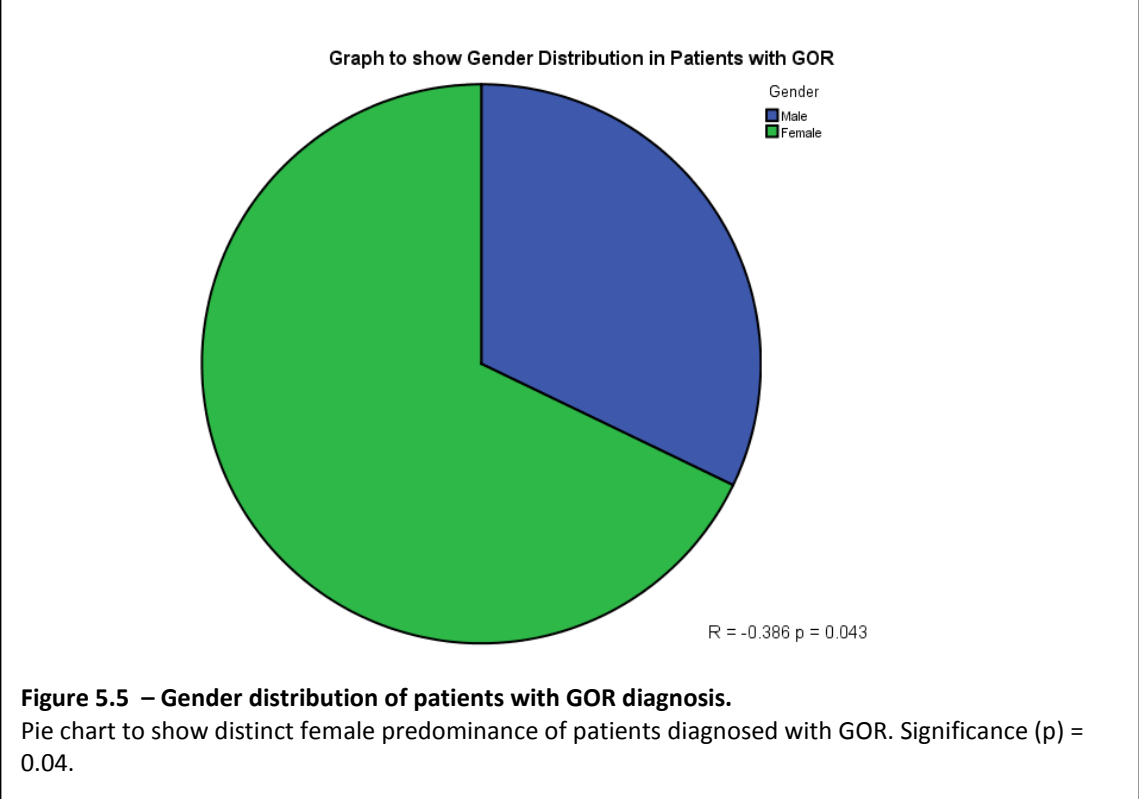
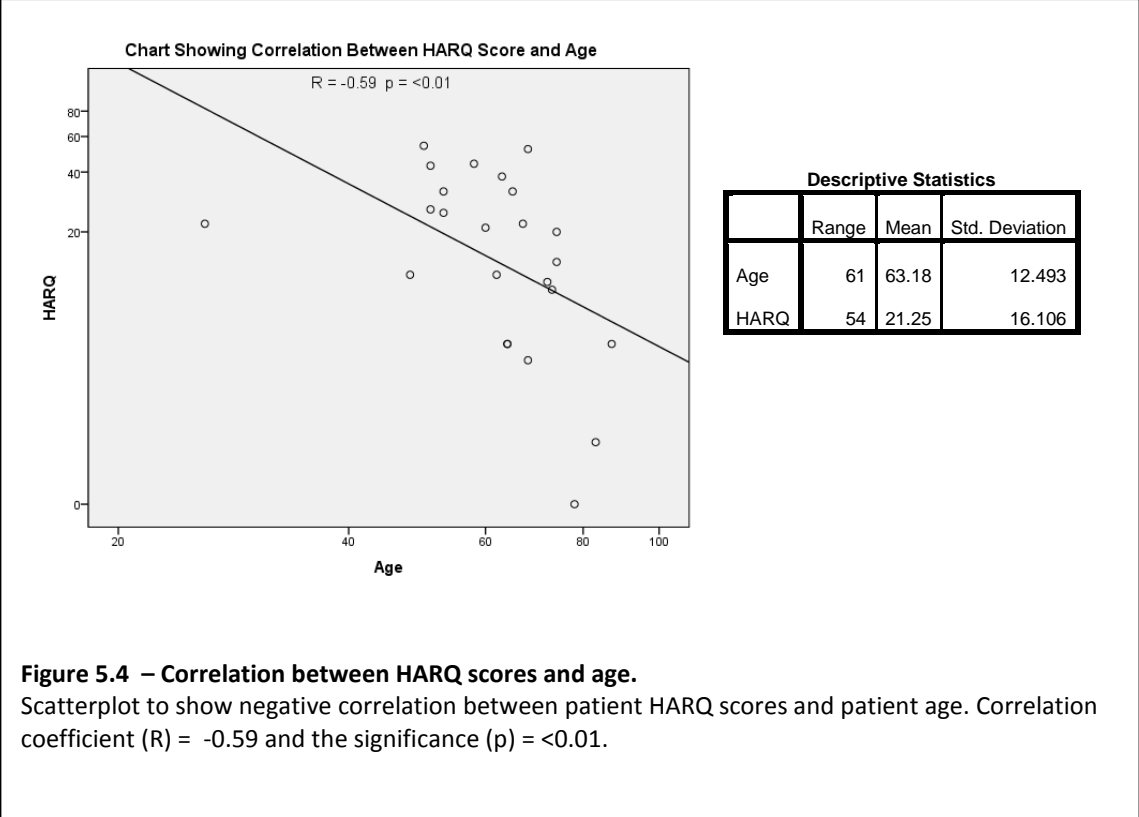
5.3.3 Statistical Analysis

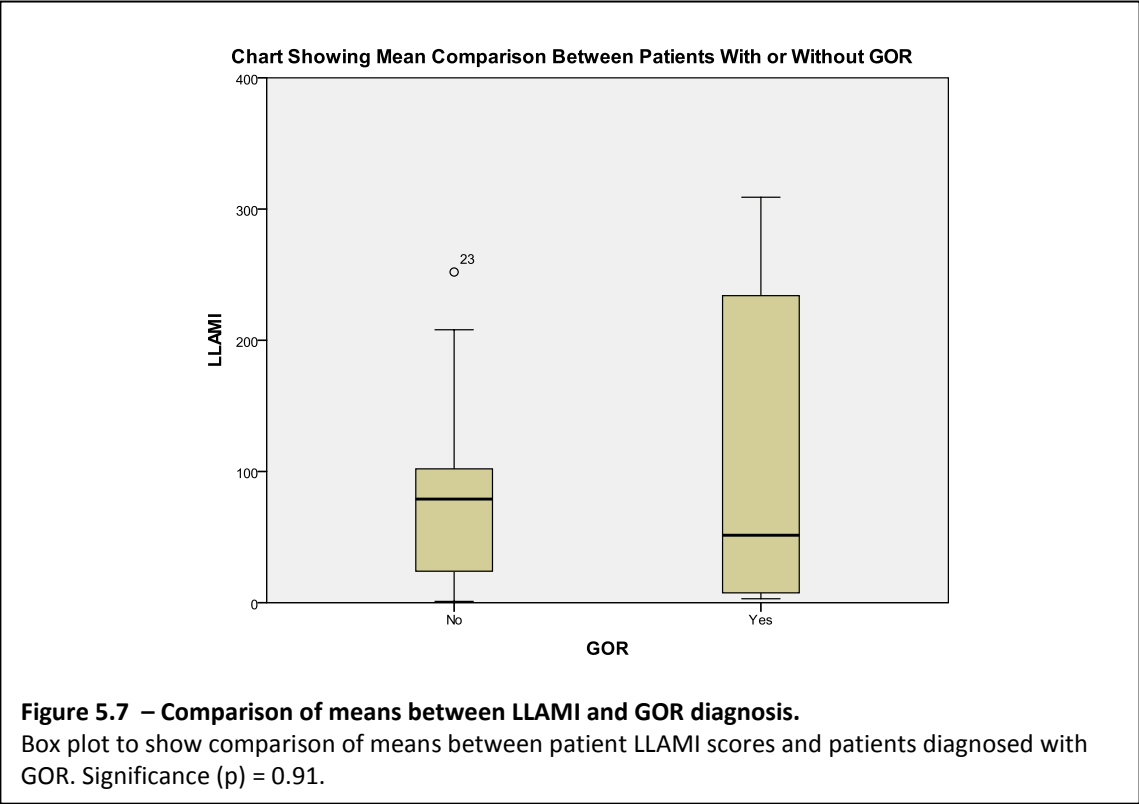
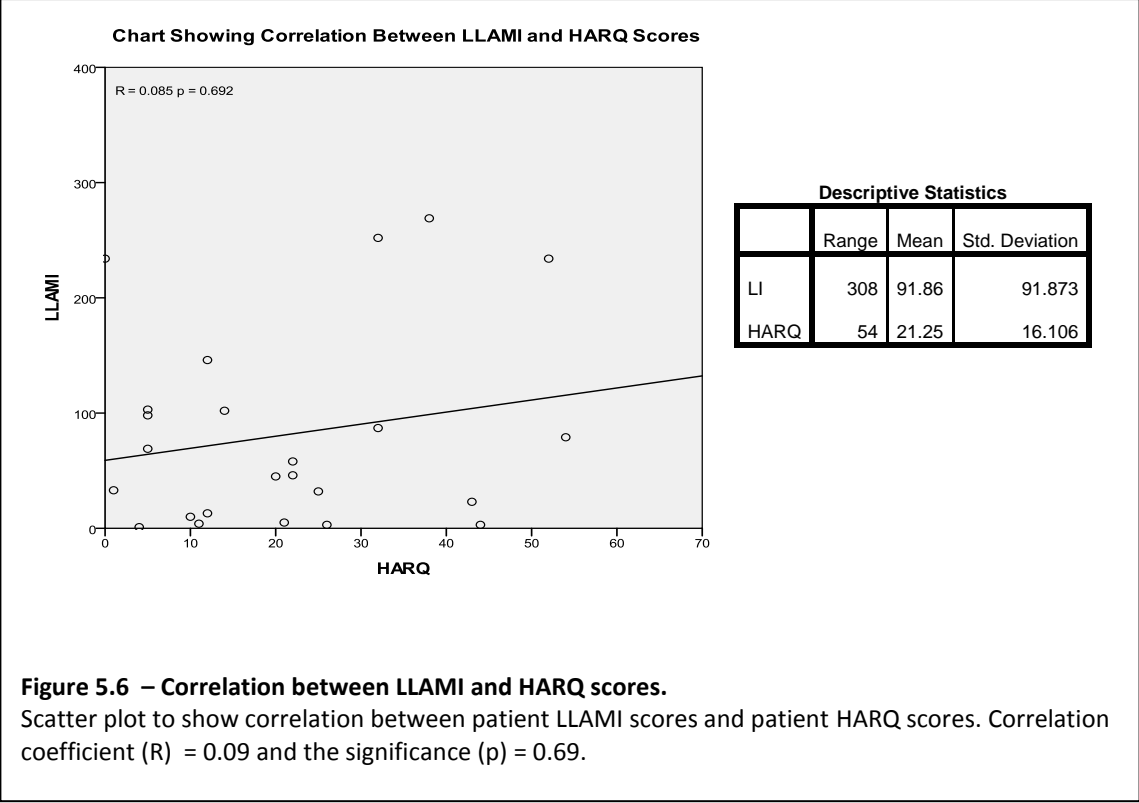
Patient data was collected and anonymised and include respiratory disease diagnosis and patient demographics. A table of these data can be seen in *table 5.1*. Statistical analysis was then performed using SPSS version 19 to highlight any possible differences and/or correlations between diseased groups and/or patient characteristics. Firstly, non-parametric Spearman rank order correlation for bi-variate statistical analysis was performed to determine any possible correlations between lipid score and patient characteristics. A significant negative correlation ($R=0.59$ $p<0.01$) was shown between HARQ score and patient age showing older patients score less on the questionnaire. The LLAMI itself showed a slight correlation (0.09) with HARQ score, although this was not statistically significant. To determine significant differences between mean data sets, a non-parametric Mann-Whitney test was then performed. A significant correlation was shown between HARQ score and age ($R = -0.59$, $p = <0.01$) shown in *figure 5.4* and a significant predominance of females diagnosed with GOR ($p=0.04$) shown in *figure 5.5*. A minor correlation was shown between LLAMI and HARQ score ($R=0.09$) shown in *figure 5.6*, however there was no significant difference between LLAMI in patients diagnosed with or without GOR as shown in *figure 5.7*.

Sample	Sex	Age	HARQ	LLAMI	Diagnosis
1	F	83	1	33	Pulmonary embolism and aspiration pneumonia and COPD.
2	F	50	54	79	Idiopathic cough
3	M	63	38	269	Interstitial lung disease and GOR.
4	M	53	25	32	Sarcoidosis and hiatus hernia and GOR.
5	F	67	22	58	Brochiectasis and GOR.
6	F	78	0	234	Late onset asthma and reflux and alveolar Cell Carcinoma.
7	F	67	MD	208	COPD.
8	F	68	52	234	GOR.
9	F	64	5	103	Brochiectasis.
10	F	87	5	69	Cancer
11	M	74	20	45	COPD and GOR
12	F	60	MD	98	Cancer.
13	F	74	14	102	Cancer
14	M	62	12	146	COPD
15	M	72	11	4	Chest infection, metallic breath and GOR.
16			MD	309	COPD, recurrent chest infection and GOR.
17	M	65	32	87	Cancer
18	M	55	MD	76	GOR,
19	F	75	MD	24	Cancer
20	F	48	12	13	AML with fungal chest infection
21	F	64	5	98	Bronchiectasis
22	M	58	44	3	GOR.
23	F	53	32	252	Hiatus hernia
24	F	26	22	46	Organising pneumonia
25	F	51	43	23	Idiopathic cough
26	F	60	21	5	GOR
27	F	51	26	3	Organising pneumonia
28	M	68	4	1	Rhumatoid lung
29	F	73	10	10	Adenenocarcinoma and GOR

Table 5.1 – Patient Data

Table showing BAL patient characteristics, HARQ score, LLAMI and clinical diagnosis. (M=male, F=female, MD=missing data)





5.4 Discussion

Using the lipid laden macrophage scoring system (LLAMI) first described by Colombo and Hallberg (1987), we wanted to undertake a study to determine the tests potential use as a diagnostic marker of aspiration. Unlike other studies, we wanted to include patients with silent or non-acid reflux, in addition to acid reflux, based on clinical history and Hull Airway Reflux Questionnaire (HARQ) scores (Morice et al., 2011). This questionnaire has the capacity to distinguish patients with cough hypersensitivity syndrome, with 94% sensitivity and 95% specificity, which is due to a symptom of both acid and non-acid reflux.

A total of 29 patients undergoing diagnostic bronchoscopy consented to the use of, and were able to provide, sufficient excess BAL sample fluid to allow ORO staining and LLAMI scoring. Of the 29 patients, 11 were diagnosed with GOR either previously or as a result of clinical investigation relating to the bronchoscopy. Patient ages ranged from 26-87 years old with a mean of 63.2. HARQ scores ranged from 0-54 out of a possible 70 with a mean of 21.3. LLAMI scores ranged from 1-309 with a mean of 91.9. A significant association was shown between gender and GOR, diagnosis demonstrating a distinct female predominance within this disease group as previously described. A significant negative correlation was also shown between HARQ score and age, demonstrating that symptoms of cough hypersensitivity may reduce with age. As symptoms of this medical phenomenon can be contributed to reflux, this result is somewhat surprising. Reflux can be attributed to loss of tone in the smooth muscle comprising the LOS, which would be expected to decrease further with age. However our data show that symptoms decrease with age, rather than increase as would be expected. Perhaps this statistic is a consequence of examining such a small cohort, however it is also possible that the sensory airway neurons become desensitised over time resulting in a tachyphylaxis effect as seen in cough challenge experiments (Morice et al., 1992).

Regarding the LLAMI index as a diagnostic tool, our experiments showed no significant correlation between LLAMI and GOR diagnosis or HARQ score. Although the correlation between LLAMI and HARQ was shown to be only slight, this may increase in strength of statistical significance with greater patient numbers. Whilst previous studies have disagreed as to the diagnostic potential of the LLAMI, we have shown that it is not a reliable in diagnostic marker of GOR, due to the lack of correlation with GOR diagnosis. Whilst we have shown that macrophages are capable of accumulating lipids directly from food material, they also accumulate lipids from the phagocytosis of other lipid containing cells which may not necessarily be available solely in the reflux associated airway pathology. However, if pH studies were to be included in the clinical workup as routine, but not as a definitive diagnostic marker, it would be interesting to see whether the LLAMI could be used to distinguish silent non-acid reflux from acid reflux and should be investigated further.

6 Macrophage Lipid Accumulation *in vitro*

6.1 Introduction

The previous chapter demonstrated the presence of lipid laden macrophages in diseased human airways. Here we wish to address the questions as to the origin of this lipid and the way in which it accumulates within the macrophage.

The human airway itself as a source of endogenous lipid is feasible. The entire lumen of the airways is coated with surfactant comprising 90% lipids (Chronos et al., 2010), which are ingested, catabolised and recycled by alveolar macrophages. However, this process is continuous as part of the normal functioning airway and seldom causes respiratory problems. In addition, surfactant lipids are comprised largely of polar lipids, such as phospholipids, which are not detectable by ORO staining.

Epithelial cells, on the other hand, are a rich source of the neutral lipids detected by ORO staining. These cells contain lipid droplets comprising triglycerides and cholesterol, either absorbed or synthesised by the cell, encapsulated in a phospholipid bilayer (Ducharme and Bickel, 2008). These lipids allow the production of eicosanoids (Luo et al., 2003, Folkerts and Nijkamp, 1998) from the modification of fatty acids such as arachidonic acid which modulate inflammatory responses in the airway. As discussed in *chapter 1.3.1*, cellular, (probably epithelial) damage occurs as a result of acidic reflux aspiration (Bathoorn et al., 2011) and so we hypothesised that normal phagocytic clearance of apoptotic airway epithelial cells results in the internalisation of epithelial cell lipid droplets by the alveolar macrophage. Platelets, too, are capable of lipid uptake and storage (Daub et al., 2010, White and Krivit, 1966) during circulation in the blood. The airway has an extensive circulatory network bringing platelets into close proximity to the alveolar macrophage and so we investigated the possibility of lipid accumulation as a result of macrophage phagocytosis of platelets also.

During silent aspiration, 'clouds' of gaseous material, which include microscopic food particles, are inhaled into the airway. This material may well include undigested or

partially digested lipids in the form of triglycerides and fatty acids. We hypothesised that during silent aspiration, alveolar macrophages accumulate these lipids directly.

Although the mechanism of fatty acid internalisation and lipid droplet formation by cells is still largely unknown (Hamilton and Kamp, 1999, Zakim, 2000, Glatz et al., 2010) it is well recognised that passive diffusion may occur by insertion of the hydrophobic fatty acids into the external surface of the plasma membrane followed by a 'flip-flop' mechanism, by which the lipid enters the cytoplasm. Indeed, circulating lipid in the form of LDL is known to enter the macrophage via both actin dependent and independent mechanisms of endocytosis (Shashkin et al., 2005), though whether this is also true in the case of unpackaged fatty acids remains unknown. It is also thought that the oxLDL scavenger receptor (CD36) is vital to foam cell formation and has been implicated in the pathological process of atherosclerosis (Endemann et al., 1993, Moore and Freeman, 2006, Postlethwait, 2007, Bobryshev, 2006). We therefore investigated the mode in which neutral lipids accumulate in macrophages by inhibiting actin-dependent phagocytosis and by blocking the CD36 scavenger receptor. In addition, we visualised accumulated neutral lipid droplets in macrophages by TEM to further investigate the formation of the lipid droplets.

6.2 Methods

6.2.1 Induction and Detection of Apoptosis in Epithelial Cells

A549 cells were grown to confluence in a 24 well tissue culture plate under conditions described in 2.1. Hydrogen peroxide (H₂O₂) was added to the culture media at final concentrations of 1-10 mM, increasing in 1 mM increments, for 24 h. Acridine orange (2.5 µg/ml) was then added to the culture media and cells visualised on an Olympus IX71 fluorescent microscope system with a FITC laser filter applied and running cell^m software.

6.2.2 Isolation of Washed Platelets

Venous blood was collected into acid-citrate dextrose (ACD; 113.8 mM D-glucose, 29.9 mM Tri-sodium citrate, 72.6 mM NaCl and 2.9 mM citric acid at pH 6.4) at a ratio of 4:1 using standard phlebotomy techniques. The whole blood/ACD mixture was centrifuged (200 x g; 20°C; 20 min.) and the platelet rich plasma transferred to a clean falcon tube using a Pasteur pipette. The pH was adjusted to 6.4 with 0.3 M citric acid and the platelets centrifuged (800 x g; 10 min.) before being re-suspended in 5 ml wash buffer (36 mM citric acid, 10 mM EDTA, 5 mM D-glucose, 5 mM KCl and 90 mM NaCl at pH 6.5). Finally the platelets were centrifuged (800 x g; 10 min.) and re-suspended in modified tyrodes buffer (15 mM NaCl, 5 mM HEPES, 0.55 mM NaH₂PO₃, 7 mM NaHCO₃, 2.7 mM KCl and 5.6 mM D-glucose at pH 7.4)..

6.2.3 Macrophage Lipid Accumulation

PMA/THP-1 cells and Daisy cells were plated at a cell density of 0.5×10^6 cells/ml in each well of a 24 well tissue culture plate containing 1 ml of cell suspension and a sterile glass cover slip. Conditions of culture are described in 2.1. After 24 h the media was replaced with media (1 ml) containing 10% v/v Calogen, apoptotic epithelial cells (2×10^5 cells/ml), or washed platelets (5×10^5 cells/ml) and the cells incubated for a further 24 h at 37°C. Cover-slips were then removed, washed 5 times in PBS and

stained with ORO and counterstained with hematoxylin. ORO staining protocol is described in 2.6.

6.2.4 Actin-dependant Phagocytosis Inhibition

PMA/THP-1 cells and Daisy cells were plated at a cell density of 0.5×10^6 cells/ml in each well of a 24 well tissue culture plate containing 1 ml cell suspension and a sterile glass cover slip. Conditions of culture are described in 2.1. After 24 hours the media was aspirated and replaced with fresh media containing 10 $\mu\text{g/ml}$ cytochalasin D, a commercially available fungal metabolite which binds actin filaments to prevent polymerisation, thus inhibiting phagocytosis. Cells were incubated with cytochalasin D for 1 h before being washed 5 times in PBS and subsequently incubated with 1 mg/ml zymosan for a further 1 h. Cover-slips containing adherent cells were then removed from the wells and washed 5 times in PBS before being differentially stained as described in 2.12.

6.2.5 Blocking Lipid Accumulation

PMA/THP-1 cells and Daisy cells were plated at a cell density of 0.5×10^6 cells/ml in each well of a 24 well tissue culture plate containing 1 ml cell suspension and a sterile glass cover slip. Conditions of culture are described in 2.1. After 24 h the media was aspirated and replaced with fresh media with or without cytochalasin D (10 $\mu\text{g/ml}$) or mouse monoclonal CD36 clone FA6-152 blocking antibody (1 $\mu\text{g/ml}$; Santa Cruz, Heidelberg, Germany). Cells were incubated for 1 h before being washed 5 times in PBS and subsequently incubated in media containing 10 % v/v Calogen for a further 4 hours. Cover-slips were then removed, washed 5 times in PBS and stained with ORO, counterstaining with hematoxylin. ORO staining protocol is described in 2.6.

6.2.6 TEM of Intra-cellular Lipid Droplets

PMA/THP-1 cells and Daisy cells were plated at a cell density of 0.5×10^6 cells/ml in T75 tissue culture flasks containing 10 ml cell suspension. Conditions of

culture are described in 2.1. After 24 h the media was replaced with media (10 ml) containing 10% v/v Calogen and the cells incubated for a further 24 h at 37°C. Cells were then washed 5 times with PBS (5 ml) and harvested by cooling to 4°C with repeated washing and agitation with ice cold PBS. Cells were then transferred on ice to the microscopy suite at the University of Hull and TEM performed as described in *section 2.4*.

6.2.7 Gene Microarray

PMA/THP-1 cells and Daisy cells were left untreated or treated with Calogen for 24 hours. Cells were then analysed for gene expression profiles as described in 2.16. Data was filtered using Microsoft Excel 2010 software to compare differences in gene expression by the fold change.

6.3 Results

6.3.1 Apoptosis Induction

To determine the optimum conditions for the induction of apoptosis, A549 cells were grown to confluence in a 24 well tissue culture plate and induced to undergo cell death by incubation with varying concentrations of H₂O₂ for 24 h. Apoptosis was then detected using acridine orange (2.5 µg/ml) to visualise nuclear condensation under fluorescence microscopy. Apoptosis was induced in A549 cells using concentrations of H₂O₂ from 1 mM-10 mM, increasing in 1 mM increments. *Figure 6.1* shows representative pictures of untreated A549 cells and cells treated with 1 mM, 5mM and 10 mM H₂O₂. Untreated cells formed a typical monolayer likened to 'crazy paving', comprising large flattened adherent cells with uncondensed nuclei. Cells treated with H₂O₂ appeared rounded, shrivelled and with much less cell-cell contact. At 1 mM H₂O₂ around 60 % of cells showed condensed nuclei, typical of apoptotic cells. At 5 mM H₂O₂ the percentage of apoptotic cells increased to 80-100 % and at 10 mM there were no detectable live cells. A concentration of 5 mM H₂O₂ was therefore utilised for future experiments to induce A549 epithelial cell apoptosis.

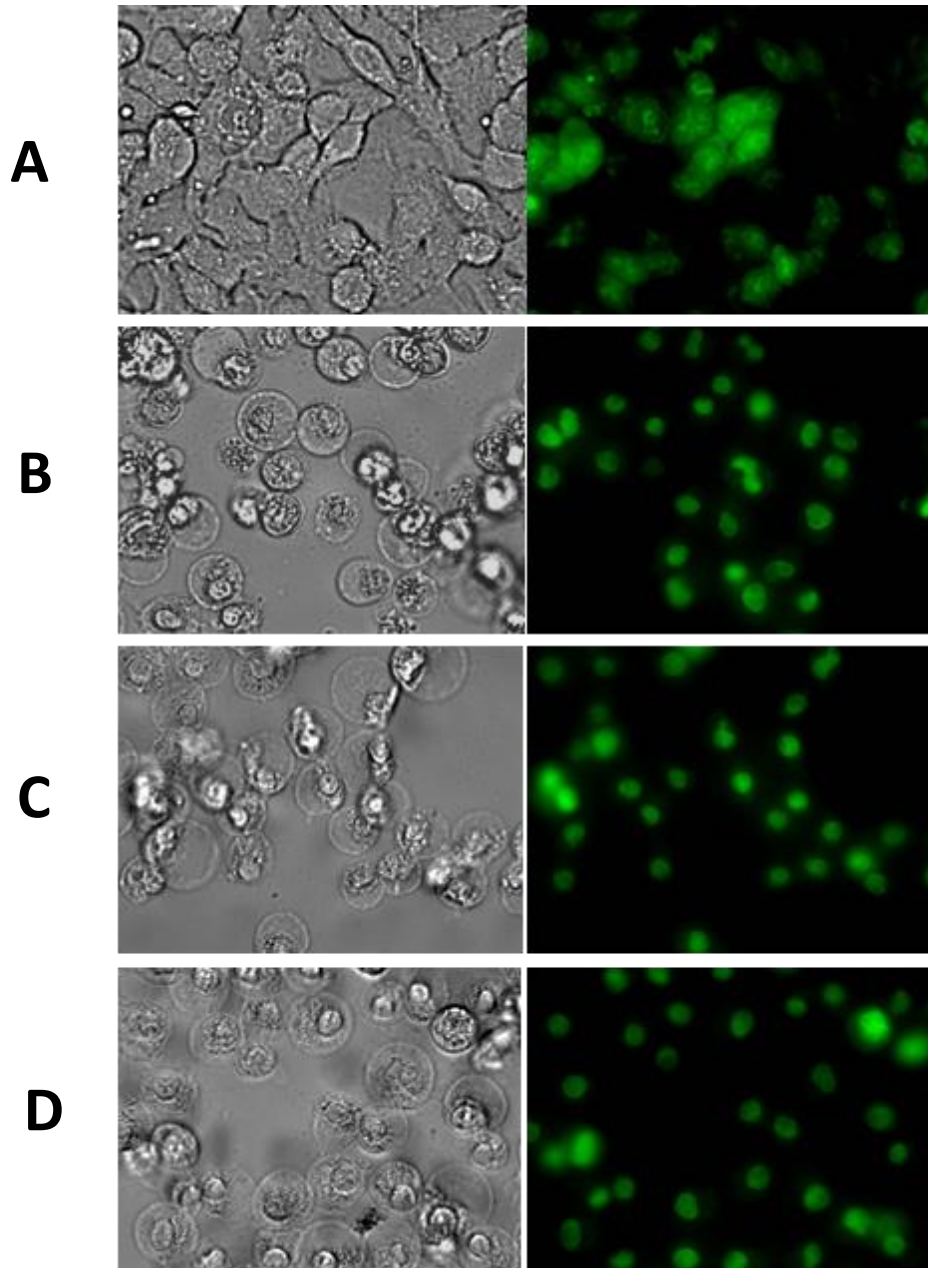


Figure 6.1 – Induction of apoptosis in A549 cells

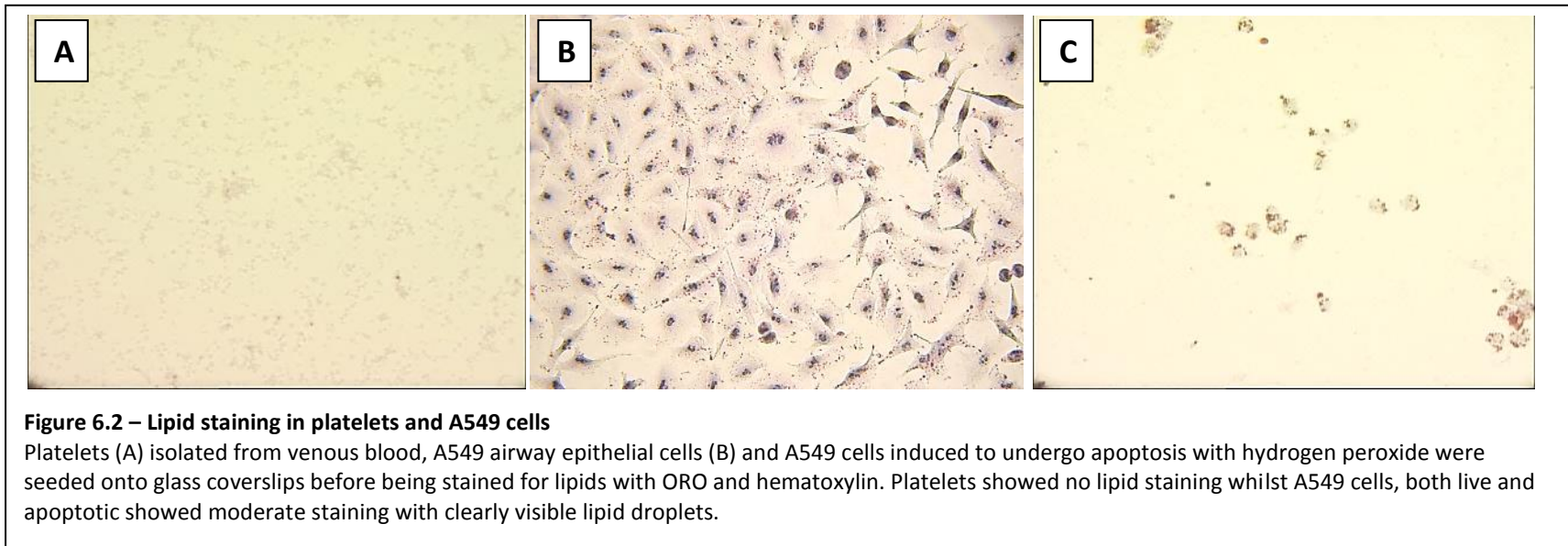
A549 cells were cultured to 80 % confluence before being incubated with H₂O₂ for 24 h. Acridine orange nuclear stain was then added to the culture media (2.5 µg/ml) and the cells visualised under brightfield (right) and fluorescence (left) microscopy. Untreated cells (A) showed flat cells, forming a 'patchwork' monolayer, with large un-condensed nuclei characteristic of live healthy cells. Cells treated with 1 mM (B) 5 mM (C) and 10 mM (D) H₂O₂ showed smaller more rounded cells, small condensed nuclei, characteristic of apoptotic cells.

6.3.2 Macrophage Lipid Accumulation

Isolated washed platelets, A549 airway epithelial cells and A549 cells induced to undergo apoptosis were washed and stained with ORO and hematoxylin to determine their potential as a source of non-polar lipids available to alveolar macrophages. Results of this staining can be seen in *figure 6.2*. Platelets showed no staining whilst A549 cells both healthy and apoptotic showed moderate staining with clearly visible lipid droplets in the cell cytoplasm.

To further investigate the origin of lipids accumulated in alveolar macrophages, PMA/THP-1 cells and Daisy cells were incubated with media (1 ml) containing either 10 % v/v Calogen representing our previously optimised model of reflux aspiration (*section 3.2.2*), apoptotic epithelial cells (2×10^5 cells/ml), or washed platelets (5×10^5 cells/ml) as a control. Cells were then washed and stained with ORO, counterstaining with hematoxylin. Results of macrophage lipid accumulation can be seen in *figure 6.3*. Untreated PMA/THP-1 cells unfortunately showed a small degree of staining with ORO indicating that perhaps the slides had not been rinsed thoroughly enough after staining, although this was seen in repeated experiments also. Cells incubated with washed platelets also showed a small degree of staining although this was comparable to the untreated cells. Cells incubated with 10 % v/v Calogen showed a high degree of staining in all cells whilst cells incubated with apoptotic A549 cells showed a moderate degree of staining in most cells.

Untreated daisy cells and cells incubated with washed platelets showed no ORO staining. Daisy cells incubated with 10 % v/v Calogen showed a high degree of staining in all cells. Daisy cells incubated with apoptotic A549 cells also showed a high degree of lipid staining although the proportion of stained cells was much less.



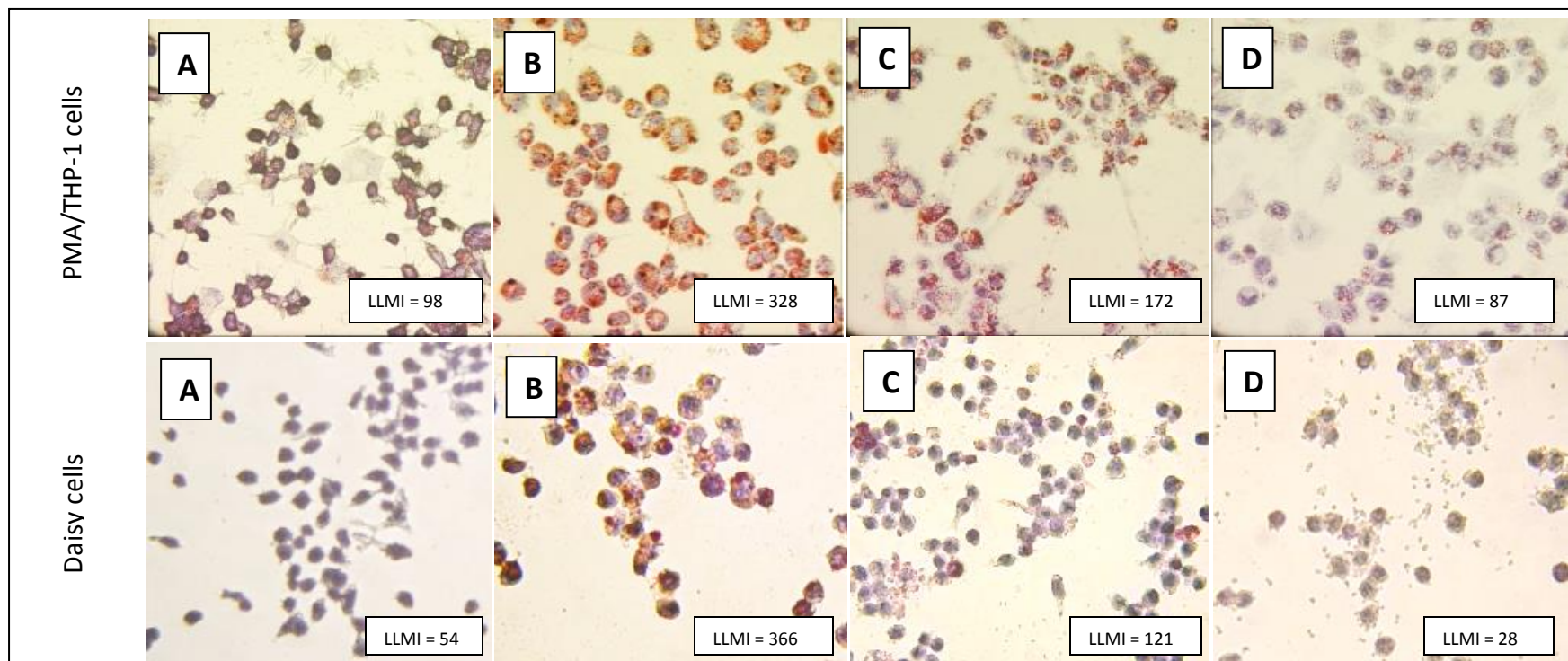


Figure 6.3 – Macrophage Lipid Accumulation

PMA/THP-1 cells and Daisy cells were incubated for 24 hours with 10% v/v Calogen (B), apoptotic A549 cells (C) and washed platelets (D) before being stained for lipids with ORO and hematoxylin and compared to untreated cells (A). Untreated PMA/THP-1 cells unfortunately showed a small degree of staining with ORO. Cells incubated with washed platelets also showed a small degree of staining although this was comparable to the untreated cells. Cells incubated with 10 % v/v Calogen showed a high degree of staining in all cells whilst cells incubated with apoptotic A549 cells showed a moderate degree of staining in most cells. Daisy cells incubated with 10 % v/v Calogen showed a high degree of staining in all cells. Daisy cells incubated with apoptotic A549 cells also showed a high degree of lipid staining although the proportion of stained cells was much less.

6.3.3 Blocking Lipid Accumulation

To optimise conditions for blockage of phagocytosis, PMA/THP-1 cells and Daisy cells were seeded onto glass cover-slips and pre-incubated with cytochalasin D for 1 h before being incubated with zymosan beads as described in section 2.13. Cover-slips were then removed, cells washed in PBS and differentially stained as described in section 2.12. Results can be seen in *figure 6.4*. Untreated cells appeared large and round with cytoplasm staining pale purple whilst the nucleus stained dark purple. Cells treated with zymosan alone showed cytoplasmic inclusions appearing as small white rings against the purple background. Cells pre-incubated with cytochalasin D showed no cytoplasmic inclusions though white rings appeared around the cell membrane. PMA/THP-1 cells also showed morphological abnormalities to the cell membranes, becoming jagged rather than round.

PMA/THP-1 and Daisy cells were then incubated with potential inhibitors of lipid accumulation prior to incubation with 10 % v/v Calogen for 24 h. Untreated cells were compared with cells treated with 10 % v/v Calogen alone, as a positive control and in the presence of cytochalasin D and CD36 monoclonal blocking antibody. In the case of cytochalasin D and CD36, inhibitors were applied for 1 hour prior to Calogen treatment. Whilst a small degree of staining was present in the untreated negative control cells, a high degree of intense staining was seen in the Calogen only treated cells. This high level of staining was also seen the cells pre-incubated with both cytochalasin D and CD36.

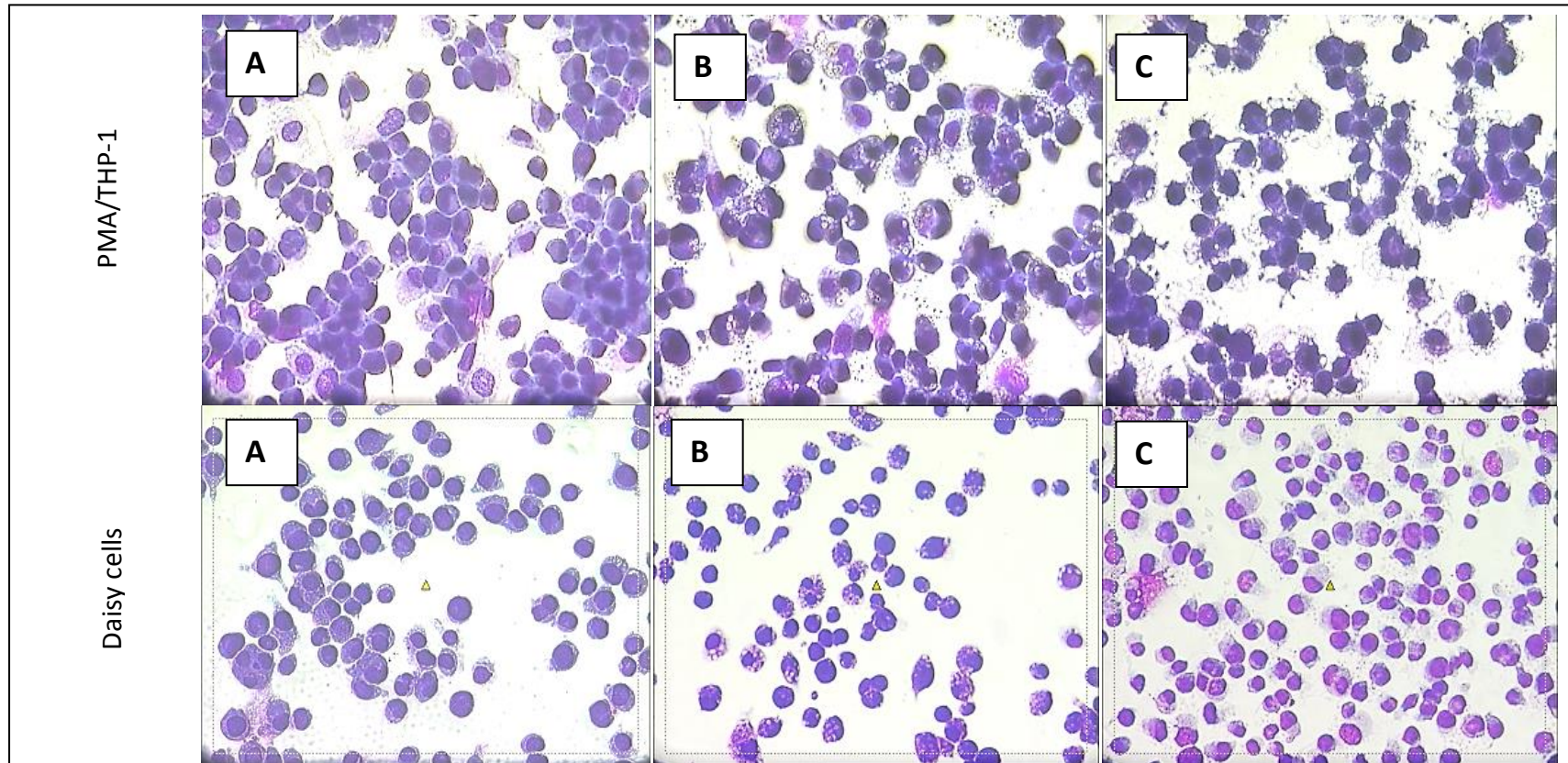


Figure 6.4 – Inhibition of Phagocytosis

PMA/THP-1 cells and Daisy cells seeded onto glass cover-slips and pre-incubated with cytochalasin D for 1 hour before being incubated with zymosan beads. Cells were washed and differentially stained. Untreated cells (A) appeared large and round with cytoplasm staining pale purple whilst the nucleus stained dark purple. Cells treated with zymosan alone (B) showed cytoplasmic inclusions appearing as small white rings against the purple background. Cells pre-incubated with cytochalasin D (C) showed no cytoplasmic inclusions.

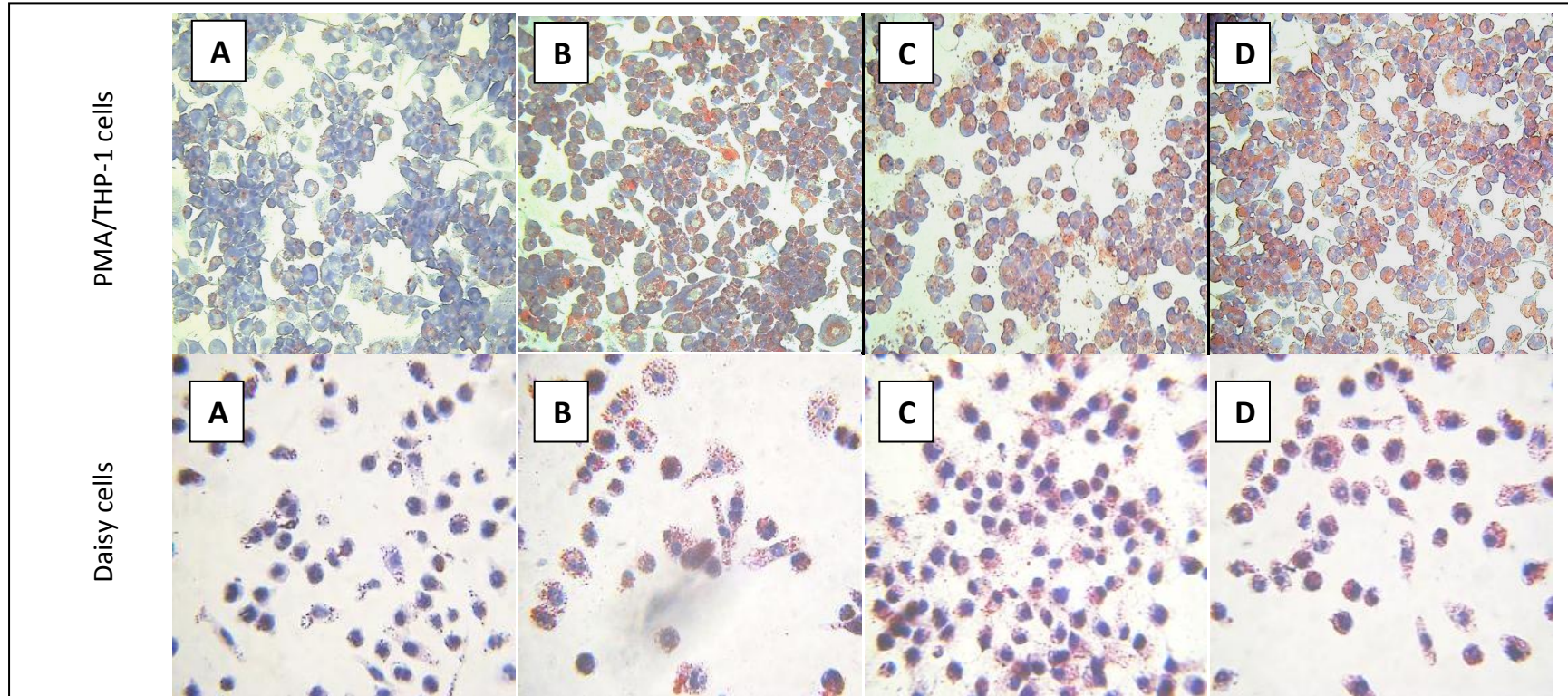


Figure 6.5 – Inhibition of Lipid Uptake

PMA/THP-1 and Daisy cells were incubated with potential inhibitors prior to incubation with 10 % v/v Calogen for 24 h. Untreated cells (A) were compared with cells treated with 10 % v/v Calogen alone (B) and in the presence of cytochalasin D (C) and CD36 monoclonal blocking antibody (D). In the case of (C) and (D) inhibitors were applied for 1 hour prior to the treatment of Calogen.

6.3.4 TEM Visualisation of Lipid Droplets

PMA/THP-1 and Daisy cells both untreated and treated with 10 % v/v Calogen for 24 h were harvested and visualised under TEM. Identified lipid droplets were then magnified for closer inspection. Images captured can be seen in *figure 6.6*. Lipid droplets were visible throughout the cytoplasm and were identifiable by dark staining of residual lipid remaining after the fixing process. These droplets were separate from, and in addition to, cholesterol clefts formed by crystallisation of cholesterol during the fixation procedure, visible as long clear spaces in the cytoplasm. Closer inspection revealed what appears to be a double membrane surrounding the lipid droplet. Lipid droplets were variable in size and shape although were roughly rounded. They appeared throughout the cytoplasm in what appeared to be random positions, well spread out and bearing no obvious association the specific organelles or structures.

6.3.5 Gene Microarray Data Analysis

To determine if Calogen treatment resulted in an alteration of gene transcription regulation, mRNA was extracted and sent for microarray analysis using an Agilent microarray system. Data was analysed using Microsoft Excel 2010 to count genes which were either up or down regulated by categorical fold changes. The result can be seen in *figures 6.7 and 6.8*.

Upon Calogen stimulation of PMA/THP-1 cells 8296 genes showed fold change differences of 2 or greater. The majority of these genes (5229) were 2-3 fold different and decreased in number as fold change increased. In addition 2 genes showed over a 100 fold change. When comparing untreated Calogen treated Daisy cells to untreated cells to Daisy cells 5229 genes showed fold change differences of 2 or greater. Again the majority of these genes (4894) were 2-3 fold different and decreased in number as fold change increased. None of the genes in this comparison showed a change greater than 100 fold. A table of the 20 genes showing the greatest change in gene regulation can be seen in *table 10.1 and 10.2* of the appendix.

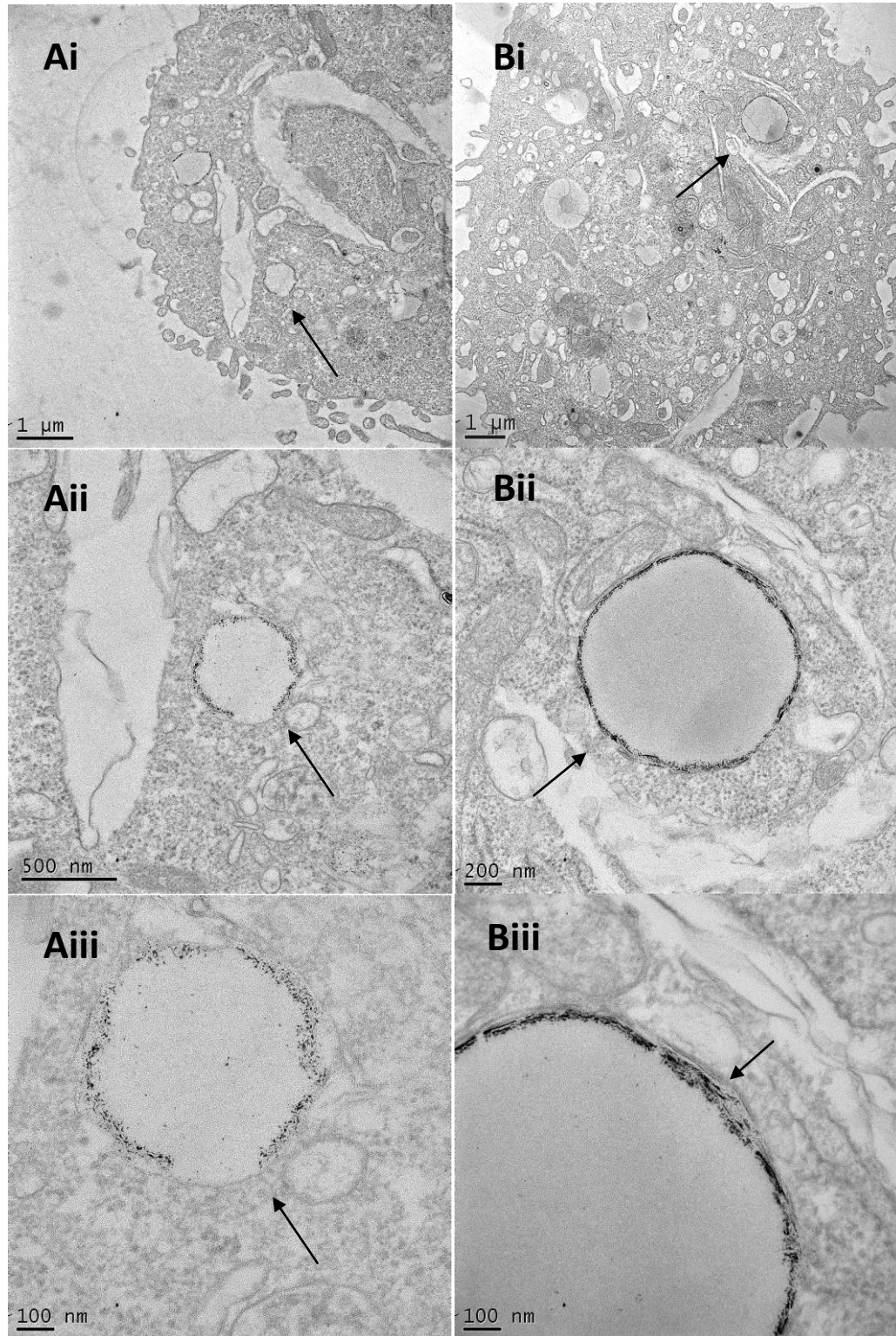


Figure 6.6 – TEM Visualisation of Lipid Droplets

Calogen treated PMA/THP-1 (Ai-iii) and Daisy cells (Bi-iii) were visualised under TEM. Lipid droplets were identified and magnified to reveal dark stained remnants of lipid encased in membrane bound vesicles.

Difference in Gene Regulation in Calogen Treated PMA/THP-1 Cells Compared with PMA only Treated THP-1 Cells

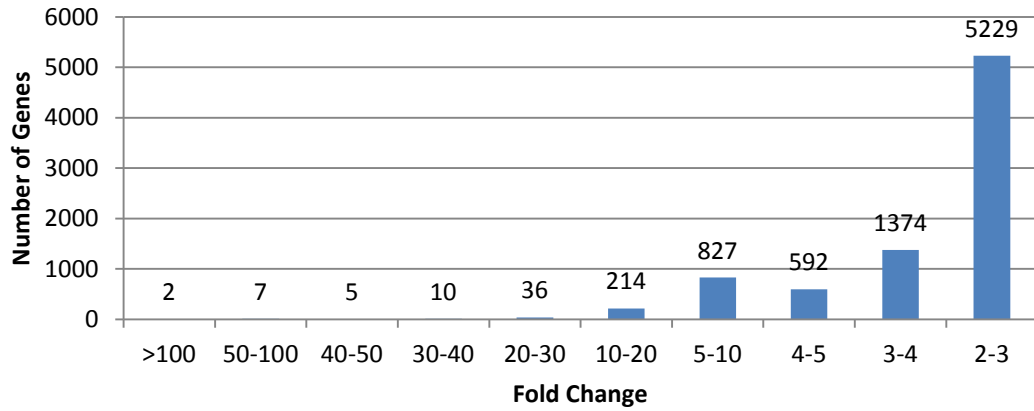


Figure 6.7 – Gene array analysis comparing Calogen Treated PMA/THP-1 Cells Compared with PMA only Treated THP-1 Cells

Gene microarray analysis of mRNA extracted from PMA/THP-1 cells with and without additional Calogen treatment. Results showed a total of 8296 genes with fold change differences of greater than 2 fold with 2 genes showing over a 100 fold change.

Difference in Gene Regulation in Calogen Treated Daisy Cells Untreated Daisy Cells

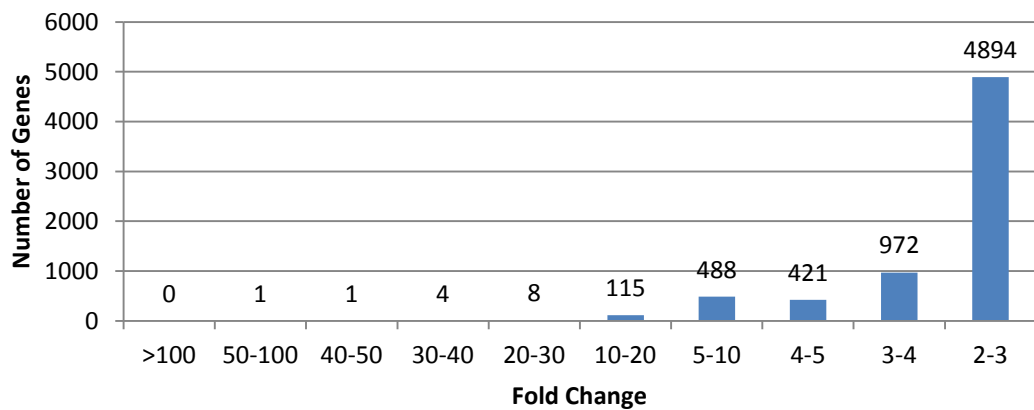


Figure 6.8 – Gene array analysis comparing Calogen Treated Daisy Cells Compared with Untreated Daisy Cells

Gene microarray analysis of mRNA extracted from PMA/THP-1 cells with and without additional Calogen treatment. Results showed a total of 6904 genes with fold change differences of greater than 2 fold with no genes showing over a 100 fold change.

6.4 Discussion

A549 cells are a human bronchial epithelial cell line. Epithelial cells are capable of leukotriene production and contain stores of lipids required for the genesis of these molecules. Platelets too are capable of lipid storage and so we investigated the potential of these cells as a source of lipid available to macrophages. Upon ORO staining A549 cells showed clearly defined lipid droplets which remained after cells were induced to undergo apoptosis with H₂O₂. Washed human platelets, on the other hand, showed no lipid staining. It is unlikely that the platelet lipid stores were depleted during processing as no detergent or solvents were used. It is however possible that as the platelets were derived from young healthy donors i.e. non-hyperlipidaemics, that these platelets naturally lacked lipid stores or stores were comprised of polar lipids and therefore did not stain. Incidentally platelets were included in further experiments as a control.

PMA/THP-1 and Daisy cells were then incubated with 10 % v/v Calogen as a model for gastric content, apoptotic A549 cells as a model for damaged airway epithelia and human washed platelets. Untreated PMA/THP-1 cells unfortunately stained slightly with ORO in this batch of experiments and this is unexplainable, however, as staining was not intense, it was accepted for use as a control slide. Both PMA/THP-1 cells and Daisy cells incubated with Calogen showed intense ORO lipid staining. As no other lipids were available to the cells this staining is likely to be caused by the direct uptake of lipids from the Calogen. Calogen contains a combination of sunflower oil and canola oil which comprise varying combinations of both long chain unsaturated (89.4 %) and long chain saturated (10.6 %) fatty acids along with a small amount of trans fats. In Calogen these fatty acids are bound to glycerol to form triglycerides however during consumption would be acted upon by lingual lipase before reaching the stomach. Lingual lipase is an enzyme secreted by serous cells on the tongue with an optimum pH range of 3.5-6, allowing it to remain active when the food bolus reaches the stomach. (Liao et al., 1984). By hydrolysing triglycerides, free fatty acids are released and this enzyme accounts for up to 30 % of dietary fat digestion. In

addition, human monocyte-derived macrophages have been shown to secrete a similar enzyme, lipoprotein lipase, as too have THP-1 cells (Chait et al., 1982, Auwerx, 1991). It is likely therefore that the triglycerides contained in Calogen are broken down to glycerol and free fatty acids before internalisation by the macrophage both *in vivo* and in our *in vitro* model of aspiration.

When incubated with apoptotic A549 cells both PMA/THP-1 cells and Daisy cells showed positive ORO staining compared with controls. This staining was largely not as intense as when cells were incubated with Calogen, though a small proportion of cells did show intense staining. This distribution of staining was comparable to some of the patient BAL sample staining seen in the previous chapter. Whilst the intensely stained cells would score maximal 3 or 4 on the lipid index, the small proportion of these cells would give an overall sample score far below the maximal 400 compared with maximal lipid scores for Calogen treated samples. This could well explain why the LLAMI has proven not to be an accurate tool for diagnosing specific airways diseases or GOR. If patients with respiratory disease experience purely acid reflux, the LLAMI would be entirely dependent on the degree of acid induced epithelial damage. If the patient experienced both acid and non-acid reflux the LLAMI would be dependent not only on acid induced epithelial damage but also on the amount of dietary lipid reaching the airways in addition to lipase activity. Hence, LLAMI by GOR would result in huge variations between patients and given that GOR can be a co-morbidity with any given disease, respiratory or not, this does not create a scheme for the most accurate diagnostic tool.

When incubated with washed human platelets, neither PMA/THP-1 cells or Daisy cells showed positive ORO staining compared with controls. This would indicate that internalisation of cells by macrophages does not result in modulation of plasma membrane lipids to produce lipid laden macrophages.

In order to decipher the mechanism by which lipids contained in Calogen, thus gastric contents, can be internalised by macrophages, we effectively inhibited actin-dependant phagocytosis by incubation with cytochalasin D. cytochalasin

D is a fungal metabolite which binds actin filaments to prevent polymerisation, thus inhibiting phagocytosis and was shown to be effective at preventing internalisation of zymosan particles. When both PMA/THP-1 and Daisy cells were pre-incubated with cytochalasin D before incubation with Calogen, lipid uptake was unaffected. This would suggest that internalisation of lipids is actin-independent and in agreement with the theory that fatty acids can diffuse across cells membranes. Cells were also pre-incubated with a commercially available antibody clone capable of blocking CD36. This also appeared to have no effect on lipid accumulation when used at the recommended concentration. It could be that the recommended concentration was too low in this experimental setting, or that fatty acids bind a separate binding site to that blocked by this antibody clone, though we suspect this not to be the case.

Upon visualisation by TEM, accumulated lipid droplets were separate from, and in addition to, cholesterol clefts. Closer inspection revealed what appears to be a double membrane surrounding the lipid droplet. Lipid droplets were variable in size and shape although were roughly rounded. They appeared throughout the cytoplasm in what appeared to be random positions, well spread out and bearing no obvious association the specific organelles or structures, suggesting passive diffusion through the cell membrane rather than production from the endoplasmic reticulum as has been suggested.

During gene microarray analysis, PMA/THP-1 cells showed that upon Calogen stimulation 8296 genes showed fold change differences of 2 or greater. The majority of these genes (5229) were 2-3 fold different and decreased in number as fold change increased. In addition 2 genes showed over a 100 fold change. Daisy cells showed that upon Calogen stimulation 5229 genes showed fold change differences of 2 or greater. Again the majority of these genes (4894) were 2-3 fold different and decreased in number as fold change increased. None of the genes in this comparison showed a change greater than 100 fold. Such a large body of data is difficult to analyse as a whole but will provide us with a base, upon which, future experimental approaches into macrophage lipid accumulation may be based. The significance of the

exact genes being up or down regulated upon Calogen stimulation remain unknown, at present and further pathway analysis is required. Once a particular gene cluster, such as T_H-2 cytokines, has been identified to be significantly up or down regulated further PCR and proteomic analysis on cell lysate for confirmation. However, the present results indicate that lipid uptake has a direct effect on cell mRNA transcription and may provide clues as to how to manipulate this process.

In conclusion, both dietary lipids and damaged epithelial cells are a feasible source of lipid for macrophages. Both these sources result in differences in staining intensity and distribution throughout a sample and could occur independently or simultaneously in patients with or without disease in addition to GOR. Dietary lipid accumulation in macrophages appears to be independent of either actin or CD36. Accumulating lipid droplets are membrane bound vesicles of varying size and apparently randomly distributed through the cell cytoplasm. Additionally, dietary lipid accumulation results directly an alteration of gene transcription.

7 Human Macrophage Activation and Polarisation

7.1 Introduction

Since the emergence of the flow cytometer, the last 30 years has seen many studies carried out on individual cell types to determine the cell surface expression of a host of antigens or molecules. The development of flow cytometry and the expansion of the antibodies commercially available with CD marker specificity have provided insight into macrophage cell origin, the process of maturation and functionality. For instance the appearance of CD14 on monocytes would indicate the cell populations progression through the myeloid cell lineage, being then down-regulated again as the cell differentiates into a macrophage. In addition, the ability of the cells to migrate from circulation into tissues, appearing as changes in adhesion molecule expression, would indicate cell maturation. Also, the ability of the cells to perform certain functions such as opsonised antigen recognition can appear as alterations in Fc receptor expression. More recent additions to the cell surface marker repertoire are reports of a small number of molecules enabling the distinction of polarised activated macrophages (Stout and Suttles, 2004, Porcheray et al., 2005, Bouhlej et al., 2007, Anderson and Mosser, 2002), which have previously been discussed in *section 1.5*.

Upon activation, macrophages are capable of eliciting an immune response by the subsequent release of pro- or anti-inflammatory mediators known as cytokines. These are discussed in *section 1.5* of the general introduction. Macrophages themselves form part of the innate cell mediated immune response, a more primitive response, capable largely of self/non-self antigen recognition. However, activated macrophages, with the release of cytokines, are capable of directing the adaptive cell-mediated arm of the immune response, by stimulating differentiation of naïve T helper lymphocytes to become type 1 pro-inflammatory cells or type 2 anti-inflammatory cells. This directed differentiation is brought about by release of IL-12 and IL-4 by M1 and M2 macrophages, respectively (Anderson and Mosser, 2002).

Macrophage activation has been found to be both inducible and reversible in mouse and man. Using lipopolysaccharide (LPS) and heat aggregated human IgG to generate activated macrophages of both M1 and M2 subtypes

respectively we therefore proposed to determine an immunophenotypical profile of M1 and M2 macrophages using current published expression markers. We aimed to compare and determine activation polarisation of lipid laden macrophages using the same panel of antibodies. The panel of antibodies and the justification of each marker are described in *table 2.2 of chapter 2 – General Methods*. We also proposed to use IL-12 and IL-4 cytokine secretion levels to identify M1 and M2 activated macrophages, comparing these with Calogen treated macrophages in order to establish the polarisation status of Calogen treated cells. In addition, alternatively activated macrophages are capable of producing a neutrophil chemoattractant, IL-8, and we proposed that Calogen treatment would enhance production of this protein, contributing to the neutrophilic non-atopic asthma profile. We also wanted to investigate the production of a further cytokine, nerve growth factor, responsible for the survival, growth and maintenance of sensory neuronal cells. We proposed that increased production of this protein would contribute to airway hypersensitivity by inducing growth of sensory neurons in the airways.

In addition, where possible, we analysed BAL fluid from patients undergoing diagnostic bronchoscopy, in order to distinguish the immunophenotypic profile of AM's from various lung pathologies including GORD.

7.2 Methods

7.2.1 Cell line treatments

THP-1, PMA/THP-1 and Daisy cells were cultured as described in 2.1. Cells were seeded at a cell density of 0.5×10^6 cells/ml into T25 tissue culture flasks containing 5 ml media. Where PMA stimulation was required; this was performed 48 h prior to treatment followed by a 24 h resting period. Cells were then washed with PBS and treated with either LPS (10 ng/ml), heat aggregated human IgG (150 ng/ml previously prepared as described in 2.14), Calogen (10% v/v), or M-CSF (50ng/ml) for 24 h. Cell culture supernatant was aspirated and stored at -80°C for cytokine analysis. Cells were washed 5 times with 5 ml PBS before being submerged in 5 ml ice cold PBS and kept at 4°C with frequent agitation until the cells detached from the flask. Cells were then centrifuged ($205 \times g$ for 5 min.) and re-suspended in 1 ml PBS. Cell surface immunophenotype was then assessed by flow cytometry as described in 2.10.

7.2.2 Enzyme-linked Immunosorbent Assay (ELISA)

Nunc MaxiSorp[®] flat bottom plates (Thermo Scientific, Loughborough, UK) were coated overnight with capture antibody diluted in PBS (100 μl at room temperature (RT)). Plates were then washed using a Wellwash 4 MK 2 plate wash system (Thermo Scientific) filling wells and aspirating 400 μl wash buffer (0.05% Tween 20, PBS, pH7.2-7.4) 3 times and leaving the wells empty. Wells were then blocked by incubation with specific block buffer (100 μl , 1 h, RT) before being washed a second time. Specific reagent preparations for each ELISA are described in *table 7.1*. Standards diluted in specific reagent diluent or undiluted sample were then loaded into specific wells and incubated (100 μl , 2 h, RT) before being washed a third time. Detection antibody diluted in specific reagent diluent was then added to each well and incubated (100 μl , 2 h, RT) before a fourth wash cycle. Streptavidin:HRP was diluted to working concentration of 1 in 200 in specific reagent diluent, added to each well (100 μl) and the plates incubated (20 min., RT) in the dark. The plate wash washed a fifth and final

time before 1-Step™ Turbo TMB-Elisa Substrate (100 µl, Thermo Scientific) was added to each well and incubated (20 min., RT) in the dark. Finally 50 µl of 2N Sulphuric Acid was added to stop the HRP-substrate reaction and the plates immediately analysed on a Multiskan FC version 1.00.79 plate-reader (Thermo Scientific) at 450 nm subtracting readings at 570 nm to correct for optical imperfections in the plate.

7.2.3 Statistical Analysis

Data was entered into SPSS Statistics version 19 software and statistically significant differences in cell surface molecule expression were calculated. Initially, an independent samples Kruskal-Wallis test was performed to highlight significant differences in expression across all 3 cells types. Subsequent post hoc testing using Mann-Whitney was then used to identify specific differences in expression.

	Reagent Diluent	Block Buffer
IL-12	1% BSA in PBS plus 2% heat inactivated goat serum added when diluting detection antibody	Reagent diluent
IL-4	0.1% BSA, 0.05% tween 20 in tris buffered saline at pH 7.2-7.4	1% BSA in PBS
IL-8	0.1% BSA, 0.05% tween 20 in tris buffered saline at pH 7.2-7.4	1% BSA, 0.05% sodium azide in PBS
β-NGF	1% BSA in PBS	Reagent diluent

Table 7.1 – Specific Elisa Reagents

Specific reagent recipes required for each ELISA duoset kit.

7.3 Results

7.3.1 Immunophenotype of Polarised and Lipid Laden Macrophages

THP-1 cells were left untreated or stimulated to differentiate with PMA as described in 2.3. PMA/THP-1 and Daisy cells were then stimulated to become M1 or M2 polarised activated macrophages with either LPS or heat aggregated human IgG as described in 7.2.1. PMA/THP-1 and Daisy cells were also treated with 10% v/v Calogen for comparison to polarised macrophages. All cells were then analysed for cell surface marker expression by flow cytometry and statistical analysis of mean fluorescence indices was performed to highlight significant differences in expression of each molecule between treatments. Results of these experiments can be seen in *figures 7.1 and 7.2*. PMA only stimulation induced significant increases in expression of CD14, CD11b, CD32, CD36, CD64 and CD86. Compared with THP-1 cells treated with PMA only, PMA plus LPS treated cells were not significantly different. Cells treated with PMA plus heat aggregated human IgG differed from cells treated only with PMA by significantly decreased expression of CD32 only. PMA plus LPS and PMA plus heat aggregated human IgG treated cells differed in expression of CD32 and CD80, both of which were reduced in heat aggregated human IgG treated cells. Calogen treated cells also showed no significant difference when compared with PMA only treated cells. When compared with PMA plus LPS treated cells, Calogen treated cells showed significantly higher CD14 expression and lower CD32 expression. Lastly when compared with PMA plus heat aggregated human IgG treated cells, Calogen treated cells were not different.

LPS treated Daisy cells were not significantly different in cell surface marker expression than untreated Daisy cells. Heat aggregated human IgG treated Daisy cells showed significantly lower expression of CD11b, CD32, CD64, CD86 and CD163. Calogen treated cells were also not significantly different from untreated cells. When comparing LPS and heat aggregated human IgG treated cells, heat aggregated human IgG treated cells showed significantly lower expression of CD14, CD11b, CD23, CD32, CD64, CD86, CD163 and CD206. Calogen treated daisy cells differed in expression

of CD163 in that expression was significantly lower than LPS treated cells and higher than heat aggregated human IgG treated cells.

THP-1 Cell Immunophenotype after Various Treatments (n=5)

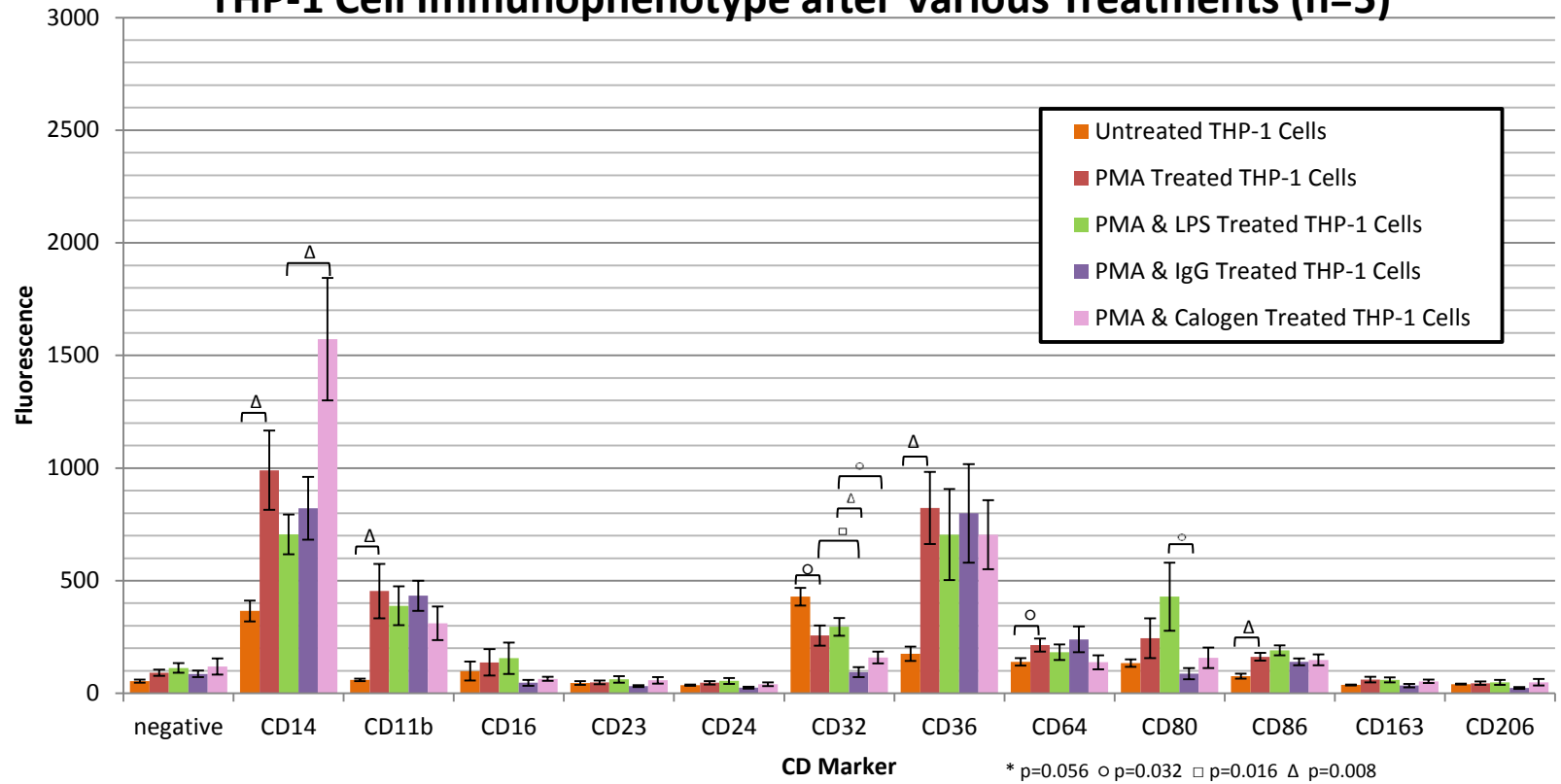


Figure 7.1 – THP-1 cell immunophenotype

THP-1 and PMA/THP-1 cells were subjected to various treatments for 24 hours to induce monocyte to macrophage differentiation (PMA) and activated macrophage polarisation (LPS for M1 or IgG for M2). Cells were also treated with Calogen for comparison and all cells analysed for cell surface marker expression by flow cytometry. Statistically significant results are shown by horizontal brackets and the level of significance indicated by shape.

Daisy Cell Immunophenotype After Various Treatments (n=5)

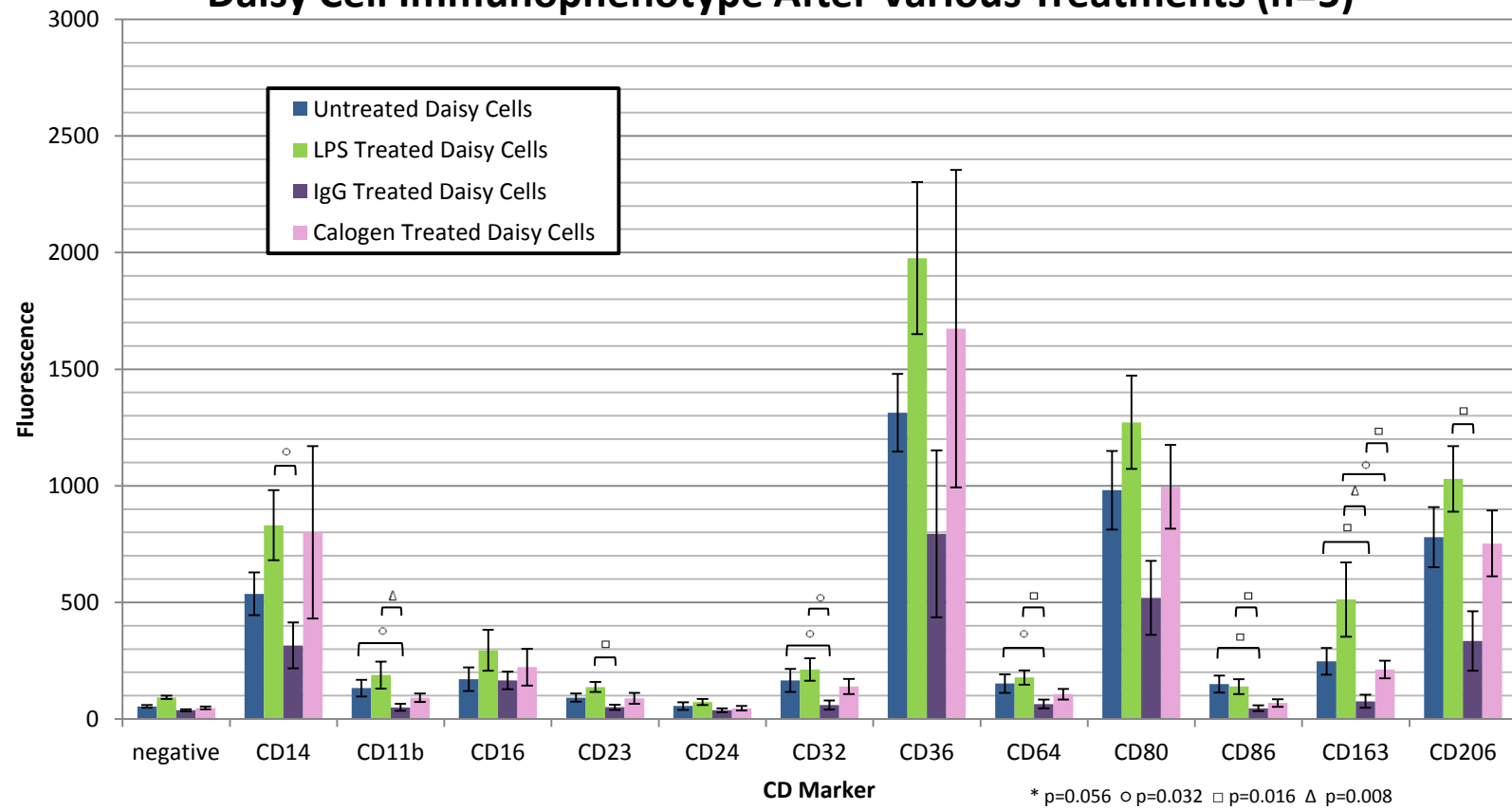


Figure 7.2 – THP-1 cell immunophenotype

Daisy cells were subjected to various treatments for 24 hours to induce activated macrophage polarisation (LPS for M1 or IgG for M2). Cells were also treated with Calogen for comparison and all cells analysed for cell surface marker expression by flow cytometry. Statistically significant results are shown by horizontal brackets and the level of significance indicated by shape.

7.3.2 Comparison of Human IgG versus M-CSF treatment

To determine the effectiveness of heat aggregated human IgG as a treatment to induce M2 polarised activation of macrophages, these cells were then compared to an alternative activation method using M-CSF and either PMA only treated THP-1 cells or untreated Daisy cells. Results of these experiments can be seen in *figures 7.3 and 7.4* respectively. PMA/THP-1 cells subsequently treated with heat aggregated human IgG showed significantly lower expression levels of CD32 when compared with either PMA only treated cells or PMA plus M-CSF treated cells. PMA plus M-CSF treated cells also showed significantly lower expression of CD163 when compared with PMA only treated cell but not PMA plus heat aggregated human IgG treated cells.

Untreated Daisy cells and M-CSF treated Daisy cells were found not to be significantly different in cell surface marker expression. Heat aggregated human IgG treated daisy cells showed significantly lower expression levels of CD36, CD163 and CD206 when compared with either untreated or M-CSF treated cells.

THP-1 cell Immunophenotype after IgG or M-CSF Treatments (n=5)

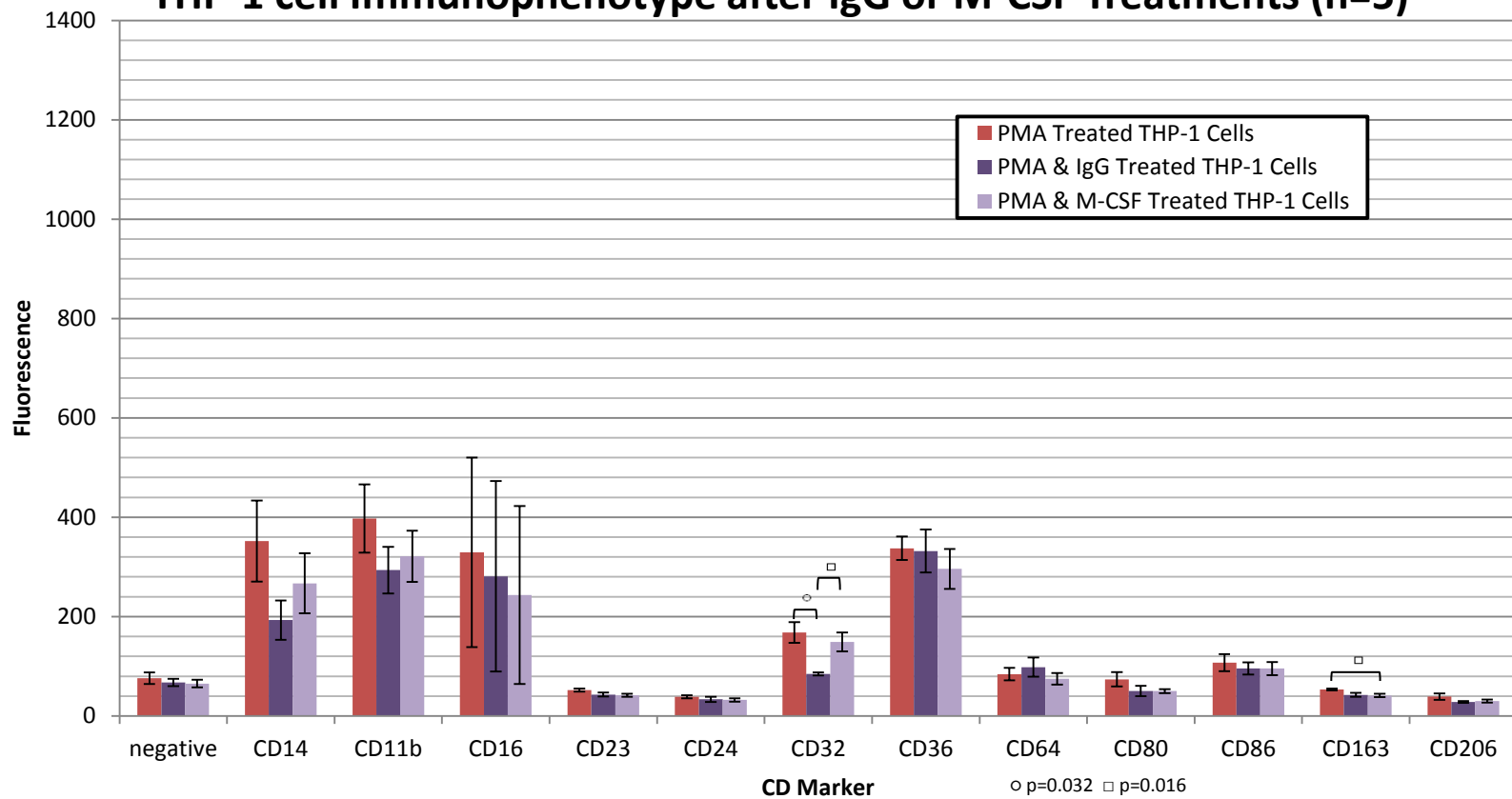


Figure 7.3 – THP-1 cell immunophenotype comparison after IgG and M-CSF treatment

THP-1 cells were stimulated with PMA to induce monocyte to macrophage differentiation. Cells were then either left untreated, treated with human heat aggregated IgG or M-CSF before being analysed for cell surface marker expression by flow cytometry. Statistically significant results are shown by horizontal brackets and the level of significance indicated by shape.

Daisy Cell Immunophenotype after IgG or M-CSF Treatments (n=5)

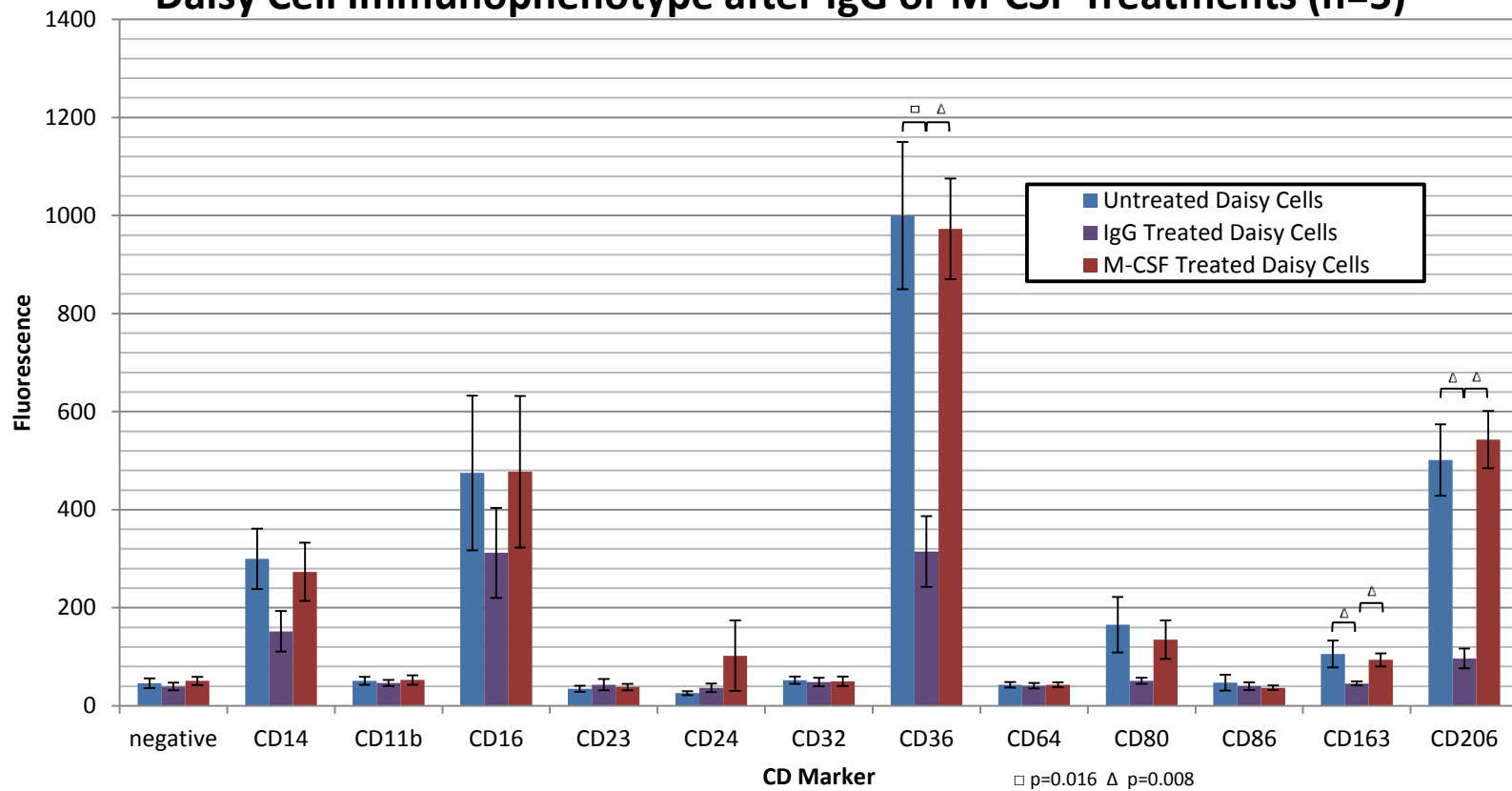


Figure 7.4 – THP-1 cell immunophenotype comparison after IgG and M-CSF treatment

Daisy cells were either left untreated, treated with human heat aggregated IgG or M-CSF before being analysed for cell surface marker expression by flow cytometry. Statistically significant results are shown by horizontal brackets and the level of significance indicated by shape.

7.3.3 Primary Human Alveolar Macrophages

When the sample size was sufficient, primary cells isolated from BAL samples of patients undergoing diagnostic bronchoscopy were also analysed for cell surface marker expression by flow cytometry. BAL fluid was collected from patients undergoing diagnostic bronchoscopy and processed as described in 2.15. Flow cytometry was then performed as described in 2.10 gating around the CD14 positive population of cells with high size and granularity light scatter profiles.

All primary macrophages showed low expression levels of CD14 and CD11b with expression being slightly higher in bronchiectasis and cancer. Of the IgG and IgE receptors, CD16, CD23 and CD64 were absent, whilst CD32 was expressed by samples from all pathologies except bronchiectasis. CD24 was expressed at low levels in the patient with GOR and very high levels in the patient with cancer. CD36 was expressed at low levels, although expression was higher in the patient with GOR. CD80 and CD86 appeared to be absent in cells from all samples from all pathologies except AML with fungal chest infection, in which CD86 was expressed at a higher level than CD80. CD163 appeared to be expressed at very low levels except in cells from the patient with AML and fungal chest infection, in which expression was higher. CD206 expression was also highest in this patient and high in the patient with cancer whilst very low in the GOR and absent in the patient with bronchiectasis.

Primary Alveolar Macrophage Immunophenotype (n=4)

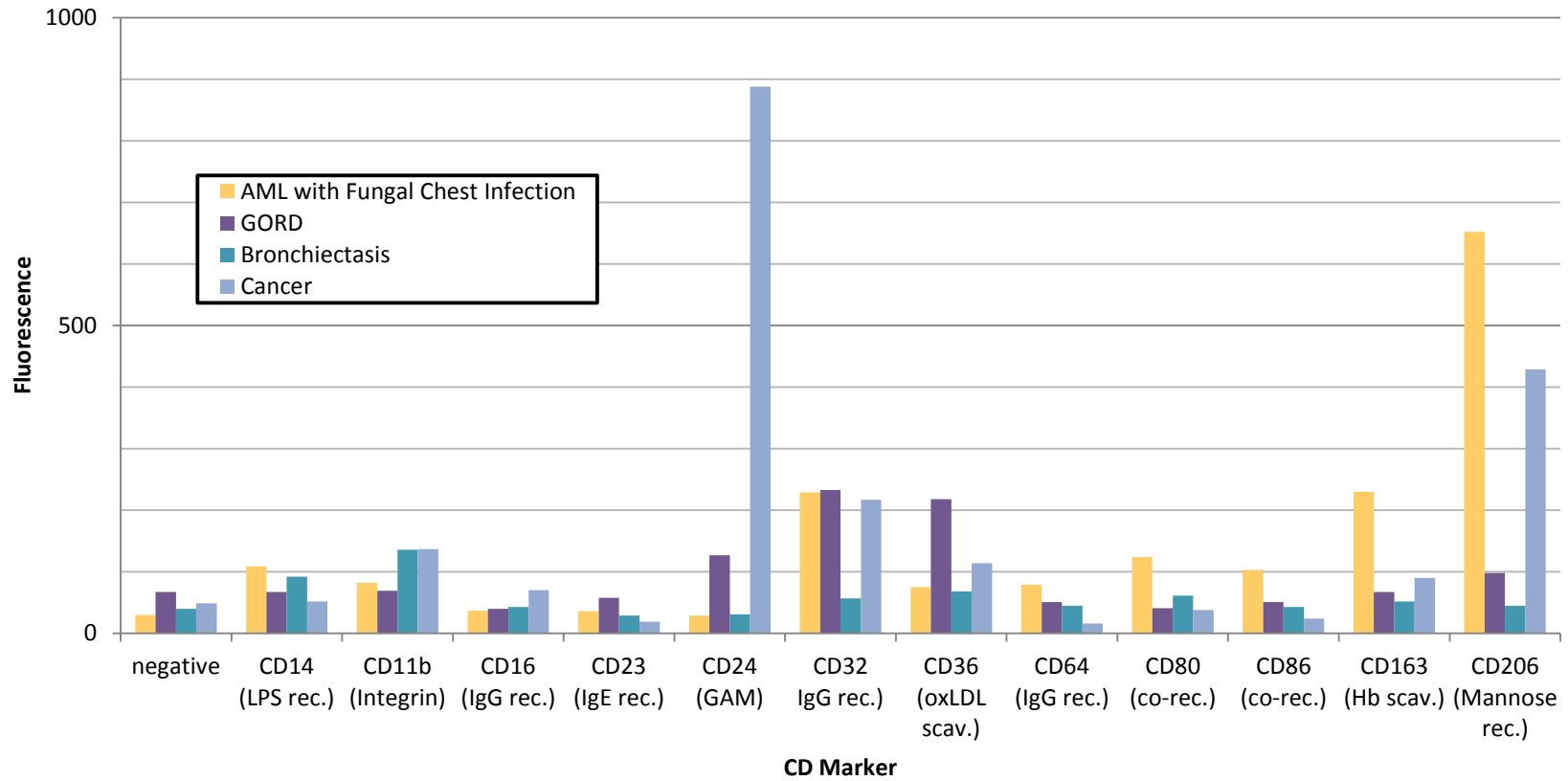


Figure 7.5 – Primary alveolar macrophage immunophenotype

Primary alveolar macrophages collected from BAL fluid of 4 patients undergoing diagnostic bronchoscopy were analysed for cell surface marker expression by flow cytometry. Cells collected from a patient with GER were distinct from cells of other pathologies showing higher CD36 expression in comparison.

7.3.4 ELISA Cytokine Analysis

Untreated THP-1, PMA/THP-1 and Daisy cells were either left untreated or, treated to induce M1/M2 cell polarisation with LPS (M1), heat aggregated human IgG or M-CSF (M2) for 24 h. Cells were also treated with Calogen as a model for the generation of lipid laden macrophages during reflux and aspiration, in order to compare with the polarised cells. Cell culture supernatants were used for ELISA detection of cytokine release. Standard curves were produced for all 4 ELISA experiments using 7 fold serial dilutions of the corresponding standard protein supplied, plotting known concentration against absorbance. These curves were then used to calculate the concentration of each cell culture supernatant sample by the inbuilt software of the ELISA plate reader.

IL-4 was used to detect M2 macrophage polarisation. Concentrations of IL-4 were detected at very low levels in supernatant taken from THP-1 cell cultures. Levels were around 100 pg/ml in all samples, with no significant difference between treatments. These results can be seen in *figure 7.6*. In Daisy cell culture supernatants, IL-4 was detected at higher levels of around 2-4 pg/ml. Again no significant difference was seen between treatments. These results can be seen in *figure 7.7*.

Regarding the neutrophil chemoattractant protein, IL-8, samples taken from untreated THP-1 cell culture showed very low level protein secretion. In samples taken from PMA/THP-1 cell culture, IL-8 protein concentrations were significantly higher in all treatments with concentrations at around 1.8 mg/ml. These results can be seen in *figure 7.8*. In samples taken from Daisy cell cultures, IL-8 protein concentrations were much lower, at around 100-400 pg/ml with no significant difference between treatments. These results can be seen in *figure 7.9*.

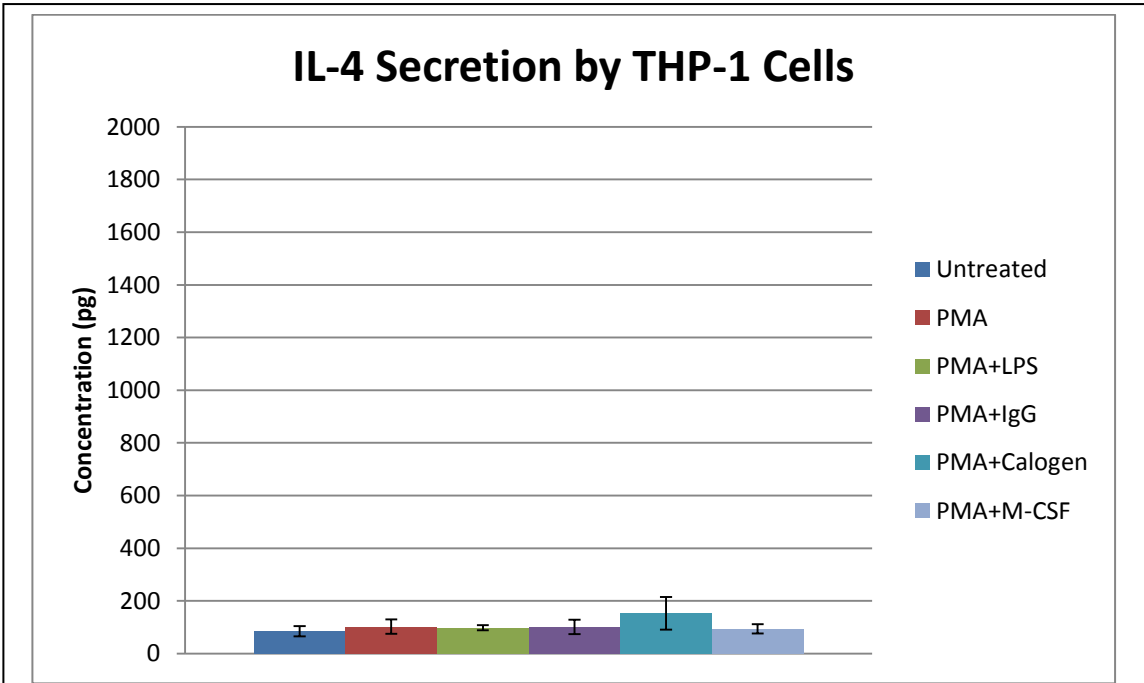


Figure 7.6 - IL-4 secretion by THP-1 cells.
 Concentrations of IL-4 protein detected by ELISA in cell culture supernatants of THP-1 cells subjected to a variety of treatments..

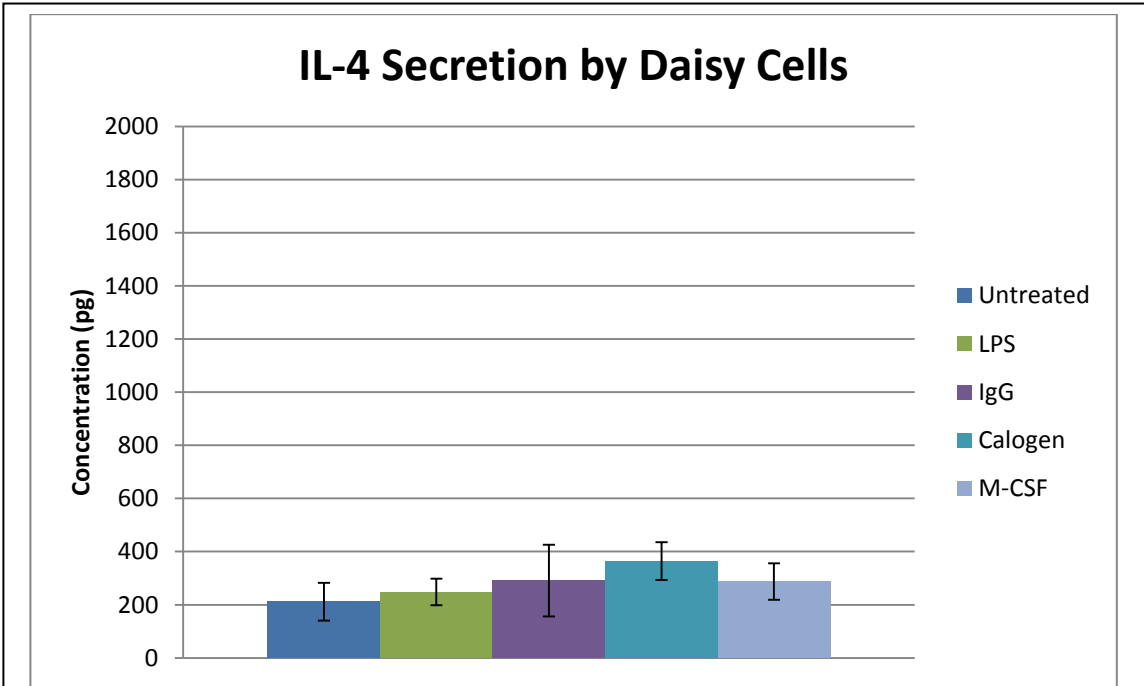


Figure 7.7 - IL-4 secretion by THP-1 cells.
 Concentrations of IL-4 protein detected by ELISA in cell culture supernatants of Daisy cells subjected to a variety of treatments.

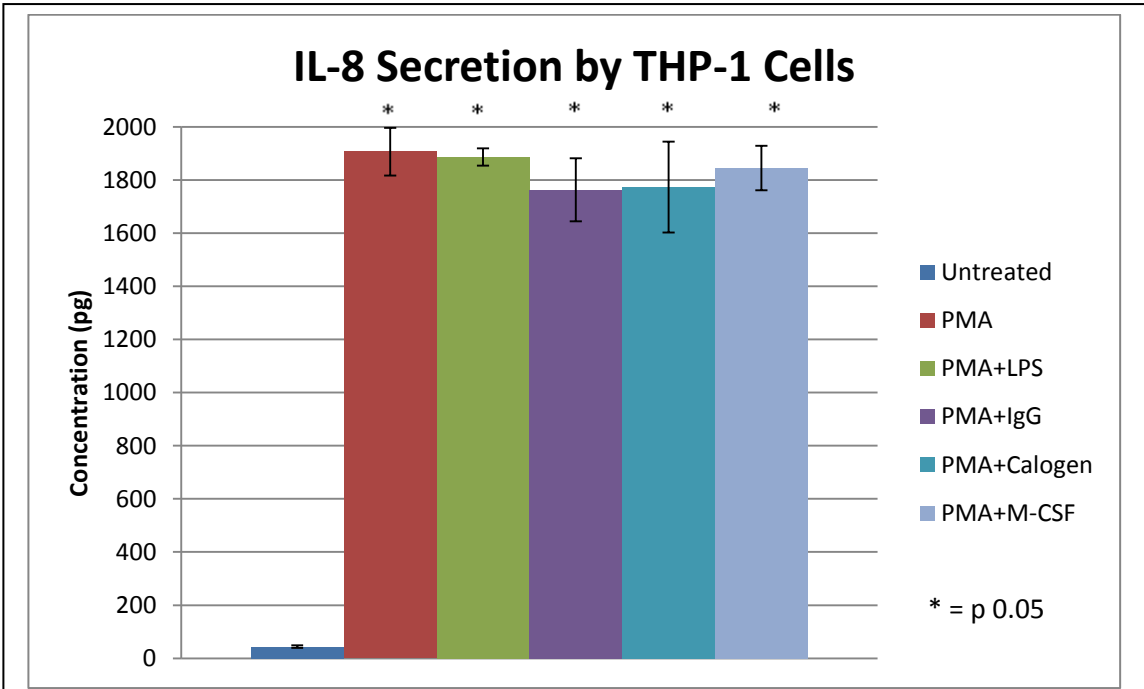


Figure 7.8 - IL-8 secretion by THP-1 cells.
 Concentrations of IL-8 protein detected by ELISA in cell culture supernatants of THP-1 cells subjected to a variety of treatments. Statistical significance is $p < 0.05$.

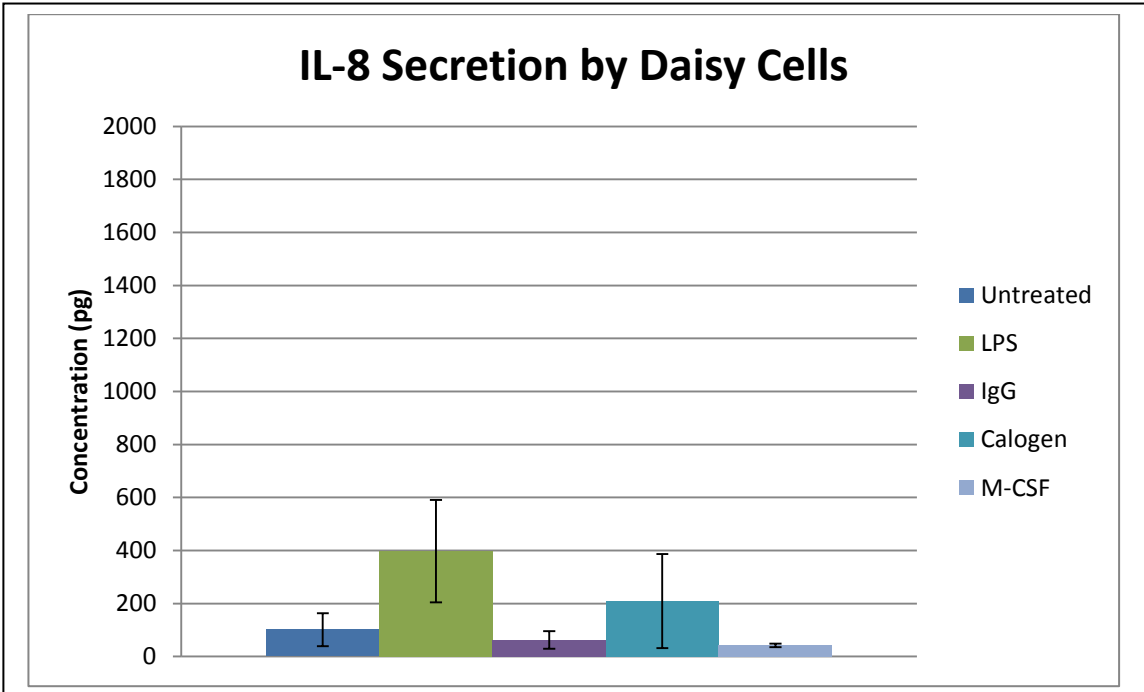
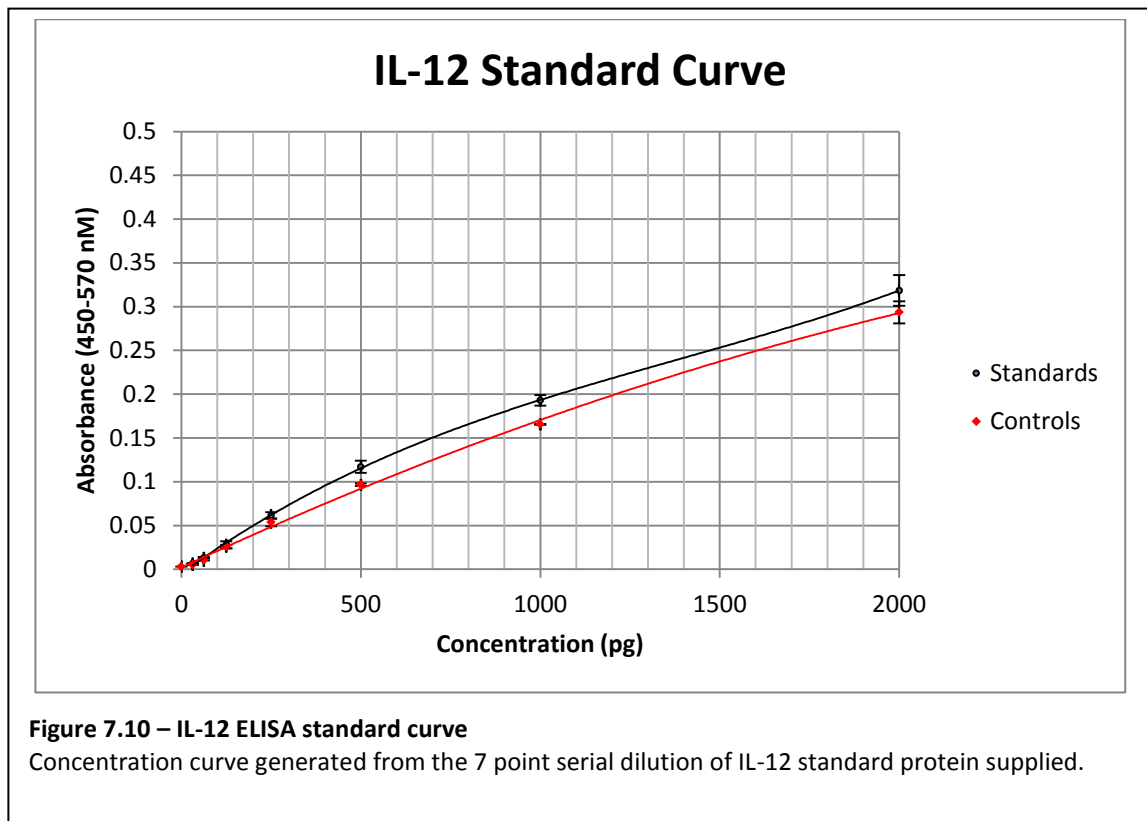
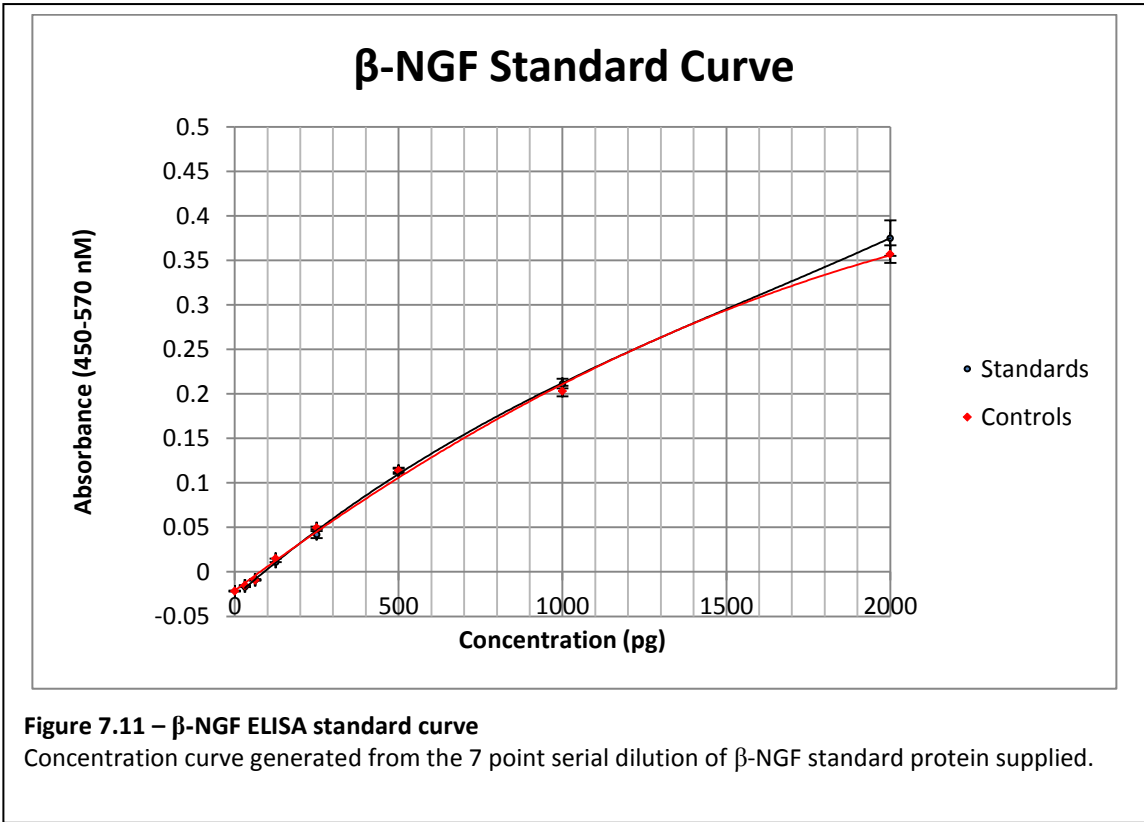


Figure 7.9 - IL-4 secretion by THP-1 cells.
 Concentrations of IL-8 protein detected by ELISA in cell culture supernatants of Daisy cells subjected to a variety of treatments.

Levels of both IL-12, the M1 macrophage marker and NGF were undetectable in samples taken from either THP-1 or Daisy cell culture although standards were detectable. Therefore, in order to determine the effect of cell culture media on the sensitivity of the ELISA test, standards were compared with standards of the same concentrations diluted in media rather than reagent diluent, as controls. Whilst the absorbance of controls was very slightly lower than the absorbance of the standards, proteins were detectable when diluted in cell culture media. These results can be seen in *figures 7.10 and 7.11*.





7.4 Discussion

The purpose of this chapter was to generate *in vitro* cell cultures of activated macrophages polarised to both the M1 inflammatory phenotype and the M2 anti-inflammatory phenotype in order to compare with lipid laden macrophages. Stimulation of THP-1 cells was required to induce monocyte to macrophage differentiation prior to treatment. As a result of PMA stimulation during cell surface marker analysis cells showed a significant increase in CD14 expression which would be expected to occur on cell differentiation. In addition THP-1 cells showed a significant increase in the integrin molecule, CD11b expression, also expected as cells become adherent upon differentiation to macrophages. THP-1 cells also indicated a change in functionality upon differentiation by a significant decrease in expression of low affinity IgG receptor (CD32) with increased expression of the high affinity IgG receptor (CD64). The lipid scavenger receptor (CD36) and the T-cell co-stimulatory molecule, CD86, were also significantly raised, showing that THP-1 cells stimulated with PMA differentiate from suspended monocyte like cells into adherent, mature, functioning 'macrophage-like' cells. Daisy cells did not require PMA stimulation in order to become 'macrophage-like'.

Upon stimulation with LPS, we expected PMA/THP-1 cells and Daisy cells to polarise to an inflammatory M1 macrophage phenotype with increased expression of all 3 IgG receptors (CD16, CD32 and CD64) and possibly increased expression of CD80, the co-stimulatory molecule required for T_H1 cell differentiation. In fact, PMA/THP-1 cells did show an increase in any of these markers except CD64, whilst Daisy cells showed an increase in all 4 molecules. However, none of these observed changes in expression were shown to be statistically significant.

Using IL-12 as a marker of M1 inflammatory macrophages, it was expected that cells treated with LPS would produce higher levels than those treated with heat aggregated human IgG or M-CSF. Unfortunately, IL-12 was not detectable in any of the samples of cell culture supernatant; therefore a control ELISA was performed. Cell culture media was used to dilute IL-12 protein standards to the same

concentrations as the standards used to produce the standard curve. IL-12 was detectable in the samples although the absorbance was slightly lower. This was most likely due to the colour difference of the cell culture media, being red, and the clear reagent diluent used for the standards. This therefore confirmed that had IL-12 been released from the cells into the culture media, it would have been detectable. However, the absorbance of the standards used was lower than expected so it is perhaps possible that the detection reagent used was not as sensitive as some others available. If this was the case then very low levels of protein, below that of the lowest standard (31.5 pg/ml) may not be detected. This was also the case when probing for NGF.

Upon stimulation with heat aggregated human IgG, we expected PMA/THP-1 cells and Daisy cells to polarise to an anti-inflammatory M2 macrophage phenotype with increased expression of the IgE receptor (CD23), up-regulation of the haemoglobin and mannose receptors (CD163 and CD206) and possibly with increased expression of CD86, the co-stimulatory molecule required for TH2 cell differentiation. Heat aggregated human IgG treated PMA/THP-1 cells showed only a significant decrease in CD32 compared with PMA only treated cells which does not indicate cell polarisation. Daisy cells showed a significant decrease in CD11b, CD32, CD64, CD86 and CD163 with a visible, yet non-specific, reduction in most other markers. Given the previous finding discussed in *chapter 4*, that Daisy cells have a higher affinity for opsonised antigen than PMA/THP-1 cells, this would indicate a possible blocking effect occurring whereby the heat aggregated human IgG prevents binding of the primary antibody to the CD antigen, rather than down regulation of the molecule itself.

For this reason we compared heat aggregated human IgG stimulation with an alternative method for inducing M2 polarisation, namely M-CSF. In PMA/THP-1 cells, the IgG receptor CD32 appeared significantly reduced with heat aggregated human IgG stimulation but not M-CSF stimulation compared with PMA only cells. This would suggest a blocking effect seen by heat aggregated human IgG but no effect with

M-CSF. A small but significant reduction in CD163 was observed with M-CSF treated cells compared with controls which would indicate that both heat aggregated human IgG and M-CSF were ineffective at generating M2 polarised macrophages. Daisy cells treated with heat aggregated human IgG showed significant reductions in CD36, CD163 and CD206 whilst cells treated with M-CSF showed no significant difference from untreated cells. Again this would suggest that both heat aggregated human IgG and M-CSF were ineffective at generating M2 polarised macrophages based upon the cell surface marker expression we expected. The first thing to consider would be whether the concentration of M-CSF was sufficient and whether this could be investigated in future experiments. A second consideration would be whether, as some review articles suggest, alternative activation requires not one but two concurrent forms of stimulation (Anderson and Mosser, 2002, Tierney et al., 2009). Perhaps both heat aggregated human IgG and M-CSF simultaneously would have been more effective.

Using IL-4 as a marker of M2 anti-inflammatory macrophages, it was expected that cells treated with heat aggregated human IgG or M-CSF would produce higher levels than those treated with LPS. IL-4 was detected in cell culture supernatant from all the treatments, at 100 pg/ml from THP-1 cells and at around 200-400 pg/ml from Daisy cells. Whilst IgG treated Daisy cells appeared to produce more IL-4 than LPS treated cells, the difference was not significant, perhaps owing to the small number of repeats (n=3).

When comparing cells treated with Calogen to all other cells in the THP-1 cell experiments, the only significant differences were in that CD14 was more highly expressed in Calogen treated cells than LPS treated cells and CD32 was less expressed in the same cell comparison. In the Daisy cell experiments, Calogen treated cells showed significantly less CD163 expression than LPS treated cells but not different from untreated cells. It would appear then that our attempts to generate and immunophenotypically distinguish between M1 and M2 macrophages were not as useful as we hoped in *in vitro* cell culture and perhaps further experiments would prove

fruitful. However, given that the current literature fails to report any definitive marker of activated macrophage cell polarisation, I would think this is unlikely.

IL-8, a cytokine which functions as a neutrophil chemo-attractant protein was also probed for and detected in all samples. In untreated THP-1 cell culture supernatant, levels of IL-8 were particularly low. However, when THP-1 cells were stimulated with PMA, IL-8 levels were significantly raised regardless of the secondary stimulation. This would indicate that the PMA stimulation itself, used to differentiate THP-1 monocyte like cells into macrophages, is responsible for the increased IL-8. Indeed in Daisy cell culture samples, where PMA stimulation was not required, IL-8 concentrations were much lower. Compared with untreated Daisy cells, LPS treated Daisy cells appeared to produce IL-8 at a higher concentration, although this was not significant. As neutrophilic infiltration of the airways is a clinical feature of infectious inflammatory airways diseases, this finding was not surprising. What was interesting however, was that although again not significant, Calogen treated cells also appeared to produce higher concentrations of IL-8 than untreated cells. This may contribute to the non-atopic asthma profile which presents a neutrophilic inflammation of the airways as opposed to the eosinophilic inflammation seen in atopic, or allergic asthma. Although experiments were repeated 3 times, further repeats are required in order to allow stronger parametric statistical testing to be performed. In addition, repeats using a more sensitive detection reagent are required, which may also uncover very low levels of IL-12 and or NGF before any final conclusions can be drawn.

In addition to cell culture experiments, sufficient BAL fluid collected from 4 patients undergoing diagnostic bronchoscopy were also analysed for cells surface marker expression. All samples showed low CD14 and low CD11b expression indicative of a mature differentiated alveolar macrophage cell phenotype. CD11b expression was however slightly raised in both the patient with acute myeloid leukaemia (AML) and fungal chest infection and the patient with bronchiectasis. CD11b is an adhesion

molecule responsible for firm adhesion, usually of monocytes, to the endothelial wall before the cell exits the circulation. In the patient with cancer this may reflect a tumour associated increase in vasculature and the macrophage innate immune response to infiltrate the cancerous tissue. In the patient with bronchiectasis, the significance is less clear. The IgE receptor, CD23, was absent from cells of all samples. As IgE is the predominant antibody in allergic response this finding is of no surprise. The IgG receptors, CD16 and CD64, were also either absent or expressed at very low levels. However CD32 was expressed at much higher levels in all samples except that taken from a patient with bronchiectasis. The clinical significance of a lack of low affinity IgG receptor in the airways of patients with bronchiectasis is not clear, however if this finding were to extend to a larger cohort then perhaps further investigation would be warranted. The granulocyte adhesion molecule, CD24, was found to be expressed at low levels in cells from the patient with GOR but at very high levels in cells from the patient with cancer. CD24 is not only expressed by granulocytes but also dendritic cells. These cells have strikingly similar origins to that of the macrophage and also have similar morphology. It would appear then that in this patient at least, dendritic cells predominate over macrophages in the airway. Expression levels of the oxLDL receptor, CD36, were low in all cells from all pathologies except GOR. Although our *in vitro* experiments failed to show CD36 as a significant facilitator of lipid accumulation, this may not be the case in primary cell culture. Also, the LLAMI of this patient was 74, not one of the highest by far so expression levels of this molecule may distinguish between lipid accumulation by GOR or by phagocytosis of epithelial cells. Either way, this molecule should be investigated further in primary cell culture. The T-cell co-stimulatory molecules CD80 and CD86 were expressed at low levels only by cells from the patient with AML and fungal infection, of which CD80 was expressed at the highest level. This would indicate that the macrophages in the airways of this patient are responding to the fungal infection and directing a T-cell mediated response. Given that CD80 is expressed at a higher level than CD86, we would predict that this would be an inflammatory T_H1 response, as would be expected with a fungal infection. Lastly the 2

reported markers of M2 polarised activated macrophages, CD163 and CD206 were expressed at high levels in cells from the AML patient with fungal infection, and to a slightly lesser extent, the patient with cancer. In conjunction with the high CD24 seen in cells from the patient with cancer, this would confirm dendritic cell phenotype. In the case of AML with fungal infection it would be more likely that the presence of CD163 and possibly CD206 are due to the leukaemic cell immunophenotype, rather than to the infection.

In conclusion, our *in vitro* attempts to generate and immunophenotypically distinguish M1 and M2 polarised macrophages were disappointing. As a result, we were not able to determine the polarisation status of lipid treated cells. We did, however, demonstrate that PMA stimulation of THP-1 generates mature macrophage-like cells and results in significant changes in cell surface molecule expression. We also demonstrated that Daisy cells have a higher antibody complex binding ability than PMA/THP-1 cells, as shown by an antibody blocking effect resulting from treatment with heat aggregated human IgG. We also demonstrated heterogeneity among primary macrophage cells isolated from BAL fluid collected from patients with varying pathologies. Of particular interest is the finding that macrophages isolated from a patient with GOR showed higher CD36 expression than any other pathology. This finding, however, needs to be investigated further in a larger cohort of GOR patients with both acid and silent reflux to determine its significance.

8 General Conclusions

Asthma is a disease of the airways characterised by chronic inflammation, airway hyper-responsiveness and variable, usually reversible, airflow obstruction (Chung and Adcock, 2000, Levy and Pierce, 2005, Rees, 2000). Presenting symptoms can range from mild intermittent wheezing or cough to severe episodes of airway obstruction requiring treatment and/or hospitalisation (Chung and Adcock, 2000). The two predominant phenotype categories of this disease are allergic and non-allergic asthma (Levy and Pierce, 2005), in which patients can be divided by the presence or absence of atopy; an elevated level of serum IgE levels associated with a pre-disposition to allergic diseases. A further category termed severe or difficult asthma accounts for around 10-20% of all asthmatics (Busse, 2011, Wenzel, 2011). This represents patients who have low base-line lung function and experience almost daily symptoms and frequent exacerbations despite high dose treatment. Patients in this category often present signs of gastro-oesophageal reflux (GOR), a phenomenon which is widely observed and published, yet currently unexplained.

GOR is one of the most common causes of chronic cough (Everett and Morice, 2004) and aspiration of gastric contents (liquid or gaseous) into the airway is considered the primary cause (Shashkin et al., 2005). Diagnosis of acid reflux can be made by investigative procedures, such as 24 hour oesophageal pH monitoring with a cough diary, barium meal studies and endoscopic visualisation of the oesophagus. However, non-acid reflux is more difficult as there are no current diagnostic tests available. The alveolar macrophage makes up to 70% of the immune cells populating the airway and is capable of antigen presentation and modulation of the immune response. The alveolar macrophage is also capable of lipid uptake which may activate and induce an inflammatory phenotype by mechanisms currently unknown. Studies regarding the use of the lipid laden macrophage scoring system (LLAMI), first described by Colombo and Hallberg (1987), to quantify the levels of macrophage ingested lipids in the airways as a reliable diagnostic tool of reflux and aspiration have been extensive. Combined, these findings show an unquestionable presence of lipid laden macrophages in respiratory disease; however the diagnostic use of the LLAMI in GOR is still

debatable. Undoubtedly, the varying reports have had differing patient inclusion/exclusion criteria, in addition to differing methods of GOR diagnosis. We hypothesised that lipid droplets from undigested or partially digested food may be aspirated into the airway and accumulate in scavenging macrophages. Foam cell formation in the airway thus generates activated macrophages that interact with other immune cells and tissue to induce an asthma-like state of disease.

We collected samples of alveolar macrophages from a cohort of patients with a variety of respiratory disorders and controls, to determine a correlation between GOR and extent of foam cell formation in the airway. Unlike other studies, we wanted to include patients with silent or non-acid reflux, in addition to acid reflux, based on clinical history and Hull Airway Reflux Questionnaire (HARQ) scores (Morice et al., 2011). A total of 29 patients undergoing diagnostic bronchoscopy were able to provide sufficient excess BAL sample fluid to allow ORO staining and LLAMI scoring. Of the 29 patients, 11 were diagnosed with GOR either previously or as a result of clinical investigation relating to the bronchoscopy. A significant correlation was shown between gender and GOR diagnosis demonstrating a distinct female predominance within this disease group. A significant negative correlation was also shown between HARQ score and age, demonstrating that symptoms of cough hypersensitivity may reduce with age. Reflux can be attributed to loss of tone in the smooth muscle comprising the LOS, which would be expected to decrease further with age as smooth muscle tone deteriorates throughout the body. However our data show that symptoms decrease with age, rather than increase as would be expected. Perhaps a consequence of examining such a small cohort, however it is also possible that the sensory airway neurons become desensitised over time resulting in a tachyphylaxis effect as seen in cough challenge experiments (Morice et al., 1992).

Regarding the LLAMI as a diagnostic tool, our experiments showed no significant correlation between LLAMI and GOR diagnosis or HARQ score. We investigated the reliability of the LLAMI itself using a novel *in vitro* model for reflux aspiration, namely Calogen high fat liquid meal, as a substitute for stomach contents.

Incubation of this substance with immortalised human macrophages led to intracellular lipid droplet accumulation, which was verified in terms of origin as both untreated cells and cells treated with fat free Fortijuice showed no lipid accumulation. Hence lipid accumulation was shown to be a result of direct uptake from the Calogen, the process of which was shown to be both actin and LDL scavenger receptor (CD36) independent. Whilst investigating the sensitivity of the lipid accumulation and staining protocols optimised in this study we found that the inter-well variability of cells of the same passage, treated identically, showed a low degree of variability (2.3-5.4 %). Therefore, we have shown that whilst the LLAMI is a reliable test, it is the levels of accumulated lipid in alveolar macrophages that is variable. This variability may be a consequence of diet, the type of reflux experienced by the patient, i.e. acid/non-acid, the severity of reflux or a combination of all three. In addition reflux of stomach acid and pepsin, or indeed simply the mechanical act of coughing can induce airway epithelial damage. Further *in vitro* experiments uncovered, to our knowledge, for the first time that lipid stores found in apoptotic airway epithelial cells can be transferred to the macrophage upon normal phagocytosis creating an additional variable factor to the degree of alveolar macrophage lipid accumulation. Given that the presentation of reflux is so wildly heterogeneous amongst patients, finding a single diagnostic test seems quite unlikely. Therefore it is perhaps more suitable to incorporate a range of tests to include pH monitoring for acid reflux, pepsin on exhaled breath condensate, sputum cell differentials to determine degree of epithelial damage and LLAMI to account for non-acid reflux in the clinical workup. As reflux can occur sporadically in otherwise healthy individuals also, future studies need to be undertaken, collecting measurements from all these parameters collectively. Comparing this data between asymptomatic individuals and patients with respiratory symptoms will allow the establishment of reference ranges to be used in diagnosis.

Further to our hypothesis of lipid laden macrophages being present in

reflux associated airways disease as a result of lipid aspiration, we hypothesised that this lipid accumulation results in activated macrophage polarisation towards an M2 phenotype, capable of directing an immune T_H-2 response seen in asthmatic airways. Recently, a small number of molecules reported to enable the distinction of polarised activated macrophages (Stout and Suttles, 2004, Porcheray et al., 2005, Bouhlel et al., 2007, Anderson and Mosser, 2002), have emerged and we proposed to investigate these, and others. Using lipopolysaccharide (LPS) and heat aggregated human IgG to generate activated macrophages of both M1 and M2 subtypes respectively. We therefore proposed to determine an immunophenotypical profile of M1 and M2 macrophages and aimed to determine activation polarisation of lipid laden macrophages using the same panel of antibodies. We also wanted to investigate released cytokine profiles, as an alternative distinguishing feature and the contribution of the lipid laden macrophage to the symptoms seen in asthma/GOR patients. We proposed to use IL-12 and IL-4 cytokine secretion levels to identify M1 and M2 activated macrophages, comparing these with Calogen treated macrophages. In addition we proposed that Calogen treatment would enhance production of IL-8 neutrophil chemoattractant protein, contributing to the neutrophilic non-atopic asthma profile. We also wanted to investigate the production of a further cytokine, nerve growth factor, proposing that increased production of this protein would contribute to airway hypersensitivity by inducing innervation of the airways.

Upon stimulation, we expected PMA differentiated THP-1 cells and Daisy cells treated with LPS to polarise to an inflammatory M1 macrophage phenotype, increasing expression of CD16, CD32 and CD64 and possibly CD80 with increase release of IL-12. We also expected cells treated with heat aggregated human IgG or MCS-F to polarise to an anti-inflammatory M2 macrophage phenotype with increasing expression of CD23, CD163, CD206 and possibly CD86, with increase IL-4 production. PMA/THP-1 cells showed no significant increase in any of these markers except CD64, when treated with LPS and only a significant decrease in CD32, when treated with heat aggregated human IgG. A small but significant reduction in CD163 was observed with

M-CSF. None of which indicate cell polarisation Daisy cells showed no statistically significant changes in CD marker expression post LPS or M-CSF treatment, again demonstrating a lack of polarisation. However, Daisy cells showed a significant decrease in CD11b, CD32, CD64, CD86 and CD163 with a visible, yet non-specific, reduction in most other markers post IgG treatment. The latter finding was attributed to a possible blocking effect occurring whereby the heat aggregated human IgG prevents binding of the primary antibody to the CD antigen, rather than down regulation of the molecule itself. Neither cells showed significant changes in IL-12 or IL-4 release under any treatment regime so it would appear from these experiments that immortal macrophage cell lines are much less responsive to stimuli than primary cells of that markers of polarisation are more discrete in humans than we had hoped. NO changes were seen in expression of polarisation markers in Calogen treated cells compared with controls, therefore in this study we were unable to demonstrate the M2 polarisation we had hypothesised. We would however be encouraged by the IL-4 results produced. Although not significant here, there was a visible increase in Calogen treated cells which may become significant with further repeats. This is also true of IL-8. Primary human macrophages appeared much more heterogeneous across treatment groups with regards to cell surface markers and the increased expression of CD36 in our patient with GOR shows potential as a diagnostic marker.

In vitro experiments using human macrophages currently require mitogenic stimulation of a macrophage precursor cell line or *ex vivo* maturation of circulating primary monocytes. We have derived a unique sub-clone of the THP-1 cell line capable of spontaneous perpetual differentiation into macrophage-like cells termed 'Daisy' and alongside the main purpose of this study aimed to characterise this cell line and investigate its potential advantage over the THP-1 cell line. We confirmed that the Daisy cells were not activated by mycoplasma, given that the initiating differential stimulus was, and is, unknown to us. In the absence of PMA stimulation, unlike unstimulated THP-1 cells, Daisy cells were adherent and morphologically

resembled human differentiated macrophages under both light and TEM microscopy. A higher proportion of euchromatin was seen in PMA stimulated THP-1 cells than Daisy cells which would signify increased DNA transcription processing. The significance of this finding is that PMA stimulation is potent and long lasting, which may mask any subsequent activity during *in vitro* experiments. Daisy cells showed much less loosely coiled chromatin which could indicate these cells are in a more 'resting' state which may be advantageous in the experimental setting. When THP-1 cells were stimulated with PMA, IL-8 levels were significantly raised regardless of the secondary stimulation. This demonstrates that the PMA stimulation itself, used to differentiate THP-1 monocyte like cells into macrophages, is responsible for the increased IL-8. Indeed in Daisy cell culture samples, where PMA stimulation was not required, IL-8 concentrations were much lower, therefore Daisy cells showed a distinct advantage with regards to PMA. Daisy cells were shown to phagocytose zymosan particles with greater though not significant capacity than PMA/THP-1 cells and both cell types were shown to be equally capable of lipid accumulation as demonstrated with ORO staining and lipid index quantification methods. The ability of PMA/THP-1 and Daisy cells to bind opsonised antigen was determined by incubation of the cells with fluorescent antibody coated BSA particles. Surprisingly PMA/THP-1 cells were barely able to bind these particles despite subsequently showing expression of all three IgG receptors (CD16, CD32 and CD64). However, Daisy cells were able to bind large amounts of opsonised antigen indicating a significant difference between the two cell types and one which needs further investigation.

Cell surface phenotype studies showed significant differences between PMA/THP-1 cells and Daisy cells, as did gene microarray analysis. Daisy cells expressed significantly less CD14 and CD11b than PMA/THP-1 cells indicating a more differentiated state. Daisy cells also expressed significantly more CD80, CD163 and CD206 than PMA/THP-1 cells, indicating a phenotype more similar to an M2 polarised macrophage without stimulation. This may account for the lack of polarisation discussed previously. Perhaps PMA stimulation of THP-1 cells renders them insensitive

to further stimulation, whereas Daisy cells are already polarised and unable to be reversed back to a resting state. During gene array analysis, Daisy cells expressed almost 40000 genes with at least a 2 fold difference in levels of transcription regardless of whether we compared them to THP-1 cells or PMA stimulated THP-1 cells. This demonstrates that the Daisy cell line has become distinct, on a genetic level, from its progenitor the THP-1 cell.

In conclusion, we have shown in our study that the LLAMI is incapable of distinguishing GOR and non-GOR patients. We showed that macrophages are capable of direct dietary lipid uptake, independently of actin or CD36. However, alveolar macrophage lipid accumulation also results from the phagocytic clearance of apoptotic epithelial cells, a previously un-reported finding, which may account for the lack of LLAMI specificity for GOR. Our *in vitro* attempts to generate and distinguish M1 and M2 polarised macrophages were unsuccessful and as a result, we were not able to determine the polarisation status of lipid treated cells. We did, however, demonstrate heterogeneity among primary macrophage cells isolated from BAL fluid collected from patients with varying pathologies. Of particular interest is the finding that macrophages isolated from a patient with GOR showed higher CD36 expression than any other pathology. Daisy cells are genetically distinct cells which appear to be macrophage-like cells morphologically, functionally and phenotypically. Phagocytosis, lipid accumulation and opsonised antigen binding assessments all show these cells to be functionally mature. Whilst DNA transcription activity appears low by TEM, phenotype analysis shows these cells to be active in, most likely, an alternative fashion. It is our opinion that the Daisy cells have potential utility for future studies with the ability to spontaneously replicate and differentiate. This gives the Daisy cells an advantage over THP-1 cells which require potent and long lasting PMA stimulation, rendering them insensitive to secondary stimuli.

9 Bibliography

- ADAMS, R., RUFFIN, R. & CAMPBELL, D. (1997) The value of the lipid-laden macrophage index in the assessment of aspiration pneumonia. *Aust N Z J Med*, 27, 550-3.
- AHRENS, P., NOLL, C., KITZ, R., WILLIGENS, P., ZIELEN, S. & HOFMANN, D. (1999) Lipid-laden alveolar macrophages (LLAM): a useful marker of silent aspiration in children. *Pediatr Pulmonol*, 28, 83-8.
- ALLEN, C. J. & ANVARI, M. (1998) Gastro-oesophageal reflux related cough and its response to laparoscopic fundoplication. *Thorax*, 53, 963-8.
- ALLEN, G. B., LECLAIR, T. R., VON REYN, J., LARRABEE, Y. C., CLOUTIER, M. E., IRVIN, C. G. & BATES, J. H. (2009) Acid aspiration-induced airways hyperresponsiveness in mice. *J Appl Physiol*, 107, 1763-70.
- ANDERSON, C. F. & MOSSER, D. M. (2002) A novel phenotype for an activated macrophage: the type 2 activated macrophage. *J Leukoc Biol*, 72, 101-6.
- ASANO, K. & SUZUKI, H. (2009) Silent acid reflux and asthma control. *N Engl J Med*, 360, 1551-3.
- ASTHMAUK (2010) For journalists: key facts & statistics.
- AUWERX, J. (1991) The human leukemia cell line, THP-1: a multifaceted model for the study of monocyte-macrophage differentiation. *Experientia*, 47, 22-31.
- BALBO, P., SILVESTRI, M., ROSSI, G. A., CRIMI, E. & BURASTERO, S. E. (2001) Differential role of CD80 and CD86 on alveolar macrophages in the presentation of allergen to T lymphocytes in asthma. *Clin Exp Allergy*, 31, 625-36.
- BARBAS, A. S., DOWNING, T. E., BALSARA, K. R., TAN, H. E., RUBINSTEIN, G. J., HOLZKNECHT, Z. E., COLLINS, B. H., PARKER, W., DAVIS, R. D. & LIN, S. S. (2008) Chronic aspiration shifts the immune response from Th1 to Th2 in a murine model of asthma. *Eur J Clin Invest*, 38, 596-602.
- BARDHAN, K. D., STRUGALA, V. & DETTMAR, P. W. (2012) Reflux revisited: advancing the role of pepsin. *Int J Otolaryngol*, 2012, 646901.
- BARREDA, D. R., HANINGTON, P. C. & BELOSEVIC, M. (2004) Regulation of myeloid development and function by colony stimulating factors. *Dev Comp Immunol*, 28, 509-54.
- BASSET-LEOBON, C., LACOSTE-COLLIN, L., AZIZA, J., BES, J. C., JOZAN, S. & COURTADE-SAIDI, M. (2010) Cut-off values and significance of Oil Red O-positive cells in bronchoalveolar lavage fluid. *Cytopathology*, 21, 245-50.
- BATHOORN, E., DALY, P., GAISER, B., STERNAD, K., POLAND, C., MACNEE, W. & DROST, E. M. (2011) Cytotoxicity and induction of inflammation by pepsin in Acid in bronchial epithelial cells. *Int J Inflam*, 2011, 569416.
- BATOOL, M., KHALID, M. H., HASSAN, M. N. & FAUZIA YUSUF, H. (2011) Homology modeling of an antifungal metabolite plipastatin synthase from the Bacillus subtilis 168. *Bioinformation*, 7, 384-7.
- BEEKHUIZEN, H. & VAN FURTH, R. (1993) Monocyte adherence to human vascular endothelium. *J Leukoc Biol*, 54, 363-78.

- BENDER, J. G., VAN EPPS, D. E. & STEWART, C. C. (1987) Regulation of myelopoiesis. *Comp Immunol Microbiol Infect Dis*, 10, 79-91.
- BICE, T., LI, G., MALINCHOC, M., LEE, A. S. & GAJIC, O. (2011) Incidence and risk factors of recurrent acute lung injury. *Crit Care Med*, 39, 1069-73.
- BOBRYSEV, Y. V. (2006) Monocyte recruitment and foam cell formation in atherosclerosis. *Micron*, 37, 208-22.
- BOUHLEL, M. A., DERUDAS, B., RIGAMONTI, E., DIEVART, R., BROZEK, J., HAULON, S., ZAWADZKI, C., JUDE, B., TORPIER, G., MARX, N., STAELS, B. & CHINETTI-GBAGUIDI, G. (2007) PPARgamma activation primes human monocytes into alternative M2 macrophages with anti-inflammatory properties. *Cell Metab*, 6, 137-43.
- BOWDEN, D. H. (1976) The pulmonary macrophage. *Environ Health Perspect*, 16, 55-60.
- BROWN, S. R., GYAWALI, C. P., MELMAN, L., JENKINS, E. D., BADER, J., FRISELLA, M. M., BRUNT, L. M., EAGON, J. C. & MATTHEWS, B. D. (2011) Clinical outcomes of atypical extra-esophageal reflux symptoms following laparoscopic antireflux surgery. *Surg Endosc*, 25, 3852-8.
- BTS & SIGN (2009) British Guideline on the Management of Asthma.
- BURASTERO, S. E., MAGNANI, Z., CONFETTI, C., ABBRUZZESE, L., ODDERA, S., BALBO, P., ROSSI, G. A. & CRIMI, E. (1999) Increased expression of the CD80 accessory molecule by alveolar macrophages in asthmatic subjects and its functional involvement in allergen presentation to autologous TH2 lymphocytes. *J Allergy Clin Immunol*, 103, 1136-42.
- BUSSE, W. W. (2011) Difficult-to-treat asthma: how serious is the problem and what are the issues? *European Respiratory Monograph*, 51, 1-15.
- CHAIT, A., IVERIUS, P. H. & BRUNZELL, J. D. (1982) Lipoprotein lipase secretion by human monocyte-derived macrophages. *J Clin Invest*, 69, 490-3.
- CHANG, A. B., COX, N. C., PURCELL, J., MARCHANT, J. M., LEWINDON, P. J., CLEGHORN, G. J., EE, L. C., WITHERS, G. D., PATRICK, M. K. & FAOAGALI, J. (2005) Airway cellularity, lipid laden macrophages and microbiology of gastric juice and airways in children with reflux oesophagitis. *Respir Res*, 6, 72.
- CHEN, E. & MILLER, G. E. (2007) Stress and inflammation in exacerbations of asthma. *Brain Behav Immun*, 21, 993-9.
- CHEN, R. Y. & THOMAS, R. J. (2000) Results of laparoscopic fundoplication where atypical symptoms coexist with oesophageal reflux. *Aust N Z J Surg*, 70, 840-2.
- CHENG, C. M., HSIEH, C. C., LIN, C. S., DAI, Z. K., SHIH, P. K., EVERETT, M. L., THOMAS, A. D., PARKER, W., DAVIS, R. D. & LIN, S. S. (2010) Macrophage activation by gastric fluid suggests MMP involvement in aspiration-induced lung disease. *Immunobiology*, 215, 173-81.
- CHRONEOS, Z. C., SEVER-CHRONEOS, Z. & SHEPHERD, V. L. (2010) Pulmonary surfactant: an immunological perspective. *Cell Physiol Biochem*, 25, 13-26.
- CHUNG, K. F. & ADCOCK, I. (2000) Asthma. IN CHUNG, K. F. & ADCOCK, I. (Eds.) *Asthma Mechanisms and*

Protocols. Totowa, Humana Press.

- COLOMBO, J. L. & HALLBERG, T. K. (1987) Recurrent aspiration in children: lipid-laden alveolar macrophage quantitation. *Pediatr Pulmonol*, 3, 86-9.
- DAUB, K., SIEGEL-AXEL, D., SCHONBERGER, T., LEDER, C., SEIZER, P., MULLER, K., SCHALLER, M., PENZ, S., MENZEL, D., BUCHELE, B., BULTMANN, A., MUNCH, G., LINDEMANN, S., SIMMET, T. & GAWAZ, M. (2010) Inhibition of foam cell formation using a soluble CD68-Fc fusion protein. *J Mol Med (Berl)*, 88, 909-20.
- DUCHARME, N. A. & BICKEL, P. E. (2008) Lipid droplets in lipogenesis and lipolysis. *Endocrinology*, 149, 942-9.
- ENDEMANN, G., STANTON, L. W., MADDEN, K. S., BRYANT, C. M., WHITE, R. T. & PROTTER, A. A. (1993) CD36 is a receptor for oxidized low density lipoprotein. *J Biol Chem*, 268, 11811-6.
- EVERETT, C. F. & MORICE, A. H. (2004) Gastroesophageal reflux and chronic cough. *Minerva Gastroenterol Dietol*, 50, 205-13.
- FARUQI, S., SEDMAN, P., JACKSON, W., MOLYNEUX, I. & MORICE, A. H. (2012) Fundoplication in chronic intractable cough. *Cough*, 8, 3.
- FOLKERTS, G. & NIJKAMP, F. P. (1998) Airway epithelium: more than just a barrier! *Trends Pharmacol Sci*, 19, 334-41.
- GALLOWAY, J. (1993) Oesophageal disorders. IN JONES, R. (Ed.) *Gastrointestinal Problems in General Practice*. New York, Oxford University Press.
- GLATZ, J. F., LUIKEN, J. J. & BONEN, A. (2010) Membrane fatty acid transporters as regulators of lipid metabolism: implications for metabolic disease. *Physiol Rev*, 90, 367-417.
- GORDON, S. (2007) The macrophage: past, present and future. *Eur J Immunol*, 37 Suppl 1, S9-17.
- GSCHMEISSNER, S. Macrophage cells, TEM. *SciencePhotoLibrary*.
- GUNSILIUS, E., GASTL, G. & PETZER, A. L. (2001) Hematopoietic stem cells. *Biomed Pharmacother*, 55, 186-94.
- HAIG, D. M. (1992) Haemopoietic stem cells and the development of the blood cell repertoire. *J Comp Pathol*, 106, 121-36.
- HAMILTON, J. A. & KAMP, F. (1999) How are free fatty acids transported in membranes? Is it by proteins or by free diffusion through the lipids? *Diabetes*, 48, 2255-69.
- HARMENING, D. M. (Ed.) (1997) *Clinical Hematology and Fundamentals of Hemostasis*, Philadelphia, F.A.Davis Company.
- HARRIS, N., PEACH, R., NAEMURA, J., LINSLEY, P. S., LE GROS, G. & RONCHESE, F. (1997) CD80 costimulation is essential for the induction of airway eosinophilia. *J Exp Med*, 185, 177-82.
- HOPKINS, P. M., KERMEEN, F., DUHIG, E., FLETCHER, L., GRADWELL, J., WHITFIELD, L., GODINEZ, C., MUSK, M., CHAMBERS, D., GOTLEY, D. & MCNEIL, K. (2010) Oil red O stain of alveolar

macrophages is an effective screening test for gastroesophageal reflux disease in lung transplant recipients. *J Heart Lung Transplant*, 29, 859-64.

HOWARD, M. & HAMILTON, P. (2002) *Haematology*, London, Churchill Livingstone.

ISHIZUKA, S., YAMAYA, M., SUZUKI, T., NAKAYAMA, K., KAMANAKA, M., IDA, S., SEKIZAWA, K. & SASAKI, H. (2001) Acid exposure stimulates the adherence of *Streptococcus pneumoniae* to cultured human airway epithelial cells: effects on platelet-activating factor receptor expression. *Am J Respir Cell Mol Biol*, 24, 459-68.

JANOWITZ, H. D. (1994) Acid in the gullet: Heartburn, Esophagitis and Hiatal Hernia. *Indigestion*. New York, Oxford University Press Inc.

JAOUDE, P. A., KNIGHT, P. R., OHTAKE, P. & EL-SOLH, A. A. (2010) Biomarkers in the diagnosis of aspiration syndromes. *Expert Rev Mol Diagn*, 10, 309-19.

KAZACHKOV, M. Y., MUHLEBACH, M. S., LIVASY, C. A. & NOAH, T. L. (2001) Lipid-laden macrophage index and inflammation in bronchoalveolar lavage fluids in children. *Eur Respir J*, 18, 790-5.

KHLUSOV, I. A., KARLOV, A. V., SHARKEEV, Y. P., PICHUGIN, V. F., KOLOBOV, Y. P., SHASHKINA, G. A., IVANOV, M. B., LEGOSTAEVA, E. V. & SUKHIKH, G. T. (2005) Osteogenic potential of mesenchymal stem cells from bone marrow in situ: role of physicochemical properties of artificial surfaces. *Bull Exp Biol Med*, 140, 144-52.

KIERAN, S. M., KATZ, E., ROSEN, R., KHATWA, U., MARTIN, T. & RAHBAR, R. (2010) The lipid laden macrophage index as a marker of aspiration in patients with type I and II laryngeal clefts. *Int J Pediatr Otorhinolaryngol*, 74, 743-6.

KITZ, R., BOEHLES, H. J., ROSEWICH, M. & ROSE, M. A. (2012) Lipid-Laden Alveolar Macrophages and pH Monitoring in Gastroesophageal Reflux-Related Respiratory Symptoms. *Pulm Med*, 2012, 673637.

KOHRO, T., TANAKA, T., MURAKAMI, T., WADA, Y., ABURATANI, H., HAMAKUBO, T. & KODAMA, T. (2004) A comparison of differences in the gene expression profiles of phorbol 12-myristate 13-acetate differentiated THP-1 cells and human monocyte-derived macrophage. *J Atheroscler Thromb*, 11, 88-97.

KOMOHARA, Y., HIRAHARA, J., HORIKAWA, T., KAWAMURA, K., KIYOTA, E., SAKASHITA, N., ARAKI, N. & TAKEYA, M. (2006) AM-3K, an anti-macrophage antibody, recognizes CD163, a molecule associated with an anti-inflammatory macrophage phenotype. *J Histochem Cytochem*, 54, 763-71.

KRAUSE, D. S. (2002) Regulation of hematopoietic stem cell fate. *Oncogene*, 21, 3262-9.

LANDSMAN, L. & JUNG, S. (2007) Lung macrophages serve as obligatory intermediate between blood monocytes and alveolar macrophages. *J Immunol*, 179, 3488-94.

LEVY, M. L. & PIERCE, L. (2005) Introduction. *Asthma*. Elsevier.

LIAO, T. H., HAMOSH, P. & HAMOSH, M. (1984) Fat digestion by lingual lipase: mechanism of lipolysis in the stomach and upper small intestine. *Pediatr Res*, 18, 402-9.

- LUO, M., LEE, S. & BROCK, T. G. (2003) Leukotriene synthesis by epithelial cells. *Histol Histopathol*, 18, 587-95.
- LUTHY, K. E., PETERSON, N. E. & WILKINSON, J. (2008) Cost-efficient treatment for uninsured or underinsured patients with hypertension, depression, diabetes mellitus, insomnia, and gastroesophageal reflux. *J Am Acad Nurse Pract*, 20, 136-43.
- MANTOVANI, A., SICA, A. & LOCATI, M. (2007) New vistas on macrophage differentiation and activation. *Eur J Immunol*, 37, 14-6.
- MAPOFMEDICINE** (2010) Chronic Asthma. *Map of Medicine*. London, Map of Medicine Ltd.
- MARTINEZ, F. O., GORDON, S., LOCATI, M. & MANTOVANI, A. (2006) Transcriptional profiling of the human monocyte-to-macrophage differentiation and polarization: new molecules and patterns of gene expression. *J Immunol*, 177, 7303-11.
- MATHEW, J. L., SINGH, M. & MITTAL, S. K. (2004) Gastro-oesophageal reflux and bronchial asthma: current status and future directions. *Postgrad Med J*, 80, 701-5.
- MAUS, U., HUWE, J., ERMERT, L., ERMERT, M., SEEGER, W. & LOHMEYER, J. (2002) Molecular pathways of monocyte emigration into the alveolar air space of intact mice. *Am J Respir Crit Care Med*, 165, 95-100.
- MAY, L., CARIM, M. & YADAV, K. (2011) Adult asthma exacerbations and environmental triggers: a retrospective review of ED visits using an electronic medical record. *Am J Emerg Med*, 29, 1074-82.
- MCNALLY, P., ERVINE, E., SHIELDS, M. D., DIMITROV, B. D., EL NAZIR, B., TAGGART, C. C., GREENE, C. M., MCELVANEY, N. G. & GREALLY, P. (2011) High concentrations of pepsin in bronchoalveolar lavage fluid from children with cystic fibrosis are associated with high interleukin-8 concentrations. *Thorax*, 66, 140-3.
- MICILLO, E., BIANCO, A., D'AURIA, D., MAZZARELLA, G. & ABBATE, G. F. (2000) Respiratory infections and asthma. *Allergy*, 55 Suppl 61, 42-5.
- MIDULLA, F., STRAPPINI, P. M., ASCOLI, V., VILLA, M. P., INDINNIMEO, L., FALASCA, C., MARTELLA, S. & RONCHETTI, R. (1998) Bronchoalveolar lavage cell analysis in a child with chronic lipid pneumonia. *Eur Respir J*, 11, 239-42.
- MISE, K., CAPKUN, V., JURCEV-SAVICEVIC, A., SUNDOV, Z., BRADARIC, A. & MLADINOV, S. (2010) The influence of gastroesophageal reflux in the lung: a case-control study. *Respirology*, 15, 837-42.
- MOORE, K. J. & FREEMAN, M. W. (2006) Scavenger receptors in atherosclerosis: beyond lipid uptake. *Arterioscler Thromb Vasc Biol*, 26, 1702-11.
- MOREHEAD, R. S. (2009) Gastro-oesophageal reflux disease and non-asthma lung disease. *Eur Respir Rev*, 18, 233-43.
- MORICE, A. H. & BUSH, A. (2003a) Chronic Cough in Adults. IN SHAW, P. (Ed.) *Cough*. London, Current Medical Literature Ltd.
- MORICE, A. H. & BUSH, A. (2003b) Chronic Cough in Children. IN SHAW, P. (Ed.) *Cough*. London, Current

- MORICE, A. H., FARUQI, S., WRIGHT, C. E., THOMPSON, R. & BLAND, J. M. (2011) Cough hypersensitivity syndrome: a distinct clinical entity. *Lung*, 189, 73-9.
- MORICE, A. H., HIGGINS, K. S. & YEO, W. W. (1992) Adaptation of cough reflex with different types of stimulation. *Eur Respir J*, 5, 841-7.
- MOSSER, D. M. & EDWARDS, J. P. (2008) Exploring the full spectrum of macrophage activation. *Nat Rev Immunol*, 8, 958-69.
- MULLER, T., HLINAK, A., MUHLE, R. U., KRAMER, M., LIEBHERR, H., ZIEDLER, K. & PFEIFFER, D. U. (1999) A descriptive analysis of the potential association between migration patterns of bean and white-fronted geese and the occurrence of Newcastle disease outbreaks in domestic birds. *Avian Dis*, 43, 315-9.
- MULLER, W. A. & RANDOLPH, G. J. (1999) Migration of leukocytes across endothelium and beyond: molecules involved in the transmigration and fate of monocytes. *J Leukoc Biol*, 66, 698-704.
- ORLOVSKAYA, I., SCHRAUFSTATTER, I., LORING, J. & KHALDOYANIDI, S. (2008) Hematopoietic differentiation of embryonic stem cells. *Methods*, 45, 159-67.
- PACHECO-GALVAN, A., HART, S. P. & MORICE, A. H. (2011) Relationship between gastro-oesophageal reflux and airway diseases: the airway reflux paradigm. *Arch Bronconeumol*, 47, 195-203.
- PARAMESWARAN, K., ANVARI, M., EFTHIMIADIS, A., KAMADA, D., HARGREAVE, F. E. & ALLEN, C. J. (2000) Lipid-laden macrophages in induced sputum are a marker of oropharyngeal reflux and possible gastric aspiration. *Eur Respir J*, 16, 1119-22.
- PATTI, M. G. & WAXMAN, I. (2010) Gastroesophageal reflux disease: From heartburn to cancer. *World J Gastroenterol*, 16, 3743-4.
- PETERSON, K. A., SAMUELSON, W. M., RYUJIN, D. T., YOUNG, D. C., THOMAS, K. L., HILDEN, K. & FANG, J. C. (2009) The role of gastroesophageal reflux in exercise-triggered asthma: a randomized controlled trial. *Dig Dis Sci*, 54, 564-71.
- PORCHERAY, F., VIAUD, S., RIMANIOL, A. C., LEONE, C., SAMAH, B., DEREUDDRE-BOSQUET, N., DORMONT, D. & GRAS, G. (2005) Macrophage activation switching: an asset for the resolution of inflammation. *Clin Exp Immunol*, 142, 481-9.
- POSTLETHWAIT, E. M. (2007) Scavenger receptors clear the air. *J Clin Invest*, 117, 601-4.
- RAGHAVENDRAN, K., NEMZEK, J., NAPOLITANO, L. M. & KNIGHT, P. R. (2011) Aspiration-induced lung injury. *Crit Care Med*, 39, 818-26.
- REES, J. (2000) Asthma in Adults. *ABC of Asthma*. 4th ed. London, BMJ Books.
- RICHES, D. W. & HENSON, P. M. (1986) Functional aspects of mononuclear phagocyte involvement in lung inflammation. *Ann N Y Acad Sci*, 465, 6-14.
- ROSSEAU, S., SELHORST, J., WIECHMANN, K., LEISSNER, K., MAUS, U., MAYER, K., GRIMMINGER, F.,

- SEEGER, W. & LOHMEYER, J. (2000) Monocyte migration through the alveolar epithelial barrier: adhesion molecule mechanisms and impact of chemokines. *J Immunol*, 164, 427-35.
- SCHWEITZER, A. N. & SHARPE, A. H. (1998) Studies using antigen-presenting cells lacking expression of both B7-1 (CD80) and B7-2 (CD86) show distinct requirements for B7 molecules during priming versus restimulation of Th2 but not Th1 cytokine production. *J Immunol*, 161, 2762-71.
- SCOTT, H. A., GIBSON, P. G., GARG, M. L. & WOOD, L. G. (2011) Airway inflammation is augmented by obesity and fatty acids in asthma. *Eur Respir J*, 38, 594-602.
- SHANG, X. Z., LANG, B. J. & ISSEKUTZ, A. C. (1998) Adhesion molecule mechanisms mediating monocyte migration through synovial fibroblast and endothelium barriers: role for CD11/CD18, very late antigen-4 (CD49d/CD29), very late antigen-5 (CD49e/CD29), and vascular cell adhesion molecule-1 (CD106). *J Immunol*, 160, 467-74.
- SHASHKIN, P., DRAGULEV, B. & LEY, K. (2005) Macrophage differentiation to foam cells. *Curr Pharm Des*, 11, 3061-72.
- SHIMIZU, Y., DOBASHI, K., ZHAO, J. J., KAWATA, T., ONO, A., YANAGITANI, N., KAIRA, K., UTSUGI, M., HISADA, T., ISHIZUKA, T. & MORI, M. (2007) Proton pump inhibitor improves breath marker in moderate asthma with gastroesophageal reflux disease. *Respiration*, 74, 558-64.
- STEFANIDIS, D., HOPE, W. W., KOHN, G. P., REARDON, P. R., RICHARDSON, W. S. & FANELLI, R. D. (2010) Guidelines for surgical treatment of gastroesophageal reflux disease. *Surg Endosc*, 24, 2647-69.
- STOUT, R. D. & SUTTLES, J. (2004) Functional plasticity of macrophages: reversible adaptation to changing microenvironments. *J Leukoc Biol*, 76, 509-13.
- STROBER, W. (2001) Trypan blue exclusion test of cell viability. *Curr Protoc Immunol*, Appendix 3, Appendix 3B.
- TIERNEY, J. B., KHARKRANG, M. & LA FLAMME, A. C. (2009) Type II-activated macrophages suppress the development of experimental autoimmune encephalomyelitis. *Immunol Cell Biol*, 87, 235-40.
- TRAORE, K., TRUSH, M. A., GEORGE, M., JR., SPANNHAKE, E. W., ANDERSON, W. & ASSEFFA, A. (2005) Signal transduction of phorbol 12-myristate 13-acetate (PMA)-induced growth inhibition of human monocytic leukemia THP-1 cells is reactive oxygen dependent. *Leuk Res*, 29, 863-79.
- VALLY, H., DE KLERK, N. & THOMPSON, P. J. (2000) Alcoholic drinks: important triggers for asthma. *J Allergy Clin Immunol*, 105, 462-7.
- VAN VEEN, I. H., TEN BRINKE, A., STERK, P. J., RABE, K. F. & BEL, E. H. (2008) Airway inflammation in obese and nonobese patients with difficult-to-treat asthma. *Allergy*, 63, 570-4.
- VCU (2009) Gastroesophageal Reflux Disease (GERD)/Heartburn. Virginia, Virginia Commonwealth University.
- VERRECK, F. A., DE BOER, T., LANGENBERG, D. M., VAN DER ZANDEN, L. & OTTENHOFF, T. H. (2006) Phenotypic and functional profiling of human proinflammatory type-1 and anti-inflammatory type-2 macrophages in response to microbial antigens and IFN-gamma- and CD40L-mediated costimulation. *J Leukoc Biol*, 79, 285-93.

- WAGERS, A. J., CHRISTENSEN, J. L. & WEISSMAN, I. L. (2002) Cell fate determination from stem cells. *Gene Ther*, 9, 606-12.
- WEBSPIDERSLIMITED (2012a) *Nutricia Advanced Medical Nutrition*. Lancashire, UK, NuBlue Web Solutions.
- WEBSPIDERSLIMITED (2012b) *Nutricia Advanced Medical Nutrition*. NuBlue Web Solutions.
- WENZEL, S. E. (2011) Characteristics, definition and phenotypes of severe asthma. *European Respiratory Monograph*, 51, 50-58.
- WHITE, J. G. & KRIVIT, W. (1966) The ultrastructural localization and release of platelet lipids. *Blood*, 27, 167-86.
- XU, W., SCHLAGWEIN, N., ROOS, A., VAN DEN BERG, T. K., DAHA, M. R. & VAN KOOTEN, C. (2007) Human peritoneal macrophages show functional characteristics of M-CSF-driven anti-inflammatory type 2 macrophages. *Eur J Immunol*, 37, 1594-9.
- ZAKIM, D. (2000) Thermodynamics of fatty acid transfer. *J Membr Biol*, 176, 101-9.
- ZHU, J. & EMERSON, S. G. (2002) Hematopoietic cytokines, transcription factors and lineage commitment. *Oncogene*, 21, 3295-313.

10 Appendix

Fortijuice		AVERAGE CONTENTS			
		UNIT	per 100ml	per 100kcal	
Description Fortijuice is a Food for Special Medical Purposes for use under medical supervision. Fortijuice is a juice tasting, high energy (1.5kcal/ml), ready to drink, juice style nutritional supplement for the dietary management of disease related malnutrition. Fortijuice can be used to supplement the diet of patients unable to meet their nutritional requirements from other foods and for those who do not like, or tire of, milk tasting supplements. Fortijuice is fat free and is suitable for patients on a low fat diet. Fortijuice is available in 200ml bottles, with a flexible straw attached, in 7 flavours: Lemon, Apple, Orange, Strawberry, Tropical, Forest Fruit, and Blackcurrant.		Energy:	kcal	150	100
			kJ	640	420
Indications For enteral use only. ACBS approved, prescribable on form FP10 (GP10 in Scotland) for the following indications: short bowel syndrome; intractable malabsorption; pre-operative preparation of undernourished patients; inflammatory bowel disease; total gastrectomy; dysphagia; bowel fistulae; disease related malnutrition.		Protein:	g	4.0	2.7
		nitrogen	g	0.6	0.4
Contraindications Not for intravenous use. Not suitable for children under 3 years of age. Not suitable for patients with galactosaemia.		NPC:N		212:1	212:1
		% of total energy	%	11	11
Precautions Not suitable as a sole source of nutrition. Only to be used as a supplement to the normal diet.		Carbohydrate:	g	33.5	22.3
		polysaccharides	g	20.3	13.5
Directions for use Fortijuice is best served chilled. Shake well before opening.		sugars	g	13.1	8.8
		lactose	g	<0.025	<0.025
Storage Store in a dry, cool place (5-25°C). Shake well before use. Once opened store bottles in a refrigerator for a maximum of 24 hours.		% of total energy	%	89	89
		Fat:	g	0	0
Shelf life 9 months. Best before date: see side of bottle.		saturates	g	0	0
		% of total energy	%	0	0
Ingredients (Lemon flavour*) Water, glucose syrup, maltodextrin, milk protein, sucrose, flavour (lemon), acidity regulator (citric acid), choline chloride, calcium chloride, L-ascorbic acid, emulsifier (polysorbate 80), potassium chloride, ferrous lactate, sodium chloride, magnesium chloride, zinc sulphate, DL- α -tocopheryl acetate, colour (curcumin), nicotinamide, copper gluconate, sodium selenite, manganese sulphate, calcium D-pantothenate, chromium chloride, pteroylmonoglutamic acid, D-biotin, pyridoxine hydrochloride, thiamin hydrochloride, retinyl palmitate, sodium molybdate, riboflavin, sodium fluoride, potassium iodide, cholecalciferol, phytomenadione, cyanocobalamin.		Dietary fibre:	g	0	0
		Minerals:			
*For all other flavours please see individual packaging.		sodium	mg (mmol)	9.7 (0.4)	6.5 (0.3)
		potassium	mg (mmol)	9.3 (0.2)	6.2 (0.2)
FORTIJUICE IS GLUTEN AND LACTOSE FREE.		chloride	mg (mmol)	178 (5.0)	119 (3.4)
		calcium	mg (mmol)	30 (0.8)	20 (0.5)
		phosphorus	mg (mmol)	12 (0.4)	8 (0.3)
		magnesium	mg (mmol)	2.0 (0.1)	1.3 (0.1)
		iron	mg	3.0	2.0
		zinc	mg	2.3	1.5
		copper	mcg	338	225
		manganese	mg	0.63	0.42
		fluoride	mg	0.19	0.13
		molybdenum	mcg	19	13
		selenium	mcg	11	7
		chromium	mcg	13	8
		iodine	mcg	25	17
		Vitamins:			
		vitamin A	mcg RE	188	125
		vitamin D	mcg	1.3	0.9
		vitamin E	mg α TE	2.3	1.6
		vitamin K	mcg	10.0	6.7
		thiamin	mg	0.29	0.19
		riboflavin	mg	0.32	0.21
		niacin	mg NE	3.4	2.3
		pantothenic acid	mg	1.00	0.67
		vitamin B6	mg	0.33	0.22
		folic acid	mcg	50	33
		vitamin B12	mcg	0.39	0.26
		biotin	mcg	7.5	5.0
		vitamin C	mg	19	13
		Others:			
		choline	mg	69	46
		Water:	g	75	50
		osmolarity	mOsm/l	750	750
		osmolality	mOsm/kg H ₂ O	955	955
		potential renal solute load	mOsm/l	285	285

Figure 10.2 – Fortijuice Nutritional Information

Information regarding the contents of Fortijuice no fat liquid meal used in this thesis. Information taken from (WebSpidersLimited, 2012a)

No	Fold-Change	Direction of Regulation	Gene Description
1	971.6562	down	Homo sapiens interleukin 8 (IL8), mRNA [NM_000584]
2	108.3099	up	UI-E-EJ1-ajw-b-14-0-UI.r1 UI-E-EJ1 Homo sapiens cDNA clone UI-E-EJ1-ajw-b-14-0-UI 5', mRNA sequence [BQ188485]
3	85.65689	down	Homo sapiens angiopoietin-like 4 (ANGPTL4), transcript variant 1, mRNA [NM_139314]
4	78.47773	up	Homo sapiens membrane-spanning 4-domains, subfamily A, member 6A (MS4A6A), transcript variant 2, mRNA [NM_022349]
5	71.98305	up	Homo sapiens glycoprotein A33 (transmembrane) (GPA33), mRNA [NM_005814]
6	71.01142	up	Homo sapiens membrane-spanning 4-domains, subfamily A, member 6A (MS4A6A), transcript variant 1, mRNA [NM_152852]
7	63.26204	down	Homo sapiens chemokine (C-X-C motif) ligand 3 (CXCL3), mRNA [NM_002090]
8	55.52314	down	Homo sapiens F-box and WD repeat domain containing 10 (FBXW10), mRNA [NM_031456]
9	55.23933	up	Homo sapiens murine retrovirus integration site 1 homolog (MRV1), transcript variant 2, mRNA [NM_130385]
10	46.03313	down	Homo sapiens chemokine (C-C motif) ligand 20 (CCL20), transcript variant 1, mRNA [NM_004591]
11	45.20027	down	Homo sapiens G protein-coupled receptor 56 (GPR56), transcript variant 3, mRNA [NM_201525]
12	42.40099	up	Homo sapiens chemokine (C-X3-C motif) receptor 1 (CX3CR1), transcript variant 4, mRNA [NM_001337]
13	41.91654	down	Homo sapiens adenosine A2a receptor (ADORA2A), mRNA [NM_000675]
14	40.72517	up	Homo sapiens G protein-coupled receptor 34 (GPR34), transcript variant 4, mRNA [NM_001097579]
15	39.76677	down	Homo sapiens chemokine (C-C motif) ligand 4 (CCL4), transcript variant 1, mRNA [NM_002984]
16	39.43316	down	interleukin 8 [Source:HGNC Symbol;Acc:6025] [ENST00000401931]
17	38.51062	up	Homo sapiens energy homeostasis associated (ENHO), mRNA [NM_198573]
18	37.83438	down	Homo sapiens chemokine (C-C motif) ligand 4 (CCL4), transcript variant 1, mRNA [NM_002984]
19	36.57692	down	Homo sapiens aldo-keto reductase family 1, member C4 (chlordecone reductase; 3-alpha hydroxysteroid dehydrogenase, type I; dihydrodiol dehydrogenase 4) (AKR1C4), mRNA [NM_001818]
20	35.904	down	Homo sapiens interleukin-1 receptor-associated kinase 2 (IRAK2), mRNA [NM_001570]

Table 10.1-Gene array data from Calogen treated PMA/THP-1 cells compared with PMA/THP-1 cells. Table showing top 20 genes with the highest fold change difference in gene regulation in PMA/THP-1 cells after treatment with 10 % v/v Calogen for 24 hours.

No	Fold-Change	Direction of Regulation	Gene Description
1	62.85637	down	BROAD Institute lincRNA (XLOC_007963), lincRNA [TCONS_00017157]
2	46.2115	down	Homo sapiens Wolf-Hirschhorn syndrome candidate 1 (WHSC1), transcript variant 1, mRNA [NM_133330]
3	39.66701	up	-
4	37.54233	up	Homo sapiens thyroid hormone receptor associated protein 3 (THRAP3), mRNA [NM_005119]
5	36.70439	up	Homo sapiens centromere protein M (CENPM), transcript variant 2, mRNA [NM_001002876]
6	33.46999	up	Homo sapiens inositol(myo)-1(or 4)-monophosphatase 2 (IMPA2), mRNA [NM_014214]
7	24.53069	up	Homo sapiens ribosomal protein L3 (RPL3), transcript variant 1, mRNA [NM_000967]
8	23.57528	up	Homo sapiens histone cluster 1, H2bi (HIST1H2BI), mRNA [NM_003525]
9	22.29274	up	Homo sapiens non-SMC element 1 homolog (<i>S. cerevisiae</i>) (NSMCE1), mRNA [NM_145080]
10	21.16814	up	Homo sapiens RNA, U4atac small nuclear (U12-dependent splicing) (RNU4ATAC), small nuclear RNA [NR_023343]
11	20.89432	up	Homo sapiens histone cluster 1, H2bm (HIST1H2BM), mRNA [NM_003521]
12	20.33614	up	-
13	20.30559	up	high mobility group nucleosomal binding domain 2 pseudogene 25 [Source:HGNC Symbol;Acc:39392] [ENST00000450495]
14	20.21342	up	Homo sapiens ribonuclease H2, subunit B (RNASEH2B), transcript variant 2, mRNA [NM_001142279]
15	19.83491	up	BROAD Institute lincRNA (XLOC_l2_009172), lincRNA [TCONS_l2_00017177]
16	19.55909	up	-
17	19.35775	up	Homo sapiens NDC80 homolog, kinetochore complex component (<i>S. cerevisiae</i>) (NDC80), mRNA [NM_006101]
18	18.61815	up	PREDICTED: Homo sapiens density-regulated protein-like (LOC100652897), miscRNA [XR_132765]
19	18.28983	up	Homo sapiens ribosomal protein L21 (RPL21), mRNA [NM_000982]
20	18.06763	up	PREDICTED: Homo sapiens 60S ribosomal protein L12-like (LOC648771), miscRNA [XR_133285]

Table 10.2-Gene array data from Calogen treated Daisy cells compared with untreated Daisy cells.

Table showing top 20 genes with the highest fold change difference in gene regulation in Daisy cells after treatment with 10 % v/v Calogen for 24 hours.